UNIVERSITÉ DE SHERBROOKE
Faculté de Génie
Département de Génie Civil

# VALORISATION DE LA FIBRE D'ASCLÉPIADE POUR LE RENFORCEMENT DE MATRICES ORGANIQUES

Thèse de doctorat
Spécialité : génie civil

Pierre OVLAQUE

Sherbrooke (Québec) Canada
Juin 2019

# MEMBRES DU JURY

Pr. Mathieu ROBERT

Directeur

Pr. Saïd ELKOUN

Codirecteur

Pr. Jérémie SOULESTIN

Évaluateur

Pr. MohammadReza FORUZANMEHR

Évaluateur

Pr. Brahim BENMOKRANE

Rapporteur

# Résumé

Ce projet vise à étudier les composites à matrice thermoplastique renforcés par fibres naturelles creuses d'asclépiade. Les fibres d'asclépiade sont des fibres unitaires, fines et creuses dont l'effet renforçant en tant que fibres cellulosiques courtes dans une matrice thermoplastique n'a pas été étudié. Le projet cherche donc à évaluer si la morphologie atypique de la fibre d'asclépiade permet de renforcer efficacement une matrice organique thermoplastique, et si la faible densité des fibres induit une baisse de celle du composite.

Les résultats présentés dans ce document démontrent que la fibre d'asclépiade possède un lumen très large occupant environ 70% du volume, et par conséquent une densité très faible pour une fibre naturelle cellulosique. Il a également été démontré que les fibres d'asclépiade possèdent une rugosité de surface et des propriétés mécaniques significativement plus faibles que les fibres libériennes comme le lin par exemple. Cependant, malgré de plus faibles propriétés mécaniques, les composites formés d'acide polylactique (PLA) et de fibre d'asclépiade se sont révélés au moins aussi performants que ceux produits avec les fibres de lin. Néanmoins, il a été démontré que la qualité de l'interface entre le PLA et la fibre d'asclépiade demeure très faible.

À la suite de ce constat, les traitements de surface de silanisation et de mercerisation ont été appliqués à la fibre d'asclépiade et ont permis d'améliorer l'adhésion interfaciale avec le PLA. Ces deux traitements usuels pour les fibres naturelles ont induit une amélioration notable de la résistance maximum à la traction des composites. Cependant, les traitements induisent une profonde altération de la fibre qui se caractérise par une baisse notoire des propriétés mécaniques des fibres.

Devant les effets secondaires néfastes liés à l'application d'un traitement de surface sur ce type de fibre, une matrice possédant une affinité naturelle avec les fibres naturelles a été utilisée pour évaluer le renforcement lié à l'ajout d'asclépiade. Les propriétés mécaniques, d'interface et la baisse de densité ont été mesurées et démontrent que l'asclépiade peut renforcer une matrice organique, si les conditions de mise en forme sont adéquates.

**Mots clefs :** Asclépiade, Composite, Thermoplastiques, Fibres naturelles

# Remerciements

Je souhaite remercier en premier lieu mes deux directeurs de thèse, les professeurs Mathieu Robert et Saïd Elkoun pour m'avoir fait confiance et pour la liberté accordée sur le déroulement de ce projet de recherche.

Je souhaite également remercier les membres du jury d'avoir accepté de prendre le temps d'évaluer et d'assister à cette thèse de doctorat.

Je remercie Stéphane et Charles pour les bons moments passés devant le FEG et les coupes cryogéniques.

Merci à Patrice pour ses conseils, son aide, les légumes et la découverte du 24 juin.

Merci à Reza, surtout pour le support et les conseils qui ont permis de lancer ce sujet de recherche il y a 3 ans, mais aussi pour m'avoir demandé de chanter « Bistro d'oyé barman » a mainte reprise…

Merci à Jérémy pour les bons moments passés ensemble, les play-offs NBA, la vente de garage finale et les beach-volleys. La pétanque n'est pas un sport. Merci d'avoir supporté la minimale de la chanson du dimanche et des fatals Picards pendant nos nombreux trajets Granby-Sherbrooke.

Merci à Florent qui n'est pas innocent dans cette histoire de thèse au Canada. La piste numéro 11 de l'album de FFS t'est associée. Merci pour les 3 premiers mois phénoménaux à Sherbrooke, le pot de miel, le légendaire marcel rouge, et la dernière ascension du mont Bellevue...

Merci à Lina pour tes très bons conseils techniques sur les fibres naturelles et la découverte du za'atar, du tahini, du halva, du baba ghanouj et des baklavas…

Merci à Amélie pour les karaokés au pub du village et l'instauration du vendredi pâtisseries.

Merci aux collègues passées par le CITE durant ces 3 années: Clément, Babak, Javad, Farnaz, Laura .

Mes remerciements s'adressent également aux stagiaires. Merci particulier à Julien Durand et Gregoire Mercusot (Aka la team bambou) pour leur excellent travail, détermination et leur bonne humeur. L'été 2018 restera celui de l'efficacité, du petit-château, des problèmes de vélo et des voitures louées sur turo…

Merci également à Michel Jaquet pour l'aide apporté sur la mise en place des tests de SFFT, la préparation des éprouvettes et le comptage des fragments de fibre.

Merci également à Ivan, Audrey, Steven et Rebecca.

Je remercie toute la famille, la belle-famille et les amis restés en France pour le support et les très bons moments passés au Québec et pendant les périodes de noël.

Pour terminer, merci à ma conjointe (de fait ☺) Marie pour l'aide et le soutien apporté durant ces trois dernières années et qui ont facilité cette aventure au Canada.

# Table des matières

# Liste des figures

# Liste des tables

# CHAPITRE 1 : INTRODUCTION

## 1.1 Contexte

La diminution des ressources pétrolières couplée à la montée de la conscience écologique depuis quelques années a ramené sur le devant de la scène les principes de durabilité et d'écoconception des objets. Ces principes prônent, entre autres, une conception pérenne limitant au maximum les impacts sur l'environnement et ne créant pas de déchets ultimes. Ces nouveaux enjeux entrent en contradiction avec l'utilisation et la production de matériaux plastiques petrosourcés. Néanmoins, ceux-ci se sont imposés et rendus indispensables dans de nombreux secteurs industriels tels que l'automobile, ou l'équipement ménager. On estime ainsi la production mondiale de plastiques, tous grades confondus, à plus de 350 millions de tonnes par an [1]. En plus d'un changement des habitudes de consommation, la plasturgie doit donc opérer une mutation vers une production respectant au maximum les principes de développement durable. Un changement de nos utilisations des matières plastiques est donc nécessaire. Heureusement, à la vue de la part croissante accordée dans les médias à la pollution induite par les plastiques, cette mutation a déjà commencé.

Une industrie de la plasturgie plus pérenne passe notamment par la diminution de sa dépendance au pétrole. On assiste ainsi depuis quelques années à l'émergence de résines biosourcées [2], [3]. La montée du prix du pétrole et la demande de matériaux plus verts ont permis le développement économique de solutions permettant de produire les résines traditionnelles par des moyens plus respectueux de l'environnement. Il est par exemple possible de produire divers grades de polyamides (PA) à partir d'huile de ricin ou encore tout récemment du polyéthylène (PE) à partir de la canne à sucre [2]. Cet engouement a aussi amené au démarrage de productions industrielles de résines biosourcées non conventionnelles telles que l'acide polylactique (PLA) ou l'acide polyglicolique (PGA). Par exemple, le PLA, connu depuis les années 1930, n'est entré en production industrielle qu'au milieu des années 2000 [4]. L'impact environnemental du PLA étant faible, il est un exemple parfait des nouveaux plastiques qui ont émergé pour relever les nouveaux défis écologiques.

Outre le fait de développer de nouveaux moyens de production plus durables, la transition des plastiques passe également par une utilisation plus raisonnée. Le renforcement mécanique des matrices polymères, dont il est question dans cette thèse, est une des solutions permettant une utilisation plus efficace des matières plastiques. En effet, l'ajout de renforts permet de diminuer la consommation de matrice et d'augmenter les propriétés mécaniques des matériaux sans modification fondamentale des techniques et savoirs. Cette augmentation des propriétés permet par ailleurs de réduire le volume des pièces pour une application. Bref, l'ajout de renforts amène à une diminution de la consommation de résine par substitution d'un volume de matrice et aussi par diminution du volume des pièces. Ce renforcement s'opère généralement, dans les matrices thermoplastiques, par l'ajout de fibres synthétiques minérales telles que les fibres de verre. Cependant à l'image des mouvements qui sont à l'œuvre concernant les résines, les fibres synthétiques sont peu à peu remplacées par des alternatives plus durables. Ainsi, les fibres naturelles cellulosiques sont de plus en plus employées pour le renforcement de matrices organiques[5].

L'utilisation des fibres naturelles est effective depuis des millénaires pour le renforcement des murs (torchis) dans de nombreuses régions. Ces fibres abondantes et diversifiées sont produites naturellement par tous les végétaux dans le monde entier. Elles sont biosourcées, biodégradables et constituent des réservoirs à $CO_2$ atmosphérique [6]. Elles sont donc des matériaux répondant parfaitement aux enjeux actuels. Leur emploi est d'autant plus vertueux que certaines d'entre elles, comme la fibre de lin canadien, sont initialement des déchets très peu valorisés et majoritairement incinérés.

Parmi la multitude de fibres naturelles, certaines comme la soie d'asclépiade présentent une morphologie très particulière. En effet, alors que la majorité des fibres naturelles sont pleines, la fibre d'asclépiade est creuse et donc extrêmement légère. La soie d'asclépiade est extraite d'une mauvaise herbe robuste parfaitement adaptée au climat nord-américain, sa culture ne nécessite donc pas d'engrais ni de pesticides. L'asclépiade est cultivée au Québec en vue de sa transformation par cardage en mats isolants. Cette production de mats entraine une séparation de la fraction de fibres ayant des longueurs trop faibles pour être entrainées dans les cardeuses. Il n'en demeure pas moins que ces fibres rejetées ne sont en aucun cas altérées, hormis leur longueur, elles conservent toutes leurs propriétés initiales. C'est de ce constat que le projet de recherche présenté dans ce manuscrit a démarré. Le but

est d'évaluer l'utilisation de ces fibres déclassées pour renforcer des matrices thermoplastiques. Malheureusement, depuis le démarrage du projet de recherche en 2016, la filière de l'asclépiade a rencontré plusieurs aléas qui l'ont amené à un repli significatif. Néanmoins, le sujet de recherche trouve une certaine universalité dans le sens où la fibre d'asclépiade est semblable à d'autres types de fibres creuses. Les travaux et les conclusions présentés ici sont donc extrapolables aux autres fibres creuses comme le kapok par exemple (100 kT produits en 2013 [7]).

## *1.2 Problématique*

Ce projet de recherche vise à valoriser la fibre naturelle d'asclépiade en tant que renfort de matrices polymériques.

La problématique est née du fait que les informations disponibles sur les caractéristiques de ces fibres sont fortement limitées. Également, il n'existe pas de retour d'expérience et d'études sur l'emploi de fibres courtes creuses en tant que renfort dans des matrices transformées par injection ou extrusion.

La question de leur utilisation dans des matrices thermoplastiques est donc truffée d'incertitudes. Il n'est pas évident, par exemple, que l'asclépiade supporte des procédés d'injection ou d'extrusion sans dommages. De même, la fibre est reconnue pour avoir une surface couverte de cire. Celle-ci pourrait conduire à des résultats négatifs concernant le renforcement des matrices thermoplastiques en limitant l'adhésion à l'interface. Également, à l'instar des fibres libériennes, l'asclépiade n'est pas une fibre structurelle pour la plante. Son effet renforçant pourrait donc être sévèrement limité. Concernant le lumen, il n'est pas possible de prédire son état de remplissage après extrusion par exemple. Ce manque d'information n'est pourtant pas à relier à un défaut d'intérêts ou de débouchés pour un tel matériau. Ce genre de composite polymérique à base d'asclépiade pourrait susciter de l'intérêt dans des domaines reliés au transport où la diminution du poids des pièces est au centre des préoccupations. En effet, une diminution de poids se répercute directement par une diminution de pollution générée lors de la phase d'utilisation pour une voiture. La fibre d'asclépiade étant creuse, elle permettrait en théorie de diminuer le poids des pièces plastiques. La requalification des fibres courtes d'asclépiade dans des matrices thermoplastiques peut donc trouver des applications concrètes.

## 1.3 Objectifs

L'objectif principal de la thèse est de vérifier si la fibre d'asclépiade, qui peut paraitre fragile et peu résistante, serait une candidate efficace pour le renforcement des matrices organiques. On cherche également à vérifier si elle amène des opportunités liées à sa structure particulière. Cet objectif de recherche amène une certaine dualité dans le projet de recherche. Tandis que la valorisation de la fibre d'asclépiade pour le renforcement des matrices thermoplastiques apparait comme un projet très appliqué, les nombreuses discussions relatives à la caractérisation des fibres et de leur efficacité s'inscrivent dans une démarche plus fondamentale. Cette approche plus théorique et fondamentale demeure nécessaire à la compréhension de cette fibre particulière et de son effet renforçant. Cette dualité se répercute logiquement dans chacun des 3 sous-objectifs présentés ci-dessous :

### 1.3.1 Preuve de concept sur l'emploi de l'asclépiade dans les composites

Dans ce premier sous-objectif, il est question de vérifier si les fibres d'asclépiade sont capables de renforcer une matrice organique. Les fibres d'asclépiade sont beaucoup plus fines et fragiles en comparaison des fibres libériennes généralement utilisées pour le renforcement de matrices (lin, chanvre, jute ou encore kenaf). Il n'est donc pas évident que les fibres puissent supporter les effets des techniques d'extrusion ou d'injection sans dommages irréversibles. Les effets renforçants induits par l'asclépiade ont été évalués sur l'acide polylactique (PLA). Le PLA est un plastique biosourcé, potentiellement biodégradable qui gagne en popularité et qui peut bénéficier d'un renforcement par des fibres naturelles. Ce sous-objectif a été traité en deux temps :

*i) Caractériser les fibres :*

Les fibres d'asclépiade sont atypiques et ne sont que très peu documentées dans la littérature. Une caractérisation des fibres a donc été effectuée en premier lieu. Cette caractérisation a permis d'établir une carte des propriétés moyennes des fibres d'asclépiade utilisées et de supporter les discussions ultérieures relatives aux composites. Afin de comparer la fibre d'asclépiade aux autres fibres naturelles, cette caractérisation a été

effectuée en parallèle sur la fibre de lin qui est une fibre libérienne très employée pour le renforcement de matrices organiques.

Les caractéristiques relatives à la morphologie des fibres (diamètre, longueur) ont été mesurées par microscopie optique (OM). La microscopie électronique à balayage (MEB) a permis d'évaluer la taille du lumen et l'épaisseur de la paroi pectocellulosique. Les propriétés mécaniques ont été calculées au moyen de tests de traction. Les propriétés thermiques, principalement les températures de dégradation des composés de la fibre, ont été évaluées par analyses thermogravimétriques (TGA). La rugosité de surface a été mesurée par microscopie à force atomique (AFM). Enfin, la densité de la fibre a été évaluée par pycnométrie.

*ii) Évaluer l'effet des fibres sur les propriétés mécaniques du PLA :*

Des composites PLA renforcés par des fibres d'asclépiade ou de lin ont été produits par injection à la suite de la caractérisation des fibres. Les morphologies et longueurs des deux types de fibres ont été mesurées après injection par OM pour évaluer la tenue de l'asclépiade aux processus d'extrusion et d'injection (comparativement au lin). Ensuite, les propriétés mécaniques en traction des composites ainsi que les propriétés thermomécaniques et les interactions à l'interface ont été évaluées par analyses mécaniques dynamiques (DMA) en simple cantilever. Les propriétés de tenue à l'impact (sollicitation Izod) des composites ont été calculées et les faciès de rupture des composites ont été observés par MEB pour visualiser la qualité de l'interface fibre/matrice. Enfin, l'absorption d'eau des composites a été mesurée et comparée à celle du lin.

Pour résumer, ce sous-objectif n°1, décrit en détail au chapitre 4, a permis de répondre aux questions suivantes :

a) *La fibre d'asclépiade présente-t-elle des propriétés intéressantes pour le renforcement de matrices organiques ?*
b) *La fibre d'asclépiade supporte-t-elle les moyens de mise en forme conventionnels ?*
c) *La fibre d'asclépiade possède-t-elle un effet renforçant dans une matrice organique (PLA) ?*
d) *La fibre d'asclépiade présente-t-elle une bonne interface naturelle avec le PLA ?*

### *1.3.2 Adhésion fibre-matrice*

Ce deuxième sous objectif découle directement des conclusions relatives à la qualité de l'interface entre l'asclépiade et le PLA. La qualité de l'adhésion entre la fibre et la matrice est cruciale pour les propriétés mécaniques finales des composites. Cependant, les fibres naturelles ne sont généralement que très peu compatibles avec les matrices organiques, la fibre d'asclépiade ne fait pas exception à la règle. La problématique liée à cette faible affinité à l'interface est généralement solutionnée par l'utilisation de traitements de surface. Ces traitements sont très efficaces sur les fibres libériennes, mais peu d'études portent sur leur application aux fibres creuses. Ce sous-objectif vise à explorer les questions relatives à l'application de traitements de surface sur la fibre d'asclépiade, leurs effets sur les fibres et les composites. Ce sous-objectif se divise en deux étapes :

*i) Traitement de surface des fibres d'asclépiade et caractérisation des fibres traitées :*

Les fibres d'asclépiade ont été traitées avec des méthodes qui ont démontré leur efficacité sur les fibres libériennes. Un traitement alcalin ainsi qu'un traitement utilisant des époxy-silanes ont été appliqués sur la fibre d'asclépiade. Le traitement alcalin consiste à libérer l'accessibilité des groupements hydroxyles de la cellulose. Il a été effectué par trempage des fibres dans la solution alcaline (5 % - 20 °C). Les effets du temps de trempage sur les diminutions des concentrations en lignines et hémicelluloses et la morphologie ont été suivis par spectroscopie infrarouge à transformée de Fourier (FTIR) et MEB, respectivement. Le traitement de silanisation consiste à greffer des molécules ayant une affinité avec la fibre et la matrice. Le traitement de silanisation passe par une hydrolyse de l'époxy-silane suivi d'un trempage des fibres dans la solution. Les fibres sont ensuite séchées pour terminer la réaction de greffage. La réussite du traitement a été suivie par FTIR et analyse dispersive en énergie (EDS).

Ces traitements peuvent être très agressifs pour les fibres d'asclépiade qui sont plus fines que les fibres libériennes, celles-ci ont donc été caractérisées avant leur utilisation dans des composites de PLA. Les propriétés mécaniques en traction des fibres traitées ont été calculées. Les modifications de la rugosité de surface ont été analysées par AFM, la morphologie par MEB et les tailles des fibres après injection ont été mesurées par OM.

*ii) Caractérisation des composites :*

Les composites ont été caractérisés suivant le même processus que pour le sous-objectif 1. Des tests de traction ont été effectués sur les éprouvettes injectées contenant des fibres modifiées soit par traitement alcalin soit par silanisation. La caractérisation s'est poursuivie par des mesures en DMA en simple cantilever et par des tests d'impact Izod. Cette caractérisation se conclut par la fractographie qui permet une visualisation directe des modifications de l'interface dans les composites.

Pour résumer, le sous-objectif 2 de la thèse tente de répondre aux questions suivantes :

*e) La fibre d'asclépiade peut-elle être traitée par des moyens conventionnels et supporte-t-elle ces traitements ?*

*f) L'application d'un traitement de surface permet-elle d'augmenter la compatibilité de la fibre d'asclépiade avec le PLA ?*

### *1.3.3 Réduction du poids et amélioration des propriétés*

Ce dernier objectif vise à trouver une matrice qui peut être utilisée avantageusement avec la fibre d'asclépiade non traitée et à évaluer la qualité de l'interface et la diminution de la densité. Cet objectif vise à s'affranchir de tout traitement de surface et obtenir une bonne adhésion interfaciale de manière naturelle. Le polyamide 11 (PA11) a été choisi, car il est connu pour présenter une bonne affinité avec les fibres naturelles cellulosiques. Les résultats obtenus avec le PA11 ont été comparés à ceux obtenus avec du polypropylène (PP), qui est un polymère couramment utilisé. Outre les propriétés mécaniques de ces composites, ce dernier objectif cherche principalement à évaluer les opportunités liées aux fibres d'asclépiade. Cette fibre présente une petite section et un très large lumen, elle devrait donc présenter une longueur critique faible et engendrer une diminution de la densité des composites. Ces caractérisations se sont déroulées en trois temps :

*i) Détermination de la longueur critique de la fibre d'asclépiade :*

La longueur critique est une indication de la qualité de l'interface entre une matrice et une fibre. Elle dépend de la géométrie de la fibre et de la qualité de l'interface avec la matrice.

Lorsque l'on connait la longueur moyenne des fibres dans un composite, la connaissance de la longueur critique permet d'évaluer l'efficacité du renforcement. La longueur critique de l'asclépiade dans le PA11 et le PP a été déterminée par des tests de fragmentation de fibre (SFFT). Ce test consiste à étirer une fine éprouvette, contenant une seule fibre alignée, et mesurer la longueur des fragments de fibre en fonction de la déformation. Ce phénomène de fragmentation est directement relié à la capacité de transfert des contraintes à l'interface et la taille de la section de la fibre.

La détermination de la longueur critique des fibres a permis de calculer le facteur d'efficience des fibres qui renseigne sur la faculté des fibres à renforcer la matrice. Ce facteur est lié à la distribution des longueurs des fibres dans le composite. Un facteur égal à 1 correspond à une situation ou les fibres sont en grande majorité longues et participent activement au renforcement. Plus ce facteur diminue, moins les fibres apportent un renforcement mécanique à la matrice.

*ii) Évaluer la diminution de la densité des composites*

La diminution de la densité se mesure directement par densitométrie dans l'éthanol pour les composites de PP et PA11. Néanmoins, les résultats de densitométrie ne renseignent pas sur la distribution et l'origine des vides. Pour connaitre le remplissage des lumens, la microtomographie à rayon X a été utilisée. Les coupes microtomographiques permettent de différencier le volume occupé par les bulles d'air de celui des lumens vides. La combinaison de la densitométrie et de la microtomographie a donc permis d'évaluer le remplissage des lumens.

*iii) Mesurer l'influence du taux de fibre sur les propriétés mécaniques des composites*

Ce sous-objectif se conclut par la caractérisation mécanique des composites de PP et PA11 ayant des taux massiques de fibre variés. La caractérisation est passée par des tests de traction, de DMA (en traction) et par la fractographie des échantillons. La connaissance des capacités de renforcement des fibres et de la distribution des vides a permis d'expliquer l'évolution constatée sur les propriétés mécaniques des composites.

Le sous-objectif 3 de la thèse répond aux questions suivantes :

g) *La fibre d'asclépiade présente-t-elle une longueur critique courte qui la rend très efficace pour le renforcement de matrices organiques ?*
h) *Le lumen des fibres d'asclépiade engendre-t-il une diminution de la densité des composites ?*

## *1.4 Originalité*

De manière générale, l'originalité principale de cette thèse est basée sur le fait de considérer la fibre d'asclépiade comme renfort de matrices organiques. À notre connaissance actuelle, il n'existe pas d'étude explorant les possibilités des fibres courtes d'asclépiade pour le renforcement de matrices thermoplastiques. Pourtant, comme mentionné dans les objectifs ci-dessus, il existe des raisons qui permettent de croire que l'asclépiade à un potentiel dans ce genre d'applications.

Comme, l'asclépiade n'est que très peu considérée pour le renforcement de matrices thermoplastiques, il n'existe naturellement pas de travaux portant sur ses propriétés d'interface. Seules quelques études de la mercerisation des fibres de kapok, une fibre similaire, sont à noter. L'originalité de cette recherche s'exprime donc aussi par la vérification de l'efficacité des traitements de surface et leurs impacts sur les fibres. En effet, la majorité des études portant sur le traitement de surface de fibres naturelles passent de l'application du traitement aux conclusions sur les composites sans s'attarder sur les effets sur les fibres.

L'originalité s'exprime également au niveau de : la mise à profit du lumen des fibres pour diminuer la densité des composites, les effets de la mise en forme par extrusion ou injection sur la morphologie des fibres creuses, les discussions apportées sur les opportunités d'avoir une géométrie creuse pour le renforcement de matrices organiques.

## *1.5 Organisation de la thèse*

Cette thèse est présentée par articles et contient 7 chapitres :

- Le chapitre 1 présente le contexte, la problématique et les objectifs liés au projet de

recherche.

- Les chapitres 2 et 3 correspondent à la revue de littérature. Le chapitre 2 aborde les notions essentielles aux discussions présentes dans les chapitres suivants. Les notions de fibre naturelles (variabilité, structure, propriétés), matrice, interface et mise en forme y sont discutées. Le chapitre 3 correspond à la revue de littérature des fibres naturelles creuses et leurs applications.

- Le chapitre 4 présente une caractérisation comparée de la fibre creuse d'asclépiade et de lin. Il est question ici de vérifier le potentiel de la fibre d'asclépiade pour le renforcement de matrices organiques. Le chapitre présente donc aussi une comparaison des propriétés mécaniques et thermiques de composites PLA renforcés de fibres de lin ou d'asclépiade.

- Le chapitre 5 s'appuie sur la conclusion du chapitre 4. Le chapitre aborde une étude sur l'application de traitements de surface (mercerisation et silanisation) sur la fibre d'asclépiade pour améliorer son adhésion avec le PLA. Les effets des traitements sur les propriétés mécaniques des fibres et des composites (matrice PLA) y sont présentés.

- Suite aux conclusions du chapitre 5, le chapitre 6 se propose de mesurer la qualité de l'interface avec une matrice démontrant une affinité naturelle avec les fibres cellulosiques (i.e. polyamide 11 (PA11)). Les notions de longueur critique et facteur d'efficience des fibres dans le PA11 et le PP y sont comparées. Les propriétés mécaniques des composites (PA11 et PP) y sont également étudiées.
- Le chapitre 7 regroupe la conclusion générale de cette thèse ainsi que les perspectives.

# CHAPITRE 2 : POLYMÈRES RENFORCÉS DE FIBRES NATURELLES CELLULOSIQUES COURTES

## 2.1 Introduction

Les polymères renforcés de fibres naturelles courtes sont des matériaux composites dont l'apparition est fortement liée à l'histoire des plastiques. La première utilisation commerciale de fibres naturelles dans une matrice polymère remonte au début du XXe siècle avec l'utilisation du coton pour le renforcement de formaldéhyde [1].

Les matrices thermoplastiques sont généralement légères, mais peu performantes sur le plan des propriétés mécaniques et notamment de la rigidité. Leur renforcement par des fibres naturelles produit des matériaux ayant un excellent ratio contrainte/poids [2]. Les composites ainsi formés présentent une bonne compétitivité économique et s'inscrivent parfaitement dans des applications pour l'automobile, la construction, l'équipement ménagé ou encore l'emballage [3].

Néanmoins, la création de composites à base de fibres naturelles présente quelques difficultés. Premièrement, à l'image des nombreux grades de matrices thermoplastiques existants, les diverses espèces de fibres naturelles possèdent des différences marquées. Deuxièmement, le composite est directement tributaire de la qualité des interactions entre les fibres et la matrice. Enfin, la technique employée pour la production et la mise en forme des composites a un impact significatif sur l'efficacité finale du matériau. Le présent chapitre vise à décrire ces différentes notions qui modèrent les propriétés des matrices thermoplastiques renforcées de fibres naturelles courtes.

## 2.2 Matériaux

Un composite à base de fibres naturelles courtes est un matériau issu de l'assemblage d'une matrice organique et de fibres naturelles. Celles-ci connaissent un gain de popularité depuis les années 90 dans le milieu de la recherche universitaire, mais également dans les secteurs industriels tels que celui de l'automobile [1]. Les fibres naturelles sont utilisées pour leurs bonnes propriétés mécaniques et supportent la charge appliquée sur le composite. La

matrice prend quant à elle le rôle de liant et assure la cohésion des fibres dans le matériau.

### *2.2.1 Fibres naturelles cellulosiques*

#### *2.2.1.1 Variabilité*

Tous les végétaux produisent des fibres cellulosiques naturelles. Néanmoins, leurs compositions, structures, morphologies ne sont pas identiques. Les variations qui peuvent exister sur ces notions sont directement reliées aux fonctions et origines des fibres et affectent, par exemple, les propriétés mécaniques des fibres.

Si l'on s'attarde sur propriétés mécaniques, leur variabilité s'explique principalement sur trois niveaux. Premièrement, au sein d'une espèce et dans une même variété, les fibres peuvent présenter des propriétés inconstantes liées à des conditions de croissance variables. Deuxièmement, au sein d'une espèce, des différences peuvent apparaitre entre les variétés. Troisièmement, la variabilité est très forte entre des fibres provenant d'espèces végétales différentes. Par analogie, discuter de manière générale des propriétés mécaniques des fibres naturelles revient à essayer de discuter du goût des fruits. On retrouve ainsi les mêmes niveaux de variation : (i) le goût des pommes d'une même variété est impacté par de nombreux facteurs tels que la qualité du sol, l'ensoleillement, la maturité ou encore la température, (ii) le goût des pommes varie en fonction des variétés (iii) le goût d'une pomme varie de celui d'une poire.

À cause de ces variations, il est usuel de séparer les fibres naturelles en différenciant les fibres issues du bois d'arbres des fibres extraites des monocotylédones (herbes et roseaux), et de celles issues des dicotylédones. Ces dernières sont généralement séparées en sous-catégories en fonction de l'origine des fibres dans la plante. On distingue ainsi les fibres issues des tiges (libériennes), de celles issues des feuilles, de celles reliées aux graines comme présenté dans la Figure 2-1. Les fibres de ces regroupements présenteront une variabilité plus faible de leurs propriétés, structure et morphologie, car leurs rôles physiologiques sont équivalents. Cette classification n'est cependant pas arrêtée, elle dépend avant tout du critère de regroupement initial.

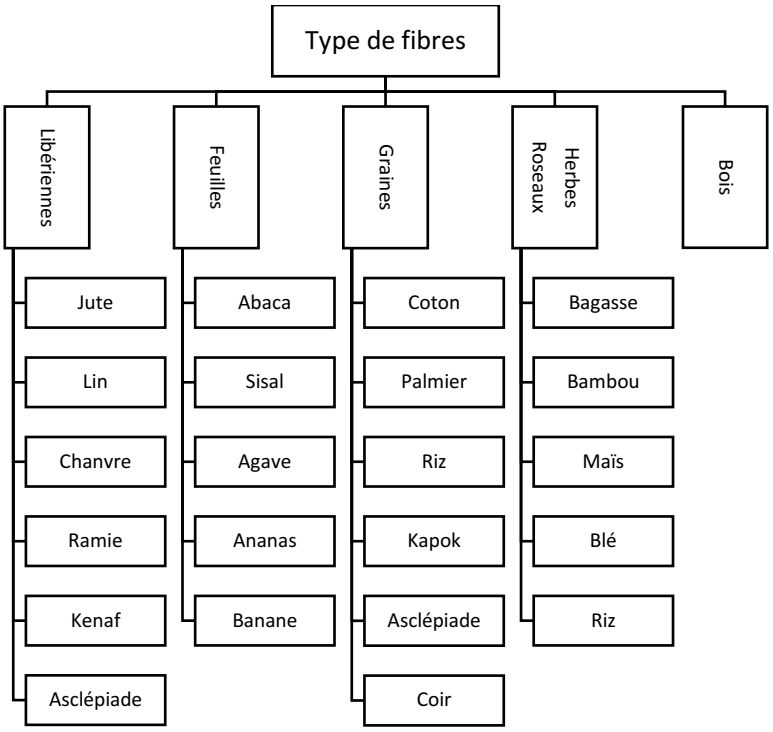


*Figure 2-1: types de fibres naturelles (d'après [11]–[13])*

### *2.2.1.2 Composition*

Les fibres naturelles, qu'elles soient libériennes, issues des graines ou extraites du bois, résultent principalement de l'arrangement de molécules de cellulose, hémicellulose et lignine en proportions variables. Plusieurs autres composés tels que les protéines, les pectines ou encore les cires entrent également dans la composition des fibres naturelles. Ils demeurent cependant très minoritaires et ne seront pas abordés ici [1], [2].

Parmi les 3 constituants principaux, la cellulose est généralement majoritaire. La cellulose est un polymère organique issu de l'arrangement linaire de molécules de glucose liées par des liaisons β(1-4) avec un degré de polymérisation pouvant varier de 200 à 15 000 [10], [11]. L'arrangement de plusieurs chaines de cellulose forme une microfibrille de cellulose. Ces microfibrilles possèdent un diamètre variant de 10 à 30 nm et peuvent démontrer un caractère cristallin local sur des longueurs allant de 30 à 60 nm [15], [17] (Figure 2-2). Ce sont les microfibrilles de cellulose qui sont responsables des bonnes propriétés mécaniques des fibres naturelles. En effet, à géométrie équivalente, on estime qu'une microfibrille de cellulose possède la même résistance à la rupture qu'un fil d'acier [17]. Néanmoins, les

propriétés mécaniques des fibres naturelles dépendent également de la cohésion de ces microfibrilles.

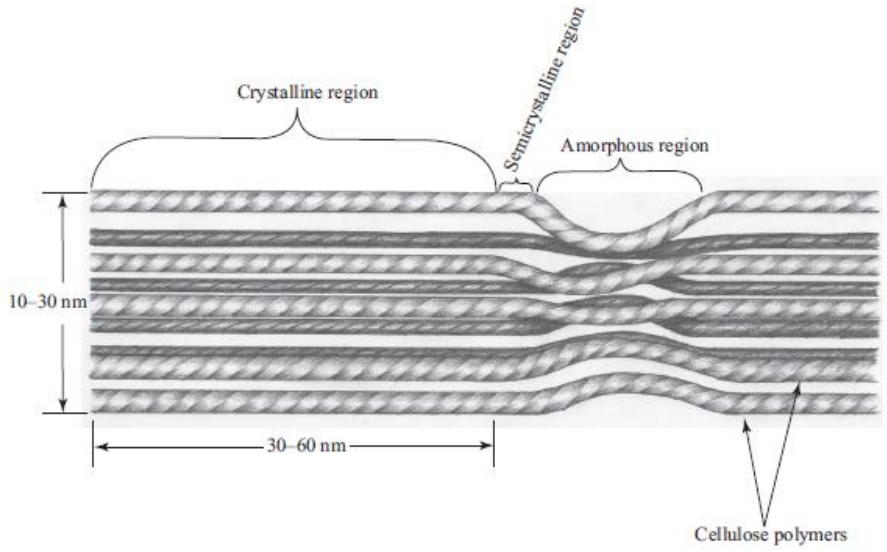


*Figure 2-2: Représentation de l'alignement des molécules de cellulose au sein d'une microfibrille [15]*

Cette cohésion est assurée par l'intermédiaire des deux derniers constituants, l'hémicellulose et la lignine. Ce sont des molécules plus courtes et ramifiées qui gainent les microfibrilles de cellulose telles qu'illustrées dans la Figure 2-3 [18]. L'hémicellulose est analogue à la cellulose, elle est également issue de plusieurs monomères de glucides, mais possède de courtes ramifications et un degré de polymérisation nettement plus faible (100-200). Les lignines sont en revanche des molécules lourdes (degré de polymérisation de 20 000 à 70 000), complexes et amorphes issues de l'arrangement aléatoire de 3 précurseurs aromatiques en proportion variable [15].

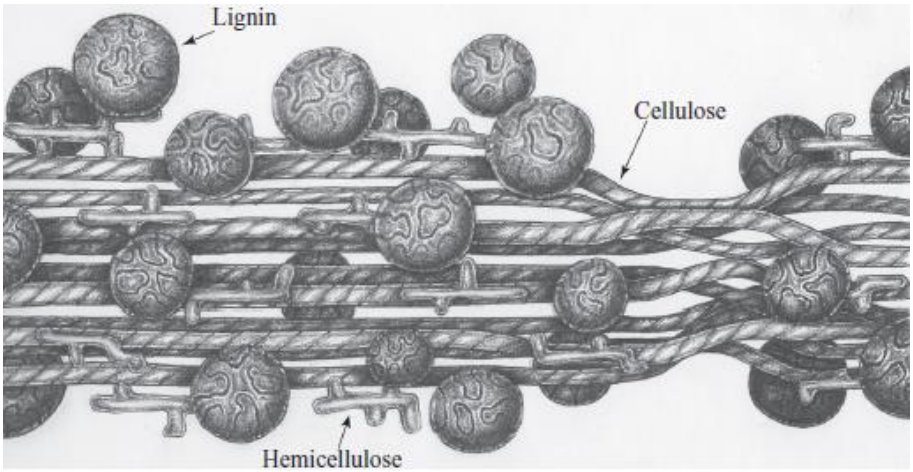


*Figure 2-3: Arrangement spatial de la cellulose, hémicellulose et lignine au sein de la paroi secondaire (la fréquence de l'hémicellulose et la lignine n'est pas représentative la réalité )[15]*

Comme mentionné plus haut, ces trois molécules sont présentes en proportions variables dans les fibres naturelles comme l'indique la Table 2-1. Néanmoins, au sein d'un regroupement, les variations sont faibles. On peut noter ainsi qu'il existe une certaine constance au niveau de la composition chimique des fibres libériennes.

*Table 2-1: composition chimique de quelques fibres naturelles*

| | | Cellulose (%) | Hémicellulose (%) | Lignine (%) | Ref. |
|---|---|---|---|---|---|
| | Bois | 45-50 | 20-30 | 22-30 | [14] |
| Graines | Coton | 92 | 2 | <1 | [19] |
| | Kapok | *43-64* | *6-32* | *13-15* | [7], [20] |
| | Asclépiade | *40-55* | *8-27* | *19-15* | [21], [22] |
| | Coir | *32-43* | <1 | *40-45* | [5] |
| Liberiennes | Lin | 71 | 19-21 | 2,2 | [5] |
| | Kenaf | 45-57 | 21 | 8-13 | [5] |
| | Chanvre | 70-74 | 18-23 | 3,7-5,7 | [5] |
| | Ramie | 69-76 | 13-17 | <1 | [5] |
| | Jute | 61-71 | 14-20 | 12-13 | [5] |

Cet arrangement particulier de la cellulose, de l'hémicellulose et de la lignine produit un matériau composite naturel qui constitue les fibres naturelles. Ainsi, les variations de composition reportées dans le Table 2-1 peuvent expliquer, en partie, les différences au niveau des propriétés mécaniques rencontrées dans les fibres naturelles. Néanmoins, l'arrangement spatial de ce matériau cellulosique possède également un impact significatif sur les propriétés mécaniques.

#### *2.2.1.3 Structure*

Les fibres naturelles présentent toutes une structure formée de plusieurs parois cellulosiques concentriques dont le nombre, la composition et l'épaisseur varient en fonction du type de fibre. Cette structure est le résultat de l'activité d'une cellule végétale et peut être considérée comme la brique élémentaire formant une fibre naturelle. En effet, à la différence des cellules animales, les cellules végétales présentent des dimensions bien plus importantes et produisent une paroi pectocellulosique. Cette paroi ne disparait pas lors de la mort de la cellule et donne une fibre végétale ultime. La Figure 2-4 présente les structures communément associées aux fibres ultimes de bois, libériennes, des graines, et des monocotylédones.

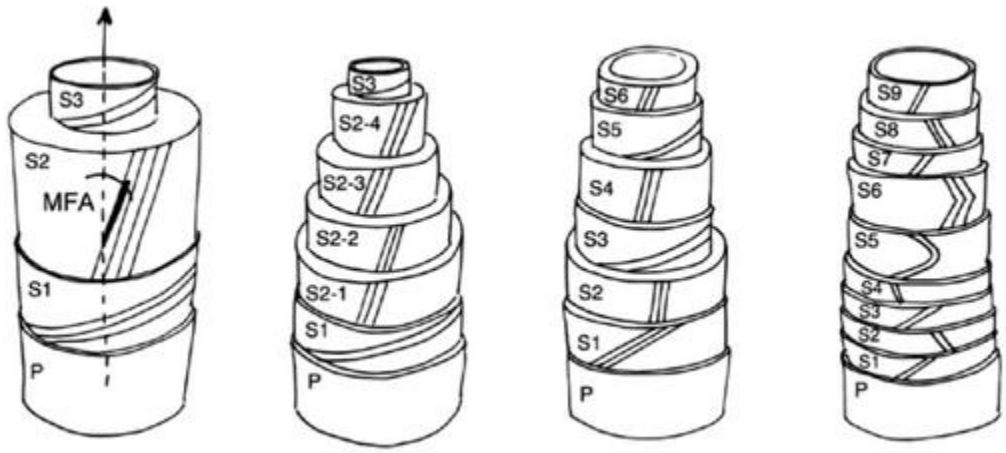


*Figure 2-4: Structures des fibres ultimes naturelles ; de gauche à droite : bois, libérienne, monocotylédone, graine[23]*

Toutes ces fibres ultimes sont formées de 3 composants.

- La première paroi, appelée paroi primaire (P), est produite par la cellule lors de sa croissance. Cette paroi ne joue pas un rôle prépondérant sur les caractéristiques mécaniques de la fibre, car elle doit demeurer souple pour suivre la croissance de la cellule [17].
- La paroi secondaire (S) est en revanche intimement liée aux propriétés mécaniques des fibres naturelles. Celle-ci possède une raideur élevée qui n'est pas compatible avec la croissance cellulaire, elle se développe donc une fois la croissance cellulaire terminée.
- Le lumen est l'espace central, ce volume vide correspond au volume occupé par la cellule avant plasmolyse (perte de l'eau et du matériel cellulaire).

L'organisation et la taille de ces trois éléments présentent des variations marquées entre les types de fibres ultimes telles que soulignées par la Figure 2-4.

Ainsi si l'on s'intéresse à la paroi S, on note que le nombre de sous-parois varie en fonction du type de fibres. On en dénombre généralement trois dans les fibres libériennes contre six pour les fibres issues des monocotylédones. La taille du lumen varie également. Les fibres issues des graines ont tendance à avoir des lumens plus larges que les fibres libériennes.

Ces variations de la structure impactent directement les propriétés mécaniques des fibres naturelles [10]. En effet, c'est principalement la sous-paroi secondaire dominante qui dicte le comportement mécanique de la fibre. Pour les fibres ultimes libériennes, c'est la

deuxième paroi secondaire (S2) qui domine avec une épaisseur 6 à 25 fois plus élevée que la paroi S1 [15], [24]. À l'inverse, les différences d'épaisseurs entre les couches S sont moins franches dans les fibres ultimes issues des graines et des monocotylédones.

Le comportement mécanique de la paroi secondaire est relié à l'angle microfibrillaire[10]. Il s'agit de l'angle formé entre les microfibrilles de cellulose et l'axe de révolution de la fibre. Plus cet angle est élevé, plus la paroi présentera un comportement ductile lors d'une mise sous contrainte axiale. Ce plateau d'écoulement est induit par le réalignement des microfibrilles sur l'axe de sollicitation. Les parois ayant un angle microfibrillaire faible présenteront un comportement bien plus fragile et élastique avec une rigidité plus élevée comme présenté dans la Figure 2-5 [12].

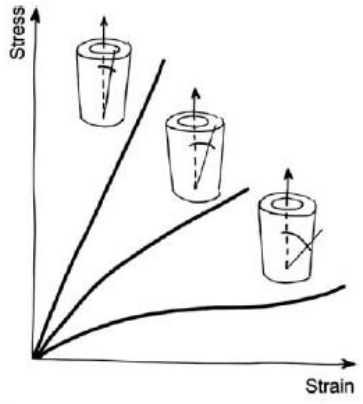


*Figure 2-5: Relation entre structure et propriétés mécaniques [23]*

Les propriétés mécaniques et donc les variations de celles-ci sont reliées directement aux variations qui ont lieu sur la paroi secondaire (structure, composition, taille, angle microfibrillaire) et qui dépendent de l'origine de la fibre naturelle.

### *2.2.1.4 Morphologie*

Comme évoqué précédemment, la variabilité des propriétés mécaniques des fibres naturelles peut s'expliquer par des différences fondamentales de structures et de composition de la paroi pectocellulosique. Cependant, ces différences ne permettent pas d'expliquer les variations morphologiques. La Table 2-2 démontre les différences de dimensions existantes entre les fibres libériennes de lin et celles issues des graines de l'asclépiade. La fibre d'asclépiade présente une longueur et un diamètre respectivement 4 et 28 fois plus faibles que les plus grandes fibres de lin.

*Table 2-2: Comparaison fibre technique (lin) et fibre ultime (asclépiade)*

| | Lin | Asclépiade |
|---|---|---|
| | 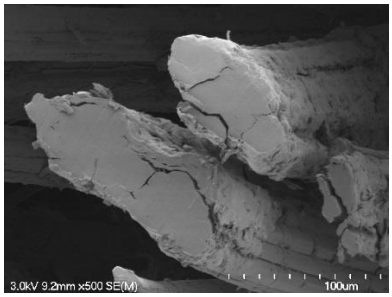  | 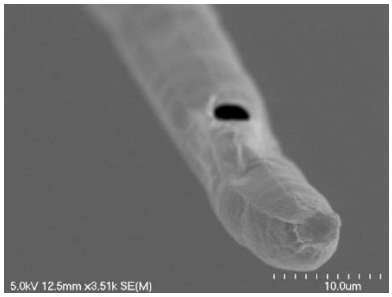  |
| Longueur (mm) | 4-80 [18] | 20 [25] |
| Diamètre (µm) | 40-620 [12] | 22 [25] |

Cette différence de taille est reliée à la notion de fibre ultime évoquée dans la section précédente. Toutes les fibres végétales sont constituées minimalement d'une fibre ultime. Les fibres naturelles issues des graines telles que la fibre de coton, de kapok ou d'asclépiade n'en sont composées que d'une. En revanche, les fibres libériennes sont issues de l'agglomération de plusieurs de ces fibres ultimes donnant ainsi une fibre plus épaisse et longue telle qu'illustrée dans la micrographie du lin dans la Table 2-2 (échelle 10 fois plus petite que pour la micrographie de l'asclépiade). Ce groupement de fibres ultimes, qui explique les différences morphologiques existantes parmi les fibres naturelles, amène à la notion de fibres naturelles techniques. Les fibres techniques sont plus volumineuses et généralement plus résistantes que les fibres ultimes grâce à l'agglomération de celles-ci.
Finalement, les notions de : fibre ultime, fibre technique, structure de paroi, angle microfibrillaire, microfibrille, cellulose et glucose qui permettent de décrire la structure et les variations des fibres naturelles peuvent être regroupées au sein du schéma présenté ci-dessous (Figure 2-6).

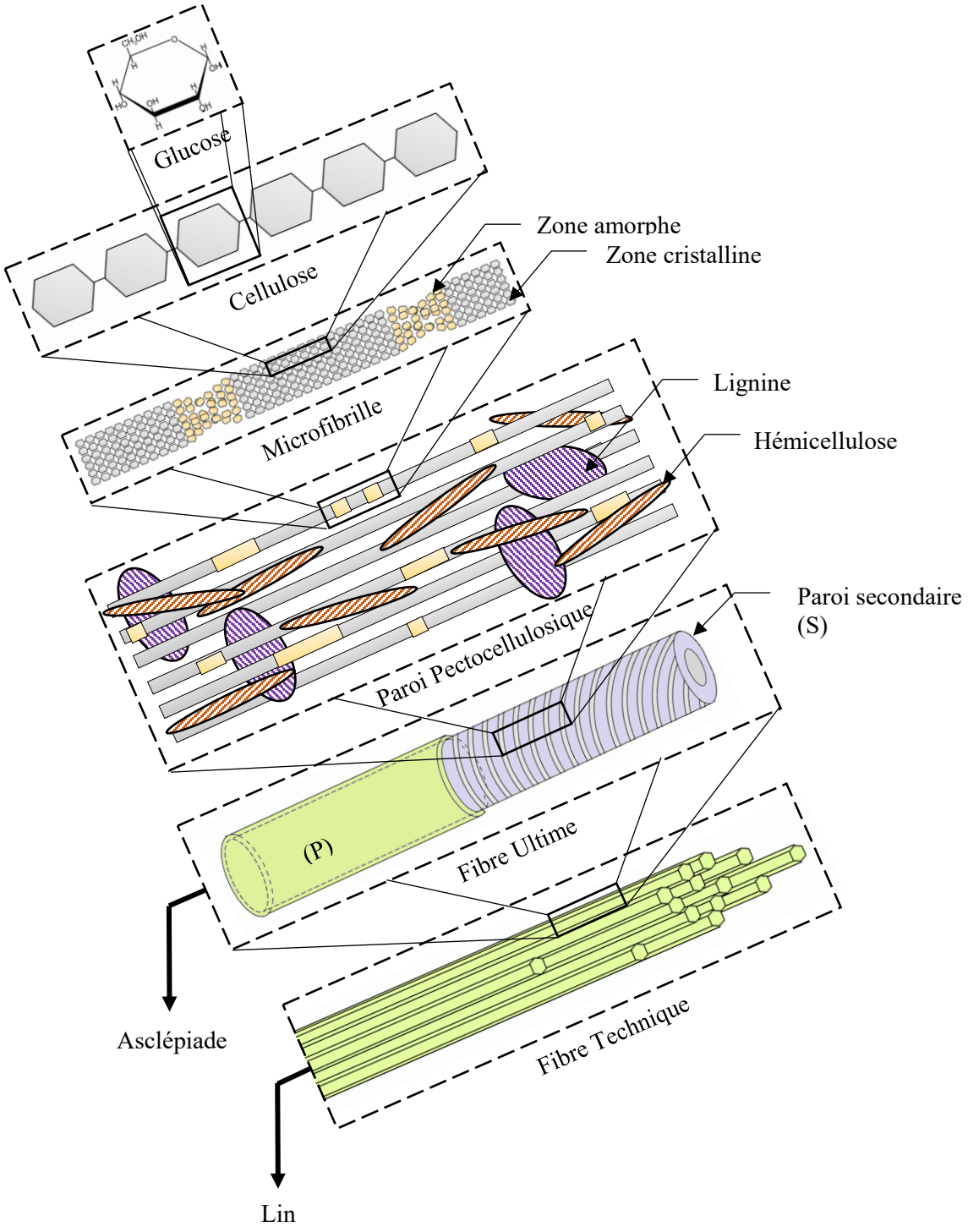


*Figure 2-6: Structure d'une fibre naturelle à partir du monomère de glucose*

### *2.2.1.5 Propriétés*

La popularité des fibres naturelles pour la production de composites est grandement liée à

leurs propriétés mécaniques, dont l'origine et la variabilité ont été vues précédemment. Comme le suggère la Table 2-3, ce sont principalement les fibres libériennes et les fibres de bois (fibres techniques) qui présentent les meilleures propriétés mécaniques. Leurs propriétés mécaniques spécifiques peuvent même surpasser celles de produits synthétiques comme la fibre de verre [26]. Ces fibres sont donc logiquement préférées pour la production de composites lorsque l'on recherche une amélioration des propriétés mécaniques par exemple.

*Table 2-3: Propriétés mécaniques de quelques fibres naturelles*

| | | Module d'Young (GPa) | Résistance à la traction (MPa) | Elongation (%) | Densité | Prix ($/kg) | Prix (k$/m3) |
|---|---|---|---|---|---|---|---|
| | Bois | 40[1] | 1000[1] | 1,5[1] | 0,4-1,4[6] | 0,25-0,3[3] | *0,1-1,8* |
| Graines | Coton | 5,5-12,6[2] | 287-597[2] | 2,0-10,0[2] | 1,5-1,6[2] | 1,8-5,1[2] | *2,7-8,2* |
| | *Milkweed* | *8,2*[4] | *296*[4] | *1,6*[4] | *0,68*[4] | 1,1-10[5] | *0,3-9,7* |
| Libériennes | Lin | 27-80[2] | 343-1035[2] | 2,7-3,2[2] | 1,4-1,5[2] | 2,5-12,7[2] | *3,6-19,1* |
| | Kenaf | 22-53[2] | 295-930[2] | 3,7-6,9[2] | 1,2-1,4[2] | 0,6-0,7[2] | *0,7-0,9* |
| | Chanvre | 3-90[2] | 580-1110[2] | 1,3-4,7[2] | 1,4-1,5[2] | 0,6-1,9[2] | *0,9-2,9* |
| | Ramie | 44-128[7] | 400-938[7] | 2.0-3.8[7] | 1.5[7] | - | - |
| | jute | 10-55[7] | 939-800[7] | 1.5-1.8[7] | 1.3-1.5[7] | - | - |

1 [14]
2 [27]
3 [28]
4 [29]
5 [30], [31]
6 [32]
7 [8]

De plus, il faut également noter que les fibres naturelles apportent certains avantages supplémentaires par rapport aux fibres industrielles. Parmi ces avantages, citons par exemple [6], [8], [10], [33]:

- Prix bas
- Recyclabilité
- Emprunte $CO_2$ faible
- Biodégradabilité
- Renouvelabilité
- Faible densité
- Bonne isolation thermique et phonique
- Non-abrasivité

Donc, avec des propriétés mécaniques sensiblement identiques, un coût plus faible et un impact environnemental diminué, les fibres naturelles peuvent surpasser les fibres

synthétiques. Elles ont donc naturellement trouvé leur place dans les secteurs du transport ou les notions de légèreté, absorption sonore et prix sont importantes.
Néanmoins certains freins demeurent à leur utilisation. Les fibres naturelles ne sont pas parfaites pour les matériaux composites car leur caractère hydrophile, leur instabilité dimensionnelle et leur biodégradabilité peuvent limiter leurs applications [8]. Si la biodégradabilité et l'absorption d'eau ne sont pas correctement gérées, la fibre peut se dégrader rapidement sous l'action des enzymes et champignons, ce qui limite leur emploi dans des applications extérieures [9]. De plus, les notions de qualité et de validation de produits sont plus difficiles à gérer par rapport à la régularité des fibres synthétiques.

### *2.2.2 Matrices*

Pour les applications de grande diffusion, les matrices thermoplastiques sont principalement privilégiées car elles sont moins toxiques, stockables dans le temps et se mettent en forme plus facilement [8]. Historiquement, les thermoplastiques de grande diffusion tels que le polyéthylène (PE) ou encore le polypropylène (PP) ont défini la carte standard des propriétés attendues par une matrice thermoplastique (i.e. capacité de production, prix, densité, module, résistance, ténacité…). L'industrie et les applications d'aujourd'hui se sont donc développées en fonction des capacités de ces matériaux synthétiques. Dès lors, les matrices et solutions plus durables émergentes comme l'acide polylactique (PLA), ou encore plus récemment les PE et PP biosourcés, doivent atteindre autant que possible ces propriétés standard pour devenir de réelles alternatives.

C'est dans la nécessité de ce réalignement que les fibres naturelles trouvent leur place. En effet, les fibres naturelles apparaissent comme une solution biosourcée et durable pour modifier certaines propriétés des matrices. De plus, une grande majorité des matrices thermoplastiques est employable avec des fibres naturelles. Leur mise en forme passe généralement par des températures relativement basses qui n'induisent pas de dégradation thermique aux fibres [23]. De manière générale, les fibres naturelles sont utilisées pour augmenter les propriétés mécaniques, diminuer la fraction de matière synthétique (donc le prix) et modifier les propriétés thermiques. Les raisons et les différentes opportunités que peuvent apporter les fibres naturelles aux matrices thermoplastiques sont discutées dans les

paragraphes suivants pour les matrices abordées dans les chapitres 4 à 6.

#### *2.2.2.1 Acide Polylactique*

Le PLA (Figure 2-7) est un polymère biosourcé qui peut se dégrader dans des conditions favorables. Il présente un faible impact environnemental, car il est issu de la polymérisation de l'acide lactique qui est produit par fermentation de sucres [34]. Le PLA est actuellement l'un des seuls bioplastiques biodégradables qui est à la fois produit à un niveau industriel (0,211 million de tonnes [35]) et qui présente une température de fusion basse (< 200 °C). La méthode de production du PLA et son rendement sont présentés à la Figure 2-8.
Sur le plan mécanique, le PLA semi-cristallin (PLLA) présente des propriétés comparables au PP pétrosourcé. Cependant, son utilisation est limitée par une fragilité très prononcée, une faible tenue en température imputable à sa température de transition vitreuse basse, et également par son prix [36].

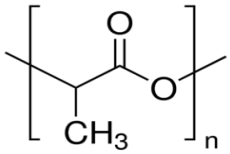


*Figure 2-7: Formule chimique du PLA*

Le renforcement du PLA par l'ajout de fibres naturelles est donc parfaitement justifiable. En effet, les fibres naturelles permettent de pallier nombre des faiblesses du PLA, notamment sa tenue en température. L'ajout de fibres de kenaf à hauteur de 70 % dans le PLA permet, par exemple, de maintenir le module de conservation jusqu'à des températures proches de 160°C [37]. Les fibres naturelles permettent également d'augmenter la ténacité. Une amélioration de plus de 300 % de celle-ci peut être atteinte avec une addition de 34 % massique de fibre de lin [38]. Également, l'addition de fibre permet de diminuer la proportion de PLA et donc le prix du produit sans compromettre son caractère durable (i.e. biosourcé et biodégradable).

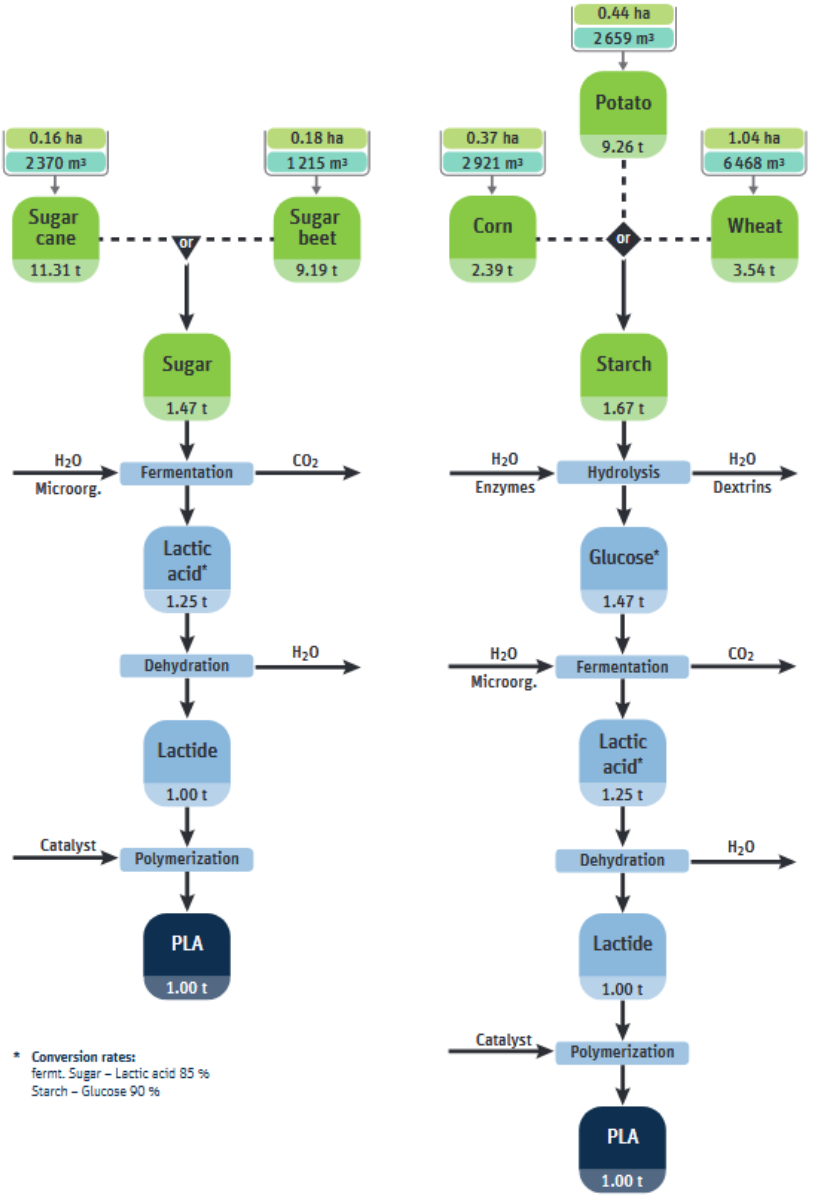


*Figure 2-8: Méthodes de production et rendement associé du PLA en fonction de la biomasse initiale[2]*

### *2.2.2.2 Polyamide 11*

Le polyamide 11 (PA11) (Figure 2-9) est un plastique organique biosourcé également (>98 % de carbone biosourcé), mais non biodégradable. Il est produit par polycondensation de l'acide aminoundecanoic extrait de l'huile de ricin [39]. La production mondiale de PA11 est comparable à celle du PLA et est estimée à 0.244 million de tonnes en 2017 [35]. La méthode de production du PA11 et la quantité d'huile de ricin à engager sont présentées à la Figure 2-10.

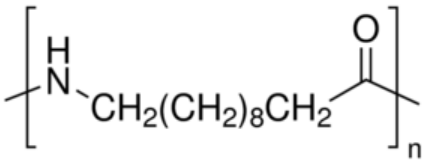

*Figure 2-9: Formule chimique du PA11*

Le PA11 est un des rares nylons à présenter une température de fusion faible (autour de 210 °C) qui n'induit donc pas de dégradation thermique aux fibres naturelles [39], [40]. Il présente également une très bonne résistance thermique, chimique, aux UV et à l'eau. Le PA11 est principalement utilisé dans des conditions d'utilisations sévères dans l'automobile ou dans les systèmes de canalisation de gaz naturel [40]. Outre les considérations environnementales, le PA11 demeure très peu compétitif face à un nylon conventionnel et pétrosourcé comme le PA6. En effet, le PA11 présente des propriétés mécaniques bien plus faibles pour un coût nettement plus élevé comme reporté dans la Table 2-4.

*Table 2-4: Propriétés mécaniques du PA6 et du PA11[41]*

| | PA 6 | PA 11 |
|---|---|---|
| Prix (CAD/kg) | 4,98 | 14,5 |
| Module d'élasticité (GPa) | 2,6 | 1,2 |
| Résistance maximum (MPa) | 86 | 57,2 |
| Allongement maximum (%) | 30-100 | 300-400 |

Cette différence au niveau des propriétés mécaniques est cependant compensable par l'addition de fibres naturelles. Le PA11 renforcé de fibres naturelles peut entrer en compétition, sur le pan mécanique, avec le PA6 grâce aux fibres. Comme dans le cas du PLA, les fibres induisent également une baisse du coût du matériau et ne suppriment pas le caractère biosourcé de celui-ci. L'addition de 50 % de fibre de bois brute (hêtre) dans le PA11 permet ainsi d'augmenter le module d'environ 260 % et la résistance de 20 %. L'ajout d'un traitement de surface permet de faire grimper ces améliorations à 290 % et 35 % respectivement [39].

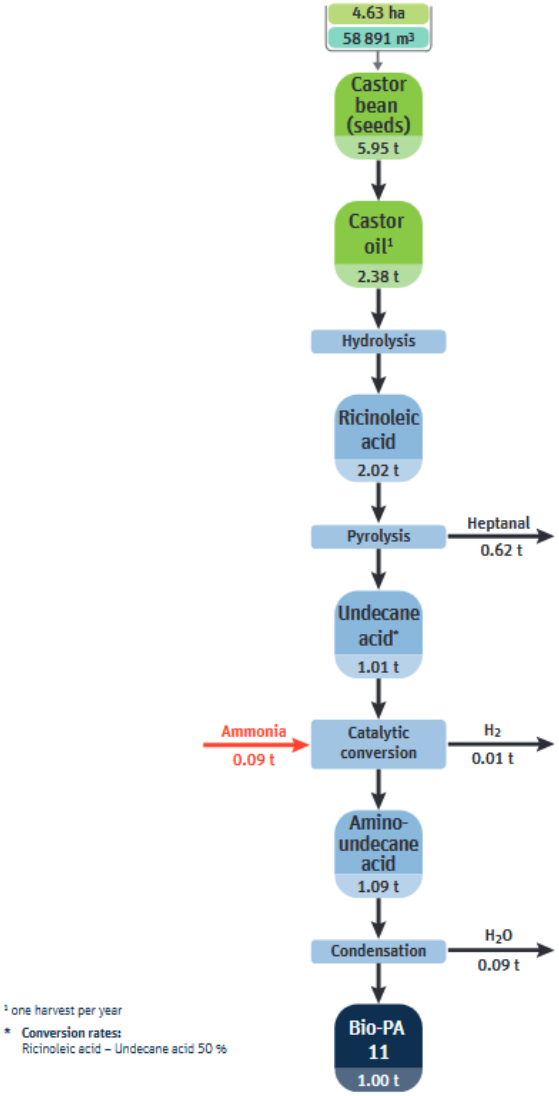


*Figure 2-10: Méthode de production du PA11[2]*

### *2.2.2.3 Polypropylène*

Le polypropylène (PP) est un plastique petrosourcé non biodégradable issu de la polymérisation du propylène (Figure 2-11). C'est l'un des plastiques le plus produits au monde avec une disponibilité d'environ 60 millions de tonnes en 2010 [42]. On retrouve le PP dans des applications allant de la simple fourniture de maison, jusqu'à des applications plus techniques pour l'automobile par exemple [43]. La très grande popularité du PP, par rapport aux autres matrices de grande diffusion, est notamment attribuable à ses nombreuses qualités telles qu'une bonne résistance à la fatigue, une bonne formabilité, un bon ratio module/densité et module/prix et un faible coût [43].

Le PP est une matrice qui pourrait devenir biosourcée dans un avenir proche. En effet, plusieurs entreprises devraient proposer des grades de PP biosourcés à horizon de 2020 [2], [44]. Également, le renforcement des lois environnementales devrait supporter une augmentation du taux de recyclage et donc de la disponibilité du PP recyclé [45], [46]. Les grades recyclés présentent généralement des propriétés mécaniques réduites dues à la dégradation des chaines polymériques, l'ajout de fibres naturelles pourrait donc pallier ces pertes [47]. Le renforcement du PP au moyen de fibres naturelles pourrait donc se justifier dans un avenir proche. Spinacé *et al.* ont ainsi démontré que l'ajout de 40 % massique de fibre d'ananas permet d'augmenter le module d'élasticité d'un PP recyclé de 75 % [48]. Néanmoins, les résultats démontrent une légère baisse de la résistance à la traction qui peut s'expliquer par un manque d'affinité au niveau de l'interface.

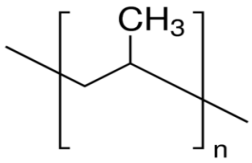


*Figure 2-11: Formule chimique du PP*

## *2.3 Propriétés*

Les propriétés des composites sont induites, en premier lieu, par le choix des fibres et de la matrice. Cependant, certains facteurs comme l'agglomération des fibres dans la matrice, les concentrations de contraintes aux extrémités des fibres, les interactions entre fibres, le taux de fibre ou encore l'orientation des fibres peuvent interférer sur les propriétés finales des composites[8], [49]. Parmi ces facteurs, la qualité de l'interface fibre/matrice est prépondérante.

### *2.3.1 Interface*

L'interface est un élément central d'un matériau composite. Elle peut être définie comme la région à 2 dimensions délimitant la fibre de la matrice qui modère toutes les interactions mécaniques, physiques ou encore chimiques entre les deux constituants. L'interface est à distinguer de l'interphase qui constitue une région à 3 dimensions (possédant une épaisseur) qui correspond à une zone de transition montrant des propriétés médianes entre les deux constituants non miscibles du composite.

De par son importance, l'étude de l'interface des composites est au centre de nombreux travaux. En effet, les propriétés finales du matériau composites sont intimement liées à la qualité de celle-ci [50]. Ainsi, pour augmenter les propriétés mécaniques, la qualité de l'adhésion fibre/matrice est souvent améliorée pour faciliter les transferts de charge de la matrice vers la fibre [9], [50]. À l'inverse, une baisse de l'affinité est souvent synonyme d'une augmentation de la résistance à l'impact [49].

#### *2.3.1.1 Longueur critique*

La qualité de l'interface influe sur les propriétés mécaniques des composites, car elle s'exprime directement sur la capacité des fibres à reprendre les contraintes. Comme souligné par la Figure 2-12, lors de la mise sous contrainte d'un composite, les fibres subissent un chargement qui varie linéairement suivant leur longueur. Par conséquent, les fibres se doivent d'avoir une certaine longueur minimale (longueur critique (Lc)) pour atteindre leur limite de résistance et donc être efficaces dans le renforcement de la matrice. Cette longueur critique dépend directement de la qualité de l'interface. Un transfert de faible qualité engendrera une mise sous contrainte difficile des fibres et donc une longueur critique élevée.

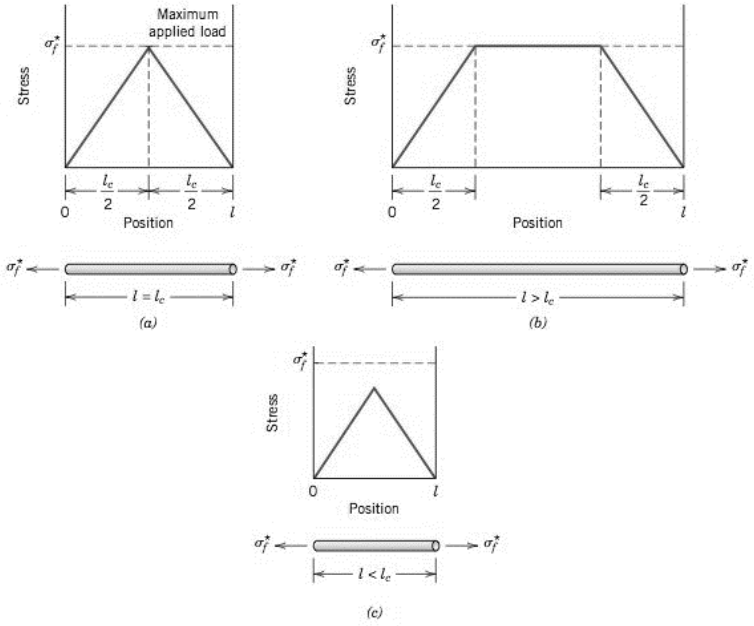


*Figure 2-12: Chargement d'une fibre dans un composite en fonction de sa longueur[51]*

La Lc des fibres dans une matrice peut être calculée en considérant les fibres comme purement élastiques, la matrice comme viscoélastique, et que le cisaillement de l'interface est limité par le cisaillement maximum de la matrice. Pour une fibre à géométrie cylindrique, les calculs amènent à la formule suivante (modèle de Kelly-Tyson) :

$$L_C = \frac{\sigma_{maxf}}{\tau_m} \times \frac{D}{2} \quad (1)$$

Avec D le diamètre de la fibre, $\tau_m$ le cisaillement maximum à l'interface qui peut être déterminé suivant les critères de Tresca ou de VonMises et $\sigma_{maxf}$ la contrainte maximale supportée par la fibre. Il apparaît nettement de cette équation que la Lc est inversement proportionnelle à $\tau_m$ et qu'elle dépend donc directement de la qualité de l'interface.

La connaissance de la Lc d'une fibre dans une matrice est un atout permettant de mesurer l'efficience du renforcement sur quelques propriétés du composite telles qu'illustrées dans la Figure 2-13 [49].

On constate ainsi que l'efficacité des fibres ($\eta_L$) est liée au rapport de la longueur des fibres à leur Lc. On considère généralement qu'une longueur de fibre au moins 5 fois supérieure à Lc permet d'obtenir un renforcement efficient de la part des fibres (88 %). De même, la connaissance de la Lc permet de connaitre la longueur optimale des fibres pour maximiser la ténacité des composites. Néanmoins, la relation à la Lc demeure complètement différente et il faut, dans ce cas, centrer au maximum la distribution des longueurs sur la valeur de la Lc.

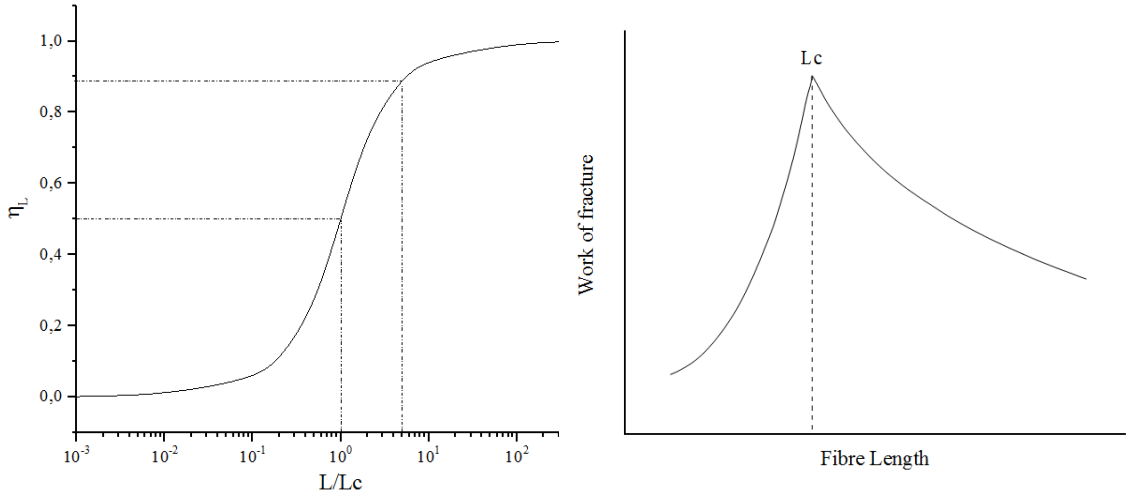


*Figure 2-13: Lien entre Lc et les propriétés mécaniques des composites*

### *2.3.2 Prédiction*

Les propriétés des composites peuvent être bornées de manière grossière par la loi des mélanges exprimée en série ou en parallèle. Cependant, cette règle n'est valable qu'à condition de considérer que les fibres et les matrices sont parfaitement élastiques, la dispersion des fibres est homogène, l'adhésion est parfaite au niveau de l'interface et qu'il y a une absence totale de vide dans le composite [52]. En réalité, ces conditions ne sont jamais rencontrées dans les composites. Ainsi, la loi des mélanges est souvent modifiée pour tenir compte des paramètres qui diminuent l'effet renforçant des fibres [49]. Les nombreux modèles qui permettent une prédiction plus fidèle des propriétés des composites (Bowyer-Bader, Cox, Cox-Krenchel, Kelly-Tyson) introduisent des paramètres d'efficacité relatifs à la longueur et l'orientation des fibres [53]. Par exemple, la règle des mélanges suivant le modèle de Kelly-Tyson peut s'écrire de la manière suivante :

$$\sigma_c = \eta_0 \eta_L V_f \sigma_f + V_m \sigma'_m \quad (2)$$

$\sigma'_m$ représente ici la contrainte supportée par la matrice pour une déformation équivalente au maximum admissible par la fibre en considérant une rupture du composite lorsque la fibre rompt. Dans cette relation, les facteurs $\eta_0$ et $\eta_L$ reflètent l'influence de l'orientation et de la longueur des fibres, respectivement. Ces deux facteurs qui varient chacun entre 1 et 0, pondèrent l'effet des fibres sur les propriétés mécaniques finales des composites. D'autres modèles plus complexes se proposent de prendre en compte la porosité, le taux d'humidité dans les fibres naturelles, le diamètre ou encore la courbure des fibres dans la détermination des propriétés mécaniques des composites [53].

#### *2.3.2.1 Facteur d'efficacité de l'orientation des fibres*

Le facteur d'orientation des fibres ($\eta_0$) peut être calculé en admettant que la fibre et la matrice subissent une déformation identique de la manière suivante [49]:

$$\eta_0 = \sum_n a_n \times \cos\theta_n{}^4 \qquad \sum_n a_n = 1 \tag{3}$$

Avec $a_n$ qui représente la proportion de fibre ayant un angle $\theta_n$ avec l'axe de sollicitation. Le calcul montre que pour un composite ayant des fibres parfaitement alignées ($a_n = 1$, $\theta_n = 0°$) $\eta_0$ tend vers 1 alors que celui-ci tend vers 0 pour des fibres perpendiculaires ($a_n = 1$, $\theta_n = 90°$). Ainsi pour des fibres perpendiculaires l'effet renforçant des fibres est nul. Dépendamment des choix de la technique de mise en forme, de la forme du moule, le facteur d'orientation et donc le renforcement induit par les fibres fluctuent. Le calcul amène à une valeur de 3/8 pour des composites ayant des fibres dispersées de manière parfaitement aléatoire. En réalité, dans le cas de l'injection ou l'extrusion, la distribution des orientations n'est pas parfaitement aléatoire. La valeur de $\eta_0$ est totalement dépendante de l'axe de sollicitation de la pièce comme illustrée par la Figure 2-14.

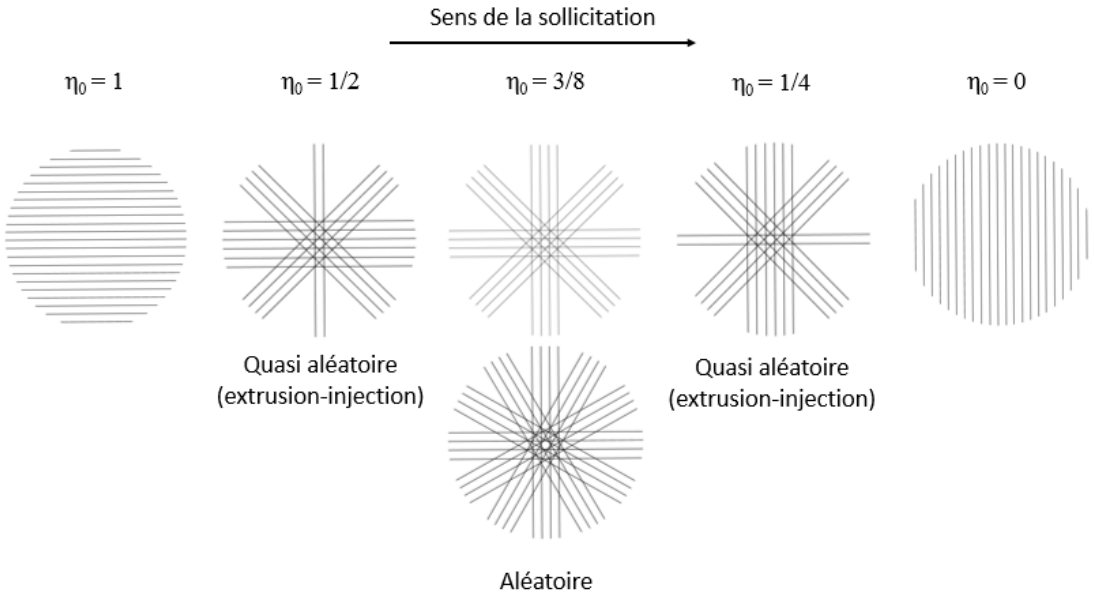


*Figure 2-14: Valeurs du facteur d'orientation des fibres pour quelques configurations*

### *2.3.2.2 Facteur d'efficacité de la longueur des fibres*

Le facteur de longueur ($\eta_L$) dépend de la distribution des longueurs des fibres par rapport à la Lc qui dépend elle-même principalement de la qualité de l'interface comme discuté

précédemment. Le facteur de longueur peut être calculé théoriquement suivant l'équation suivante (modèle de Kelly-Tyson)[49], [54], [55]:

$$\eta_L = \frac{1}{V_f}\left[\sum_i \frac{L_i V_i}{2L_c} + \sum_j V_j\left(1 - \frac{L_c}{2L_j}\right)\right] \quad (4)$$

*Sub-critique* *Super-critique*

L'équation distingue le renforcement induit par les fibres ayant une longueur sub-critique et super-critique (i.e. ayant une longueur respectivement inférieure ou supérieure à leur Lc). Le premier terme est relié aux fibres sub-critiques. La contrainte maximum admissible dans celles-ci dépend directement de la taille de l'interface et donc de leurs longueurs ($L_i$). $V_i$ représente le volume de fibre ayant une longueur $L_i$ strictement inférieur à Lc. Le deuxième terme de l'addition est associé aux fibres ayant une longueur super-critique. $V_j$ représente le volume de fibre ayant une longueur $L_j$ supérieure ou égale à Lc. Bien que la longueur soit supérieure à Lc et donc que le maximum de résistance puisse être atteint, la valeur de résistance maximum à la traction des fibres n'est pas considérée. En effet, la variation linéaire de contrainte depuis l'extrémité des fibres induit une contrainte moyenne supportée inférieure à la résistance maximum.

Il est à noter que la détermination de $\eta_L$ pour le modèle de Cox ou Cox-Krenchel demeure différente et se base sur le modèle de décalage du cisaillement à l'interface [53].

## *2.4 Optimisation*

Pour une amélioration des propriétés mécaniques, on cherche donc souvent à maximiser $\eta_0$ et $\eta_L$. Cependant le facteur $\eta_0$ n'admet que peu de latitude et est principalement induit par les choix relatifs à la mise en forme des pièces. À l'inverse, le facteur $\eta_L$ est beaucoup plus variable et est liée au rapport L/Lc. La maximisation de $\eta_L$ et donc du rapport L/Lc peut être effectué de deux manières différentes comme illustrées par la Figure 2-15 :

(i) L/Lc peut être augmenté en diminuant la valeur de la longueur critique par amélioration du transfert de charge à l'interface (traitement de surface).

(ii) L/Lc peut être augmenté en augmentant la longueur des fibres dans le composite (influence de la mise en forme).

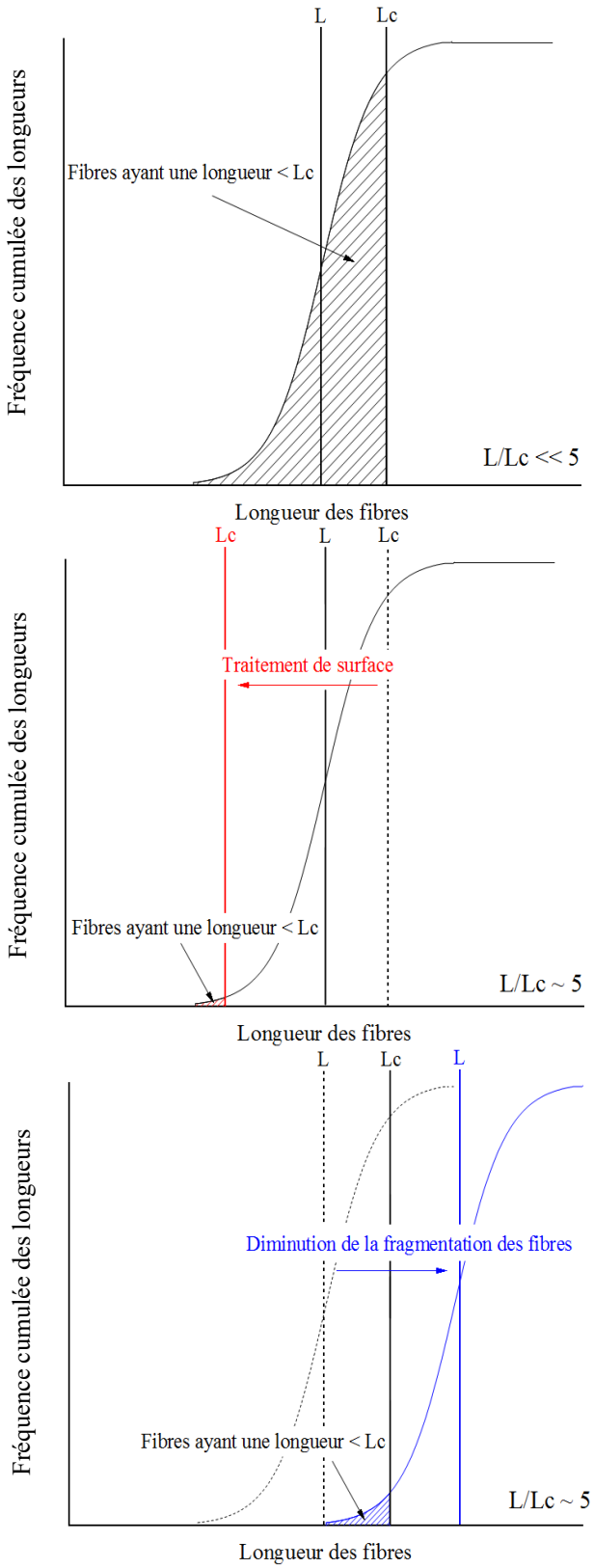


*Figure 2-15: Effet d'un traitement de surface (rouge) ou d'une augmentation de la longueur des fibres (bleu) sur la proportion de fibres n'atteignant pas Lc*

### *2.4.1 Traitement de surface*

Le traitement de surface des fibres permet de rendre efficiente une association matrice/renfort judicieuse ne présentant pas une bonne affinité naturelle.

Dans le cas du couple fibres naturelles et matrices thermoplastiques, les interfaces présentent généralement une très faible affinité naturelle qui s'explique par la différence d'hydrophilicité et de polarité entre les fibres et les matrices[9], [10], [56]. Les fibres naturelles ont tendance à être hydrophiles et polaires quand les matrices organiques présentent des propriétés hydrophobes et apolaires. Les gains théoriquement attendus sur les propriétés mécaniques des composites dévient donc souvent des résultats expérimentaux du fait de cette faible adhésion qui limite grandement la reprise de contrainte par les fibres.

Il existe plusieurs types de traitements applicables aux fibres naturelles, le chapitre 5 se penche exclusivement sur l'application de deux traitements de surface (traitement alcalin et silanisation) sur la fibre d'asclépiade et sur ses conséquences sur les propriétés du composite. Les deux solutions étudiées au chapitre 5 font appel à des mécanismes différents. Les traitements de surface peuvent induire une modification de la fibre permettant une meilleure affinité. Ils peuvent également constituer en l'addition d'une molécule médiatrice capable d'effectuer des liaisons avec les deux composants.

Les paragraphes suivants présentent les traitements les plus communs pour les fibres naturelles. Parmi les solutions populaires non abordées dans ce chapitre, citons par exemple : le greffage de monomère, l'acétylation, l'éthérification ou encore le recours aux isocyanates [10].

#### *2.4.1.1 Mercerisation*

La mercerisation ou traitement alcalin est un traitement de surface utilisant de la soude (NaOH). Ce traitement est à la fois très efficace et économique sur les fibres naturelles. Le traitement a pour effet de retirer une partie des lignines, hémicelluloses, et autres composés tels que les graisses et les cires qui gainent la fibre et limitent l'efficience de l'interface[10]. La mercerisation permet également d'exposer les microfibrilles de cellulose et d'augmenter la rugosité de surface comme illustrée dans la Figure 2-16. Le traitement amène également en finalité à une augmentation du nombre de sites pouvant amener un

blocage mécanique. L'interpénétration de la fibre et de la matrice conduit à une meilleure adhésion et un meilleur transfert de contrainte [5], [10]. Le traitement alcalin permet donc, en théorie, d'améliorer l'interface fibres/matrice indépendamment de la nature de la matrice.

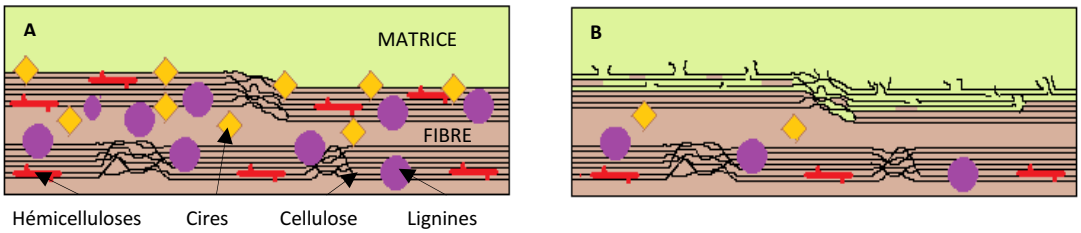


*Figure 2-16: Effet du traitement alcalin sur une fibre naturelle (A) fibre non traitée (B) fibre traitée*

Le traitement alcalin modifie la fibre et doit être contrôlé. La concentration de la solution, la température et le temps de traitement doivent être maitrisés. Un traitement trop fort pourrait conduire à une dépolymérisation de la cellulose et une délignification excessive. Un traitement excessif conduirait donc à une perte des propriétés mécaniques de la fibre et à fortiori des composites [5].

### *2.4.1.2 Silanisation*

Contrairement à la mercerisation, la silanisation n'entraine pas de modification structurale de la fibre. L'utilisation de silanols du type R-$(CH)_n$-$SI(OH)_3$ ayant un n comprit entre (0-3) permet d'augmenter les propriétés mécaniques des composites par augmentation de la qualité de l'interface. Les groupements alcool vont réagir avec les hydroxyles présents en surface de la fibre pour former une liaison covalente. Les silanols peuvent également réagir entre eux afin de former une couche de polysiloxane en surface (voir Figure 2-17) [57]. À l'autre extrémité de la chaine carbonée du silanol, la fonction organique (R) est ajustée en fonction des besoins pour la matrice. Par exemple, l'utilisation d'une fonction époxyde permet une réaction avec les groupements acides en bout de chaine du PLA [58].

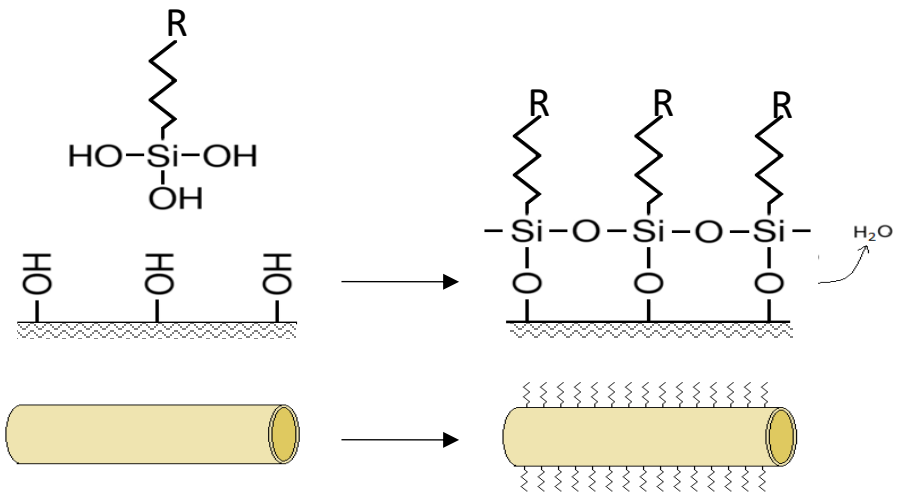


*Figure 2-17: Greffage de silanols sur une fibre naturelle*

Contrairement au traitement alcalin, la silanisation n'engendre pas de modifications de la structure de la fibre. L'ajout de molécules en surface augmente la résistance thermique des fibres [59]. Des études tendent à prouver que le traitement de silanisation des fibres naturelles tend à être plus efficace pour l'amélioration des propriétés mécaniques des composites que le traitement alcalin [59]. En revanche, la combinaison mercerisation suivie d'une silanisation diminue les propriétés mécaniques des composites [60].

### *2.4.1.3 Anhydride maléique*

L'anhydride maléique présente une similarité avec l'utilisation des silanols dans le sens où il est capable d'effectuer des liaisons à la fois avec la matrice et la fibre. L'anhydride maléique est un agent de couplage fortement utilisé sur fibres naturelles dans les matrices thermoplastiques [59]. Il peut être greffé directement sur les chaînes carbonées du PP ou encore du PLA afin d'augmenter les interactions fibres/matrice et limiter les dégradations de la fibre [61]. La Figure 2-18 présente le mécanisme de liaison de l'anhydride maléique greffé sur du polypropylène avec la fibre.

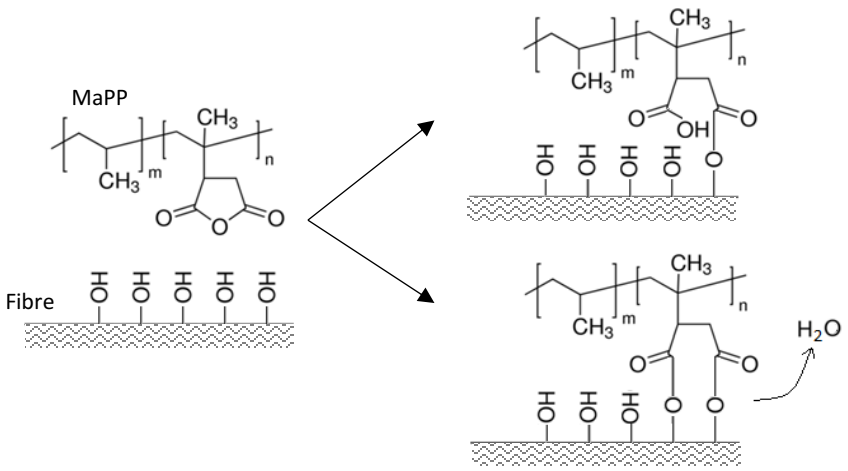


*Figure 2-18: Mode de réaction du MAPP sur une fibre cellulosique*

La fonction anhydride va réagir avec les groupements hydroxyles présents en surface des fibres pour former une ou deux liaisons covalentes [59]. L'utilisation d'anhydride maléique reste cependant délicate, le temps nécessaire à la réaction durant la mise en forme peut entrer en compétition avec des phénomènes de dégradation thermique des fibres dans certains cas.

### *2.4.2 Mise en Forme*

Les polymères thermoplastiques renforcés de fibres naturelles courtes ne nécessitent pas de moyens de mises en forme atypiques. Les techniques conventionnelles d'extrusion et d'injection peuvent être appliquées. Néanmoins, la mise en forme est une étape cruciale pour le composite, car elle possède une influence significative sur la longueur et l'orientation finale des fibres et donc sur les propriétés du composite [8], [52]. Cette influence s'exprime à travers les valeurs des facteurs $\eta_0$ pour l'orientation et $\eta_L$ pour la longueur, abordés précédemment.

La création du composite passe généralement par une étape d'extrusion (simple ou bi-vis) présentée en Figure 2-19. Cette étape consiste à insérer les fibres dans la matrice fondue et assurer leur dispersion. L'extrusion produit en finalité des granules (ou pellets) homogènes qui peuvent être ensuite utilisés en injection ou à nouveau en extrusion pour obtenir un produit fini renforcé [49]. À cause de l'orientation quasi aléatoire des fibres, le volume de fibre admissible dans la matrice demeure limité. Si l'on souhaite augmenter le ratio de

fibres, il faut se tourner vers l'enrobage de fibres (sous forme de bobine suivie de pelletisation) [49].

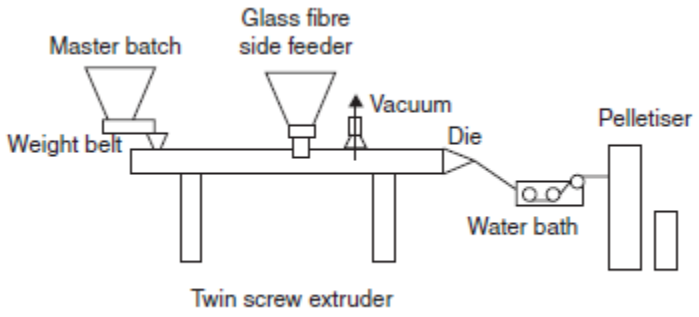


*Figure 2-19: Production de pellets de composite à fibres courtes*

### *2.4.2.1 Longueur des fibres*

De nombreux paramètres d'extrusion possèdent un impact sur la distribution des longueurs. De manière générale, on tend toujours, à diminuer la vitesse de rotation des vis de l'extrudeuse, augmenter la température au point d'insertion des fibres et limiter le parcours des fibres pour maximiser la longueur des fibres et donc le $\eta_L$ [49], [62], [63]. Le profil de la vis et notamment la présence d'éléments de mélange sont également responsables de la diminution de la longueur des fibres.

Les amplitudes admissibles sur ces paramètres restent cependant très limitées. La baisse de la vitesse de rotation de la vis est directement concurrente de la cadence de production. Il faut donc sur ce point établir un compromis entre les propriétés mécaniques du composite et son coût de production. L'augmentation de la température au point d'addition des fibres est limitée par la dégradation thermique de la matrice ou des fibres. Enfin, le parcours de fibres ou encore la présence d'éléments de mélange sur la vis sont reliés aux caractéristiques techniques de l'équipement de production.

### *2.4.2.2 Orientation*

La longueur moyenne des fibres n'est pas le seul facteur contrôlé par la mise en forme qui possède un impact notoire sur les propriétés mécaniques du composite. Alors que la longueur des fibres est impactée par les paramètres de mise en forme lors de toutes les

étapes de transformation, l'orientation n'est reliée qu'à la mise en forme du produit fini. Cette orientation des fibres dans le composite est principalement liée à l'écoulement du matériau dans la filière d'extrusion ou le moule d'injection. Les fibres auront tendance à s'aligner avec le sens d'écoulement du flux sur la couche externe de la pièce à cause du cisaillement important dans cette zone. À l'inverse, les flux divergents qui apparaissent suite à une augmentation de section par exemple peuvent amener à un alignement transversal des fibres, réduisant ainsi les propriétés mécaniques du composite dans cette zone [64]. Néanmoins, la géométrie du moule ou de la filière n'est pas le seul paramètre à considérer, la température du mélange ou encore la vitesse d'injection ont montré un effet sur l'orientation des fibres [49], [63].

# CHAPITRE 3 : FIBRES CREUSES – CARACTÉRISATIONS ET APPLICATIONS INDUSTRIELLES

***Auteurs et affiliation :***

- *Mathieu Robert : Professeur, Université de Sherbrooke, Faculté de génie, Département de génie civil*
- *Ovlaque Pierre : Étudiant au doctorat, Université de Sherbrooke, Faculté de génie, Département de génie civil.*
- *Mohammadreza Foruzanmehr : Coordinateur scientifique, Université de Sherbrooke, Faculté de génie, Département de génie civil.*

***Date d'acceptation:*** *1 juin 2018*

***Etat de l'acceptation:*** *Version finale publiée*

***Livre:*** *Chemistry of Lignocellulosics: Current Trends*

**Référence:** *M. Robert, P. Ovlaque, and M. R. Foruzanmehr, "Hollow Floss Fibers Characterization and Potential Industrial Applications," in Chemistry of Lignocellulosics: Current Trends, CRC Press, 2018, p. 516.*

## *3.1 Résumé*

L'importance de limiter la pollution de l'environnement a attiré l'attention de nombreux ingénieurs vers la recherche de nouvelles solutions telles que la substitution des matières premières synthétiques par des matières premières naturelles. Ainsi, des efforts importants sont faits pour trouver des applications à de nouvelles sources de fibres naturelles plutôt que d'utiliser les fibres synthétiques petrosourcées. Parmi les variétés de fibres naturelles connues ou redécouvertes, l'asclépiade est classée comme une fibre de substitution polyvalente aux nombreuses propriétés uniques, qui sont principalement attribuées à sa structure creuse. En effet, la présence d'un large lumen le long de la fibre induit une faible densité et de bonnes propriétés d'isolation. En raison des caractéristiques atypiques et des avantages écologiques induits par les fibres naturelles, de nombreuses applications ont pu être envisagées avec les fibres d'asclépiade.

Le présent chapitre regroupe les informations disponibles dans la littérature concernant les caractéristiques, propriétés et applications potentielles des fibres creuses.

## *3.2 Abstract*

Importance of solving the environmental pollution has attracted many designers and engineers' attentions towards finding different available solutions such as substituting polymer-based raw materials with the natural ones. Thus, significant efforts are made to find new resources of natural fibers instead of using the petroleum-based synthetic fibers. Among the variety of newly known natural resources, Milkweed is categorized as a versatile substitutive fiber with numerous unique properties, which are mainly attributed to their hollowness structures. The presence of hollow channel along the fiber length is responsible for their lightweight and good insulation properties. Because of the fibers' ecological and chemical advantages, numerous technical application fields could be considered for the eco-friendly and non-allergenic textiles made of Milkweed fibers especially in production of medical goods. Since morphological aspects as well as physical and mechanical properties of the Milkweed fibers significantly affect their functional behavior during their end uses, we are summarizing here the available information regarding the fibers' characteristics and properties. Having fundamental knowledge about the spin-ability of Milkweed fibers as well as finding the optimized process condition for their carding operation is essential for obtaining the textile products with desired properties.

## *3.3 Introduction*

The availability and the environmentally friendly nature of renewable materials have caught researchers' and industries' attention. Among the renewable materials, natural fibers do not only have good properties (lightweight, high strength), but are also fairly cheap and available when they are extracted from the remnant of the harvest. For instance, in western Canada over 600,000 to 800,000 hectares grow oilseed flax. This can potentially produce 2,000 kg/ha of flax straw annually. Currently, overall more than 75% of this amount is usually burnt or thrown away [65]. The industrial use of these materials can also promote sustainable agriculture that is the principal element of sustainable development [66], [67].

Another way to promote sustainable agriculture is promoting technologies and markets for vernacular natural fibers. By doing so, local farmers find the motivation to breed these

fibers. This can mitigate the social and economic problems of small agriculture, and reduce environmental impacts by providing renewable materials [68].

Cellulosic natural fibers can be obtained from various parts of plants, such as leaf, fruit, bast, and seed. Among them bast fibers (like flax) and seed fibers (like cotton) are more conventional [69]. The geometrical dimensions of these fibers as well as their properties depend on where the fibers are extracted. For example, fibers from seeds are shorter than fibers from stems and leaves (few centimeters versus meter). Moreover, fiber extraction from stem is time consuming and leads to heterogeneous fibers in comparison with seed fibers [70].

Some of the seed fibers (floss fibers) are hollow, as is the case with kapok, akund, and Milkweed. These fibers have an extremely wide lumen and very thin wall. In fact, they are supposed to disperse grains for germination. This special hollow structure makes these fibers lightweight and therefore it provides plenty of opportunities for creation of low-density and insulating materials.

Among the hollow floss fibers, Milkweed (*Asclepias syriaca*) is a valuable fiber because it is easy to grow and it can be harvested twice a year [71]. Milkweed is native to Northwest of North America. This territory includes the area within 35˚-50˚ latitude north (N) and 60˚-103˚ longitude west (W). In other words, the region is encircled by a line passes from New Brunswick to Virginia to Tennessee, then through Kansas to Manitoba [72].

The scientists have been interested in using Milkweed for more than a century. Milkweed has potentials of use in a variety of applications such as textile industry, composite manufacturing, paper production, oil absorbent, and thermal and sound insulation.

## *3.4 Histrory of hollow fibers*

Hollow seed fibers such as produced by members of the family of Apocynaceae have had numerous well-known applications for centuries. These plants have been used in interesting applications including textiles and medicinal [73].

*Calotropis procera* fibers were used during the 11$^{th}$ century in the former “Bilad al Sudan” empire in western Africa for fireproof textiles [74]. According to the Bulletin of Miscellaneous Information of the Royal Botanic Gardens, *Calotropis gigantea* fibers were used as stuffing materials for pillows fresh cushions in India. There are also some evidences

in the report of exploration of Ganges River by Fitch, which indicate the use of hollow fibers for clothing in 1585. Europeans also used to spin *Calotropis gigantea* fibers, though the spinning difficulties and the insufficient source of fibers caused the complete decline of these fibers uses [73]. In the meantime, *Asclepias syriaca* hollow fibers were used in North America by the Amerindian tribes in numerous applications [75]. The Amerindians transferred the knowledge of using the hollow fibers to French settlers after they started to colonize North America. The book "Traités des asclepiades" described the interest of the former French monarchy for developing an industry to exploit these fibers [76]. Even the King of France Louis XV started to use the fibers for his personal winter dressings [75]. However, these activities were discontinued by late 18$^{th}$ century as the British Empire concurred French colony in North America. In that era, the British Empire had a strong domination on the business of cotton and silk. Hence, they considered *Asclepias syriaca* as a threat for their business and hence choked the rising economy based on these fibers.

The Second World War (WWII) is an important milestone in the history of hollow floss Fibers. Since there was no technology to fabricate low-density synthetic fibers, hollow kapok fibers became ideal filler materials for life jackets [7]. During WWII Japan invaded the countries in southern Asia, which supplied kapok fibers and consequently, the US navy was forced to find an alternative for kapok fibers. Therefore, the neglected milkweed floss fibers were again harvested in a large quantity to compensate for the lack of kapok supply and sustain the life jacket industry [77]. The change in demand for Milkweed fibers due to the end of the WWII and the advent of new synthetic fibers diminished again the demand and the application of Milkweed fibers fell into oblivion.

Nowadays hollow fiber properties and functions are progressively rediscovered. In North America and especially in Canada the crop growing of *Asclepias syriaca* has started and led to the formation of private sectors which are able to process fibers for various applications [78]. This on the one hand encourages the local farmers to take advantage of growing more economic crops with higher benefits, and on the other hand, it paves the way for communities to achieve sustainable development [79].

## *3.5 Plant species*

Huge variety of plants produce hollow fibers with very similar morphologies. Although they all exhibit hollow morphologies, they have slightly different structures and are produced by different species. Moreover, as it was previously noted, these plants grow all around the world. If the members of Apocynaceae family are classified by the plant morphological characteristics, it will lead to the formation of a huge list consisting of 280 genera and 2000 species [29]. It is not possible to describe all species and thus, the most common ones that are found in the literature will be discussed in this work.

### *3.5.1 Kapok*

Generally, wild weeds or bushes produce the hollow fibers. However, kapok is the only one that is produced by trees. Kapok trees (*Ceiba pentandra*) produce kapok hollow fibers. The trees have various names such as silk-cotton tree, Ceiba and many other indigenous names. Kapok growing area extends from all sub-tropical zones of America, Africa and Asia [7]. The trees can reach a height of 45 meters and a diameter of 2 meters. There is no need to cut down the tree in order to harvest the fibers. The fibers are contained in pods and the pods can be harvested directly from the tree branches. Kapok is the most readily available hollow fiber; Almost 99 000 tons of kapok fibers were harvested in 2013 [7].

*Figure 3-1: Kapok fibers[7]*

### *3.5.2 Milkweed*

Hollow fibers produced by weeds are often known as milkweed fibers. However, other names such as Akund or Estabragh are frequently used according to the location where the plants grow. Figure 3-2 shows the common names and corresponding regions. For instance, Estabragh is a Persian name for a hollow fiber producing plant, which grows in Iran. A similar plant also grows in China, which is called Akund.

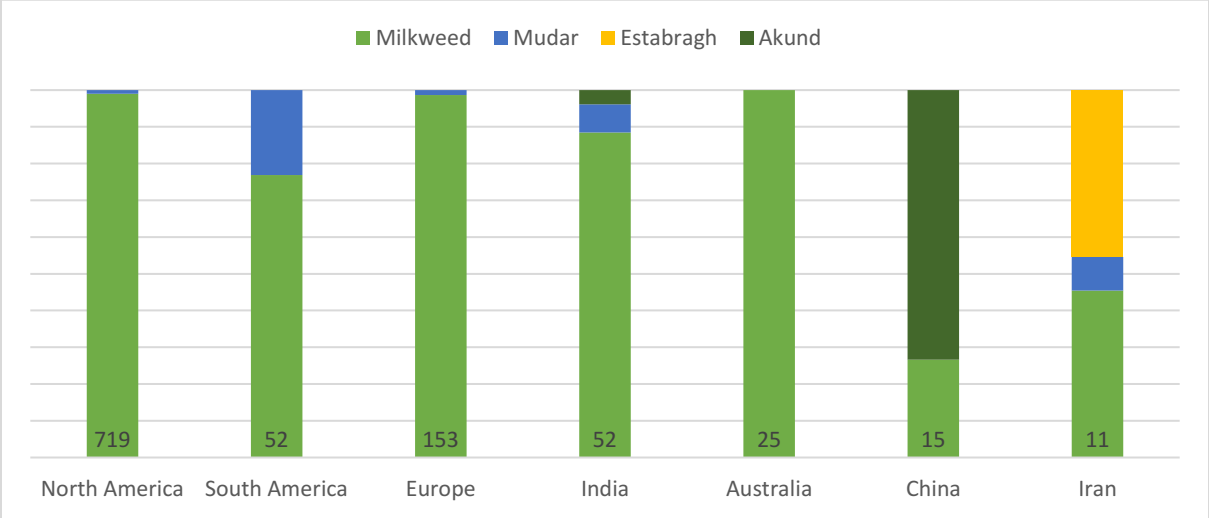


*Figure 3-2: Common names of hollow fibers used in scientific papers regarding the country of origin and the number of publications*

Figure 3-3 depicts different subcategories of hollow fibers with corresponding family, genus, and species names. Among them, the aak fibers belong exclusively to the *Calotropis procera* genus. Akund and Mudar belong to the *Calotropis procera* and *C. gigantea* genus in literature and milkweed is a common name for any species. Concerning the Persian term Estabragh, only Gharehaghaji and Davoodi have indicated a species (*Asclepias procerais*) which has also been used to designate the *Calotropis procera* species [80].

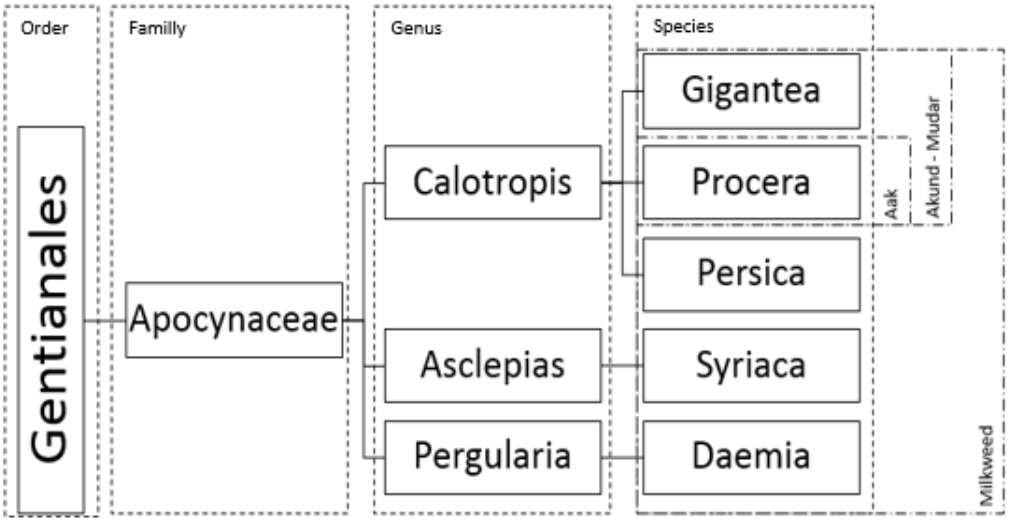


*Figure 3-3: Apocynaceae family and common names*

*Asclepias Syriaca*

This species is also called common milkweed, as it is similar to a small wild weed producing a white sap. The plant can reach up two meters in height and it grows mainly in the eastern part of northern America continent according to the USDA plant database. The *Asclepias syriaca* species has small branches with opposite oval leaves. The flowering of this species occurs during summer and floss fibers are ready to harvest at the end of September [81], [82].

*Figure 3-4: Asclepias syriaca Plant and fibers*

*Calotropis Procera* and *C. Gigantea*

The species *C.procera* can be found in North Africa and Middle East. *C.procera* has been successfully introduced in semi-arid area such as California and Australia

[72]. These species are frequently found in the region surrounded by India, China, and Philippines. Unlike *Asclepias syriaca*, *Calotropis procera* and *C. gigantea* can develop large shrubs with three meters high stems and 25cm diameter [29]. Both *Calotropis* species produce fruits that contain the floss fibers. Fruit development on shrubs are mainly occurring during hot seasons.

*Figure 3-5: Mudar shrub [29]*

## *3.6 Hollow floss fibers*

### *3.6.1 Fibers's morphology*

Unlike common natural fibers such as flax fibers, which have no lumen (a central hollow cavity in the fibers) or a tiny one, hollow floss fibers possess an enormously wide one. The lumen can form 77% of the volume of the fiber and create a particular morphology in comparison with the common natural fibers [83].

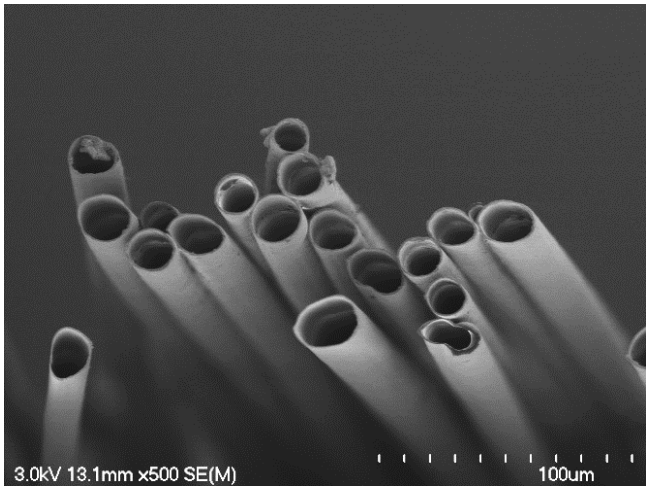


*Figure 3-6: Asclepias syriaca floss fibers*

Another particular structural feature of hollow floss fibers is the thin cellulosic cell wall of these fibers (see Figure 3-6). Normally, the natural fibers are plant cells that grow together and form the fiber bundles. The plant cells consist of a large central vacuole (i.e. a micro-organelle filled with water) which is engulfed by a cell wall (composed of cellulose, hemicelluloses, pectin and lignin). When the cell dies the membrane of vacuole is broken down so the cell loses its content except for its skeletal part, which is the cell wall. In fact, the lumen is empty space of the lost cell content and the fiber wall is the remaining skeletal part of the plant cell. The cell wall thickness has been reported to be 1.27µm for *Asclepias syriaca* [25] as compared to 2µm for kapok fibers [83]. Regarding the diameter of the fiber, an average fiber diameter is around 20µm for all types and species (see Table 3-1).

*Table 3-1: Length and diameter of hollow fibers*

| Species | Length (mm) | Diameter (µm) | Reference |
|---|---|---|---|
| **A. syriaca** | 20,1 | 22,4 | [25] |
| **C. procera** | 31 | 10-21 | [84] |
| **C. gigantea** | 17,1 | 30,4 | [29] |
| **C. persica** | 18,6 | 15,9 | [85] |
| Milkweed | 14,2 | - | [86] |
| Akund | 31,24 | 20,63 | [20] |
| Estabragh | 26,4 | 25,3 | [87] |
| Estabragh | 27,7 | 22,14 | [88] |
| Estabragh | 27,89 | - | [89] |
| Estabragh | 34,23 | 25,31 | [90] |
| Estabragh | 33,5 | - | [80] |
| Estabragh | 26,6 | 28,93 | [91] |
| **Kapok** | 19,08 | 19,28 | [20] |
| **Kapok** | 25 | 16,5 | [83] |
| **Kapok** | 27.87 | - | [92] |

Hollow fibers have a conic morphology that was reported for several species such as *Asclepias syriac*a, *Calotropis gigantea* and kapok [87], [91], [93]. The fibers can be considered as a truncated cone with a base to top diameter ratio equals to 3 [87]. Hollow fibers are shorter (20 mm) than other conventional fibers such as hemp or flax (70-80 mm) [5]. This is because the natural bast fibers consist of a bundle of individual fibers, which are intertwound, and thus have longer dimensions. However, hollow floss fibers are single ultimate fibers and consequently are very short. Unlike most of the natural fiber, hollow fibers are directly harvested at the end of fiber's life cycle with no need for retting.

### 3.6.2 Chemical composition

*Table 3-2: Chemical composition of various species of hollow fibers*

| Species | Cellulose (%) | Hemicellulose (%) | Lignin (%) | Wax (%) | Reference |
|---|---|---|---|---|---|
| **C.gigantea** | 49 | 20 | 18 | - | [29] |
| **C. procera** | 55 | 24 | 18 | 3 | [84] |
| **A. syriaca** | 54,9 | 19,3 | 19,3 | - | [21] |
| **A. syriaca** | 39,6 | 27,3 | 15,1 | - | [22] |
| **C. persica** | 53,4 | 25,2 | 17,4 | - | [85] |
| **Daemia** | 53 | 26 | 15 | 4 | [94] |
| *Milkweed* | 55 | 24 | 18 | - | [95] |
| *Milkweed* | 52 | - | 21,3 | - | [86] |
| *Akund* | 55,45 | 21,91 | 16,15 | - | [20] |
| **Kapok** | 43 | 32 | 15 | - | [7] |
| **Kapok** | 64 | - | 13 | 0.8 | [16] |

The chemical compositions of the different species are reported in Table 3-2. Values show a certain homogeneity despite the variability of plant species and the techniques used for the characterization of chemical composition. Hollow fibers exhibit a relatively lower amount of cellulose and a high amount of lignin and waxes in comparison with other conventional fibers.

The hollow floss fibers tend to have a low percentage of cellulose around 55% whereas flax or hemp fibers are usually reported having 20% higher of this amount [5]. The content of lignin in the hollow fibers varies ranging from 13 to 21.3, while, bast fibers normally possess a very low percentage of lignin in their compositions. For instance, the percentage of lignin in flax and hemp are 2.2 and 5.7 respectively [5]. Only few researches were performed on the quantification of waxes in the hollow floss fibers. The only works available on the wax content show a higher amount of wax compared to other natural fibers. As the hollow floss fibers are directly in contact with the environment, an epicuticular layer of wax may be on the surface of the fiber [96].

### 3.6.3 Structure of floss fibers

It is well understood that the natural fibers cell walls are composed of a multi-layered material. Based on the origin of the fiber the number of layers as well as their thickness

may vary. Unlike the structure of bast fibers which has been well investigated, the hollow floss fibers cell wall structure has not yet been characterized. It is possible to depict a universal structure for hollow floss fibers. However, it is better to consider the structure for seed fibers (seed fibers grow from seeds like cotton) rather than floss fibers. The structure of cotton fibers has been intensively investigated and is described as the results of several concentric layers induced by the diurnal cycles (Figure 3-8) [23] . Moreover, according to Anderson and Kerr, the layers are the results of a difference in the density of the layer induced by the activity of the cell during the development of the fiber [97], [98]. Kapok and cotton do not have the same structure despite being seed fibers Kapok fibers are produced by a tree and it may be irrelevant to generalize this model for weeds hollow fibers (*Asclepias* or *Calotropis*). Meiwu *et al.* (2010) performed a study on the structure of kapok fibers wall. They investigated the structure of the kapok fiber by transmission electron microscopy. Their study revealed clearly a 5-layer structure within the wall of kapok fiber (Figure 3-7). The fiber structure is composed of an external cuticle, a first interlaced structure , two closely packed layers and a final inner skin [16].Although, proposing a universal structure for floss fibers and especially milkweed fibers may be irrelevant, both models can be applied to the Apocynaceae family fibers for various reasons.

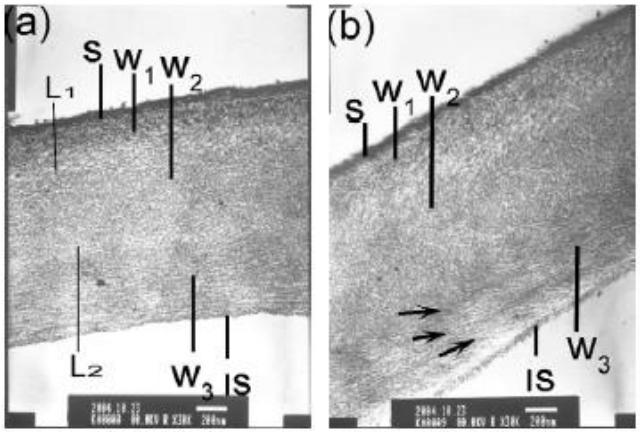


*Figure 3-7: Structure of the kapok fiber [16]*

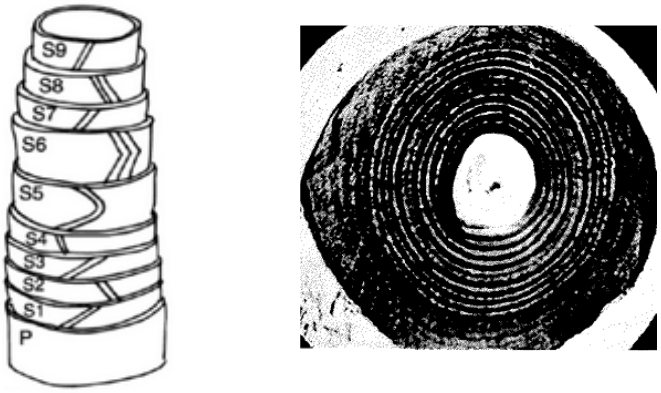


*Figure 3-8: Structure of common seed hair (left)[23] Structure of cotton fibers (right)[97]*

## *3.7 Physical properties of floss fibers*

### *3.7.1 Moisture absorption*

Moisture absorption and release of kapok and akund fibers were investigated by Yang *et al.*[19]. The study showed that the hollow fibers tended to absorb more water than the cotton fibers. The values showed that akund fibers reached an equilibrium state of 10.44% after a relatively long time. Kapok fibers reached a slightly lower than akund (9.9%) but still higher than cotton (7.5%). Moisture absorption of the common Milkweed (*Asclepias syriaca*) was studied by Drean et *al* [25]. They used ASTM D2654 to characterize the moisture absorption of Milkweed fibers and the results showed a correlation with the results found for kapok and akund. Milkweed fibers showed 9.9 wt% of moisture absorption. As the methods used in both studies are different, the absorption time was also different from one study to the other. Karthik and Murugan have studied the moisture regain of the *Pergularia daemia*. Their results showed once again that hollow fibers had a high rate of moisture absorption (10.0%) [94]. They also proved that the removal of wax on the fiber led to a higher amount of moisture absorption (12.0%). Moreover, Sakthivel *et al.* found a value of 11% regarding the moisture regain of the Mudar fibers (*Calotropis procera*) [84].

Overall, hollow fibers tend to absorb moisture around 10% of their weight regardless of the species.

### *3.7.2 Density*

Several methods have been used to characterize the density of hollow fibers. Among them gas pycnometry has also been used. However, this method always shows a value around 1.5 which is very close to the density of cellulose [99]. In fact, this method can only measure the density of solid part of the fibers and not the whole hollow fiber.

It is very important to take the lumen and its corresponding volume into account when the density of a hollow fiber is calculated. As previously explained, the hollow fibers have two main components: the cellulosic wall and the lumen. Considering the lumen as a part of the fiber has a strong influence on the density of the fiber.

Literature show very different results for the density of hollow fibers. Reddy and Yang determined a density of 0.893 on the milkweed fiber without mentioning the species of fibers [86]. The result was found using the sink-float method in xylene and carbon tetrachloride. The same method was used by Sakthivel for measuring the density of Mudar fibers (*Calotropis procera*) [84]. According to the results, the *C. procera* fibers have a density of 0.97. Ashori and Bahraini also determined the density of Mudar fibers (*Calotropis gigantea*) found a value of 0.68 while they did not indicate the method they used [29]. Bahari *et al.* also found a density of 0.9 for Estabragh fibers without explaining the methodology [89]. Another study was conducted on kapok fibers by Meiwu *et al.* and determined the density of fiber close to 0.3 [16].

With density values ranging from 0.3 to 0.9 (see Table 3-3), it is not clear what the correct density of the hollow fibers is. However, it is possible to find approximatively a value based on the geometrical calculation. As the hollow fibers are very short it is possible to assume the fiber as a cylinder for a very short length (see Figure 3-9) with an average diameter of 20µm (Table 3-1), an average wall thickness of 2µm [83] and an average density of the wall of 1.48 measured using a gas pycnometer on *Asclepias syriaca*. Theoretically, the volume of fiber is equal to the volume of cylinder and determined by the following equation:

$$V_{fiber} = \pi \times R^2 \times \delta x \quad (1)$$

With R the external diameter and $\delta x$ the length of the cylinder considered for the volume calculation. The mass of fiber is equal to the density of wall multiply by its volume. Then the mass of fiber is given by the following equation:

$$M_{fiber} = V_{wall} \times d_{cellulose} = \pi \times (R^2 - (R-e)^2) \times \delta x \times d_{wall} \quad (2)$$

With e the thickness of fiber's wall.

The theoretical density of the fiber can be calculated by the final equation below:

$$d_{fiber} = \frac{M_{fiber}}{V_{fiber}} = \frac{\pi \times (R^2 - (R-e)^2) \times \delta x \times d_{wall}}{\pi \times R^2 \times \delta x} = \frac{R^2 - (R-e)^2}{R^2} \times d_{wall} \quad (3)$$

Then by applying average values of hollow fibers, the theoretical hollow fiber density is close to 0.296 g/cm3. This value shows that the conventional methods for measuring the density of hollow fibers have undergone overestimations. A different value was found using immersion method, which can be explained by the fact that the lumen was partially filled by the liquid during the immersion test.

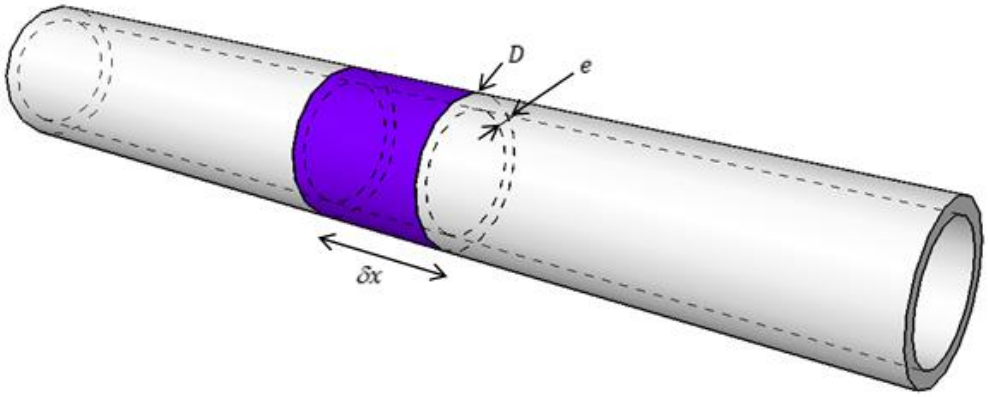


*Figure 3-9: Schematic view of the cylindrical model to calculate the volume and density of hollow fibers*

*Table 3-3: Density of hollow fibers*

| Species | Method | Density | Reference |
|---|---|---|---|
| **Gigantea** | - | 0,68 | [29] |
| **Daemia** | Sink/float in xylene | 0,8-0,9 | [94] |
| **Procera** | Sink/float in xylene and carbon tetrachloride | 0,97 | [84] |
| Estabragh | - | 0,97 | [89] |
| Milkweed | Sink/float in xylene and carbon tetrachloride | 0,893 | [86] |
| Kapok | - | 0,31-0.38 | [100] |
| Kapok | - | 0,3 | [16] |
| Kapok | - | 0,3 | [101] |

### *3.7.3 Tensile properties*

Tensile Properties of the hollow fibers are presented in Table 3-4. Few publications were found dealing with the mechanical properties of natural hollow fibers. The majority of studies has characterized the mechanical properties of fibers for the textile industry. Accordingly, the ultimate tensile stress is often expressed in g/tex instead of Pascal. Only Ashori and Bahreini have published values for the young modulus of hollow fibers [29]. Other studies were manly focused on the textile industry and only ultimate tensile stress, elongation and linear density were presented. Nevertheless, despite inhomogeneity in the results, the hollow fibers exhibit quite low tensile properties. In fact, hollow fibers are not supposed to have high mechanical properties and their purpose is to suspend the seeds in air and then disperse them as far as they can fly. However, Bast fibers grow to withstand the gravity and lateral forces. In fact, the primary function of the fibers naturally determines if they need to have high or low mechanical properties. Values of UTS in italic in the Table 3-4 were recalculated when the density values were available [102, p. 284].

*Table 3-4: Mechanical properties of hollow fibers*

| Species | Young's Modulus (GPa) | Tensile Strength (MPa) | Breaking Strenght (g/tex) | Strain (%) | Linear Density (tex) | Reference |
|---|---|---|---|---|---|---|
| **Gigantea** | 8,2 | 296 | - | 1,6 | - | [29] |
| **Procera** | - | *231* | 24,3 | 2 | 0,26 | [84] |
| Akund | - | - | 29,6 | 2,45 | 0,1 | [20] |
| Estabragh | - | *362* | 38 | 2,6 | 0,37 | [89] |
| Estabragh | - | - | 29,9 | 2,2 | 0,17 | [80] |
| Kapok | - | - | 16,7 | 3,6 | 0,68 | [20] |
| Kapok | 4 | 93,3 | - | 1,2 | - | [100] |
| Kapok | - | - | - | 1,83-4,23 | - | [101] |

Moreover, growing conditions strongly influence the mechanical properties of fibers. Yang *et al.* (2012) showed in their study that the properties of Akund changed dramatically by the environment and growing conditions [103]. In the study the effect of parameters like growing altitude, the pod size, and the location of fibers in the pod on the mechanical properties were investigated. They showed that an increase in the altitude tends to decrease the ultimate tensile strength of the fiber. They also noticed a strong correlation between the size of the pods and the properties of the fibers. The smaller the pods, the weaker the fibers are. Eventually, they found that the fibers are located in the upper part of the pods are more resistant to tensile stress than those in the lower part.

### *3.7.4 Thermal properties*

Yang *et al.* (2012) characterized the thermal properties of Akund and kapok fibers [20] (Figure 3-10). Their results were compared with the cotton fibers. Results showed that both fibers had poor thermal stability. In both cases the main onset temperature occurred few degrees before the one of cotton. Regarding the residual mass, cotton had higher values in comparison with these fibers. However, the two hollow fibers presented lower degradation speed than cotton.

The lower thermal stability of hollow fibers compared to cotton can be explained by two reasons. The content of cellulose and the degree of crystallinity. As it was presented in

Table 3-2, hollow fibers possess higher amount of lignin and hemicelluloses and lower amount of cellulose compared with cotton (92.56% of cotton is cellulose) [20]. Hemicellulose and lignin have lower molecular weight in comparison with cellulose and thus their thermal degradations start well before cellulose [95]. In addition, hollow fibers cellulose presents a degree of crystallinity of about 28.92% while cotton generally presents the degree of crystallinity close to 78.4% [20]. The higher crystallinity of cotton fibers will lead to a higher degradation temperature [104]. That is why cotton exhibits superior thermal properties compared with Akund and kapok fibers.

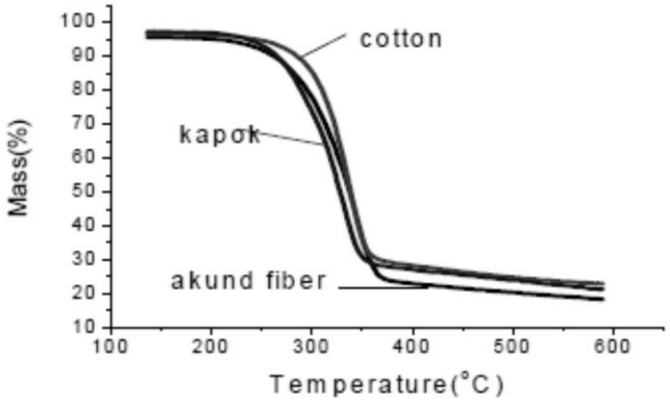


*Figure 3-10: Thermal degradation of akund and kapok fibers[20]*

### *3.7.5 Alkaline resistance*

Alkaline resistance of the hollow fiber and specially Estabragh fiber was studied by Merati [91]. The alkaline resistance of Estabragh was evaluated in cementitious materials. Merati found that Estabragh fibers had a very poor alkaline resistance. The strength of fiber decreased from 3.65 CN to 2.17 CN after 28 days in caustic soda (40g/l). According to the research done by Merati, adding the fibers to the cement did not improve the long-term strength of cement. However, the study showed that hollow fibers decreased the number of cracks appearing during the early stage of cement curing.

Alkaline resistance on the Mudar fibers (*Calotropis procera*) was also studied by Sakthivel *et al.* [84]. The study placed focus on the spinnability of hollow fibers. As hollow fibers are very smooth it is hard to manage the spinnability. Therefore, to improve the friction a short alkaline treatment was applied on Mudar fibers. The treatment involved soaking fibers in a 5% NaOH solution for 5 minutes. The fiber morphology was studied by scanning

electron microscopy and showed that the fibers geometry is strongly deteriorated by the treatment. Alkali treated fibers exhibited convoluted like morphology as well as cotton fibers. Moreover, they noticed that fibers tend to agglomerate after the treatment.

### *3.7.6 Acoustic properties*

A huge amount of void in hollow fibers provides the opportunity for these fibers to be used in sound-proofing applications. Hollow fibers acoustic properties were studied by Hasani *et al.* for the automotive application [90]. Their study showed that Estabragh presented a good acoustic performance. The noise absorption coefficient of a conventional hollow polyester web was improved by the addition of Estabragh. This study mainly attributed the high damping properties of Estabragh to the presence of the lumen in the fiber. The results showed that a pure Estabragh web has a noise absorption coefficient almost double of the one of pure polyester.

## *3.8 Industrial Applications of Floss Fibers*

### *3.8.1 Composite manufacturing*

Apocynaceae fibers have been used as reinforcements in both thermoset and thermoplastic polymers. Although, the number of studies on thermosets is higher than the one on thermoplastics, researchers and industries are interested to use hollow fibers in both resins and even in cementitious matrices.

One study was done on natural hollow fibers using polypropylene (PP) by Reddy and Yang at the University of Nebraska [86]. However, the authors did not specify the species of the fibers but it is likely *Asclepias syriaca*. The composites were fabricated using 35% and 50% fibers by thermal compression. First, the fibers were carded four times to make mats and then the composites were made by compression molding at 190 ° C for 140 seconds. The results showed that the PP/hollow fibers composites had superior mechanical properties compared to conventional PP/kenaf composites. Using 50 wt% hollow fibers as reinforcement increased two times the flexural strength and four times elastic modulus in comparison with PP/kenaf composites.

Srinivas *et al.* studied mechanical properties of *Calotropis gigantea* fibers reinforced unsaturated polyester (UP) composites [105]. The authors studied the effect of increasing the content of fiber on the mechanical properties of composites. The composites were produced by hand layup molding with fiber contents ranging from 0% to 30%. The article does not provide an indication of the state of the fibers or even their distribution in the specimens. The results showed that the addition of *Calotropis gigantea* fiber up to 30% in the polyester resulted in an increase of 100% in the tensile strength and an increase of 47% in the elastic modulus. The study also showed that the composites with 30 wt% fibers exhibited 1.54 times higher flexural modulus and 1.3 times higher impact compared with the reference. Moreover, the study could successfully decrease the density of UP by 30% for the composite with 30 wt% fibers.

Another well-known hollow fiber, which has been used in composite materials, is kapok. Like the other hollow natural fibers, very few publications have focused on the study of kapok fibers reinforced composites [106]–[110]. To the best of our knowledge, there is still no study, which shows the effect of kapok fibers on mechanical properties of thermoplastics. However, Venkata Reddy *et al.* conducted a research on the mechanical properties of kapok/UP composite. The authors found a significant increase in the mechanical properties of composites by adding 9% of fibers to the polymer. The composites were processed by reinforcing the UP using kapok fabrics. They also studied the effect of fibers pre-treatments on the mechanical properties of composites. The alkaline treatment of the fibers (30 minutes in a 2% solution of NaOH) slightly improved the properties. Although they have claimed for the amelioration in the mechanical properties of composites, they did not show any microscopy on the treated fibers. Therefore, it is not possible to check the state of the fiber to discuss the real reason for the improvements [106]–[109].

A handful of studies have been done on hollow fibers reinforced composites. Although, the studies are very different and limited, it seems that Apocynaceae fibers can improve the mechanical properties of polymeric matrices. Table 3-5 summarizes the results of these studies.

*Table 3-5: Mechanical properties of hollow fiber composites*

| | *Asclepias syriaca* [a] | *Calotropis gigantea* [b] | Kapok [c] | Alkali treated Kapok [d] | Kapok [e] | Alkali treated Kapok [f] |
|---|---|---|---|---|---|---|
| Fiber content | 50 % | 30 % | 9 % | 9 % | 5 % | 5 % |
| Polymeric matrices | PP | UP | UP | UP | UP | UP |
| Process | Thermocompression | Manual | Manual | Manual | Manual | Manual |
| Elastic modulus (Tensile mode) | + 65 % | + 57 % | - 18 % | + 19 % | - | - |
| Elastic modulus (Flexural mode) | + 392 % | + 154 % | + 723 % | + 731 % | + 303 % | + 327 % |
| Tensile strength | + 57% | + 100% | + 182% | + 232% | - | - |
| Flexural strength | + 195 % | + 80 % | + 125 % | + 160 % | + 50 % | + 56 % |
| Impact resistance | + 33 % | + 130 % | + 133 % | + 145 % | - | - |

a [86]

b [105]

c [107]–[109]

d [107]–[109]

e [106]

### *3.8.2 Oil absorbents*

Oil sorption capacities of natural fibers are generally much higher than the one of polypropylene [111]. According to Choi and Cloud, milkweed fibers are the best natural oil absorbents followed by Kapok fibers [111], [112]. Lim and Huang and Choi and Cloud have explained this high oil absorption capacity by two phenomena[83], [112]. First, hollow fibers create interaction with oil thanks to their waxy surface. This interaction is induced by a chemical compatibility with oil as both are hydrophobic [83]. Second, absorption mechanism is related to capillarity in the lumen of the fibers. Therefore, the small radius of lumen increases the capillarity pressure which promotes the oil absorption. Kobayashi *et al.* found that Kapok fibers are able to absorb more than twice the amount of oil absorbed by polypropylene which is considered as an excellent oil absorbent [113]. Kapok fibers are able to absorb almost 40g of oil per gram of fiber [83], [114]. Same trend was also found for milkweed fibers [111].

Oil absorbents made of hollow fibers can be reused even though the oil sorption capacity will be lowered by the number they are used. However, the sorption capacity remains still higher than that of new polypropylene [83].

### *3.8.3 Thermal insulation*

Down is one of the most famous materials, which has been used for thermal insulation applications. However, there are always some ethical and economic concerns with using this material. Hollow fibers can find applications in the thermal insulation with fewer concerns. The thermal insulation capacity of milkweed fibers (*A. syriaca* and *A. speciosa* blended) was studied by Crews *et al.* [115]. Winter coats isolated with Milkweed fibers, synthetic fibers or down were tested to measure their insulating efficiency. Results showed surprisingly that a coat insulated with 100 % Milkweed fibers had a very low insulation value. Moreover, they also noticed that standard commercial dry-cleaning procedures affected strongly the fiber and their insulating efficiency. Nevertheless, the 50/50 Milkweed/ down coat happened to be as effective as the pure down coat even after the cleaning process. Their conclusion showed that Milkweed fibers are very useful to decrease the use of down or feather with no loss of thermal efficiency. In addition, as the Milkweed fiber costs half of the price of the goose down, the use of Milkweed fibers may decrease the price of insulating materials.

Parmar *et al.* found a similar conclusion regarding the use of Milkweed for thermal insulation [116]. Their results showed that the addition of Milkweed fibers to common cotton or polyester fabric resulted in an increase in the thermal insulation value. Thermal insulation properties of fabrics were improved by 14% for cotton and 10% for polyester when half of the fibers are replaced by Milkweed fibers. Furthermore, they also noticed that Milkweed fibers greatly induced ultraviolet protection properties to the fabrics. Based on literature, Parmar *et al.* have explained this property due to the high percentage of lignin in Milkweed fibers.

Kapok also exhibits similar behaviors when it is used in thermal insulating applications. Cui *et al.* have shown that the thermal conductivity of wadding decreased when the share of Kapok in fabrics increased [117], [118]. Few patents have also been published on hollow fibers for different applications. For instance, in 1949 the Milkweed Products Dev Corp patented an insulated life preserver for below zero Celsius temperatures [119]. A building insulation material made from hollow fibers has also been patented recently [120].

## *3.9 Conclusions*

Hollow fibers are a truly sustainable product that can be harvested in almost all over the world with constant properties regardless of the type or species. Hollow fibers can be recognized by the following properties:

- Hollow fibers are shorter than common natural fibers.
- Hollow fibers composition is characterized by a low amount of cellulose and a high amount of lignin, hemicellulose and wax.
- Hollow fibers show higher moisture regain than common natural fibers.
- The density of hollow fibers is almost five times lower than common natural fibers.
- Tensile properties of hollow fibers are lower compared to liber fibers.
- The thermal stability is lower than common natural fibers.
- Hollow fibers are very sensitive to alkaline environment.
- The acoustic properties of hollow fibers are excellent.

In this chapter, different species of hollow fibers and their corresponding mechanical properties were described. It is quite clear that the properties of fibers do not depend directly on the species of hollow fibers. Although, there is a strong relationship between the wall structure and the tensile properties of the fibers, there is no clear link between the structure of fibers' wall and the species. Hollow fibers should not be used or considered as same as conventional natural fibers are. These fibers possess lower tensile properties in comparison with those fibers. However, hollow fibers have potentials of numerous applications such as oil absorbent or thermal insulation, which are not available for other natural fibers.

# CHAPITRE 4 : MISE EN FORME, STRUCTURE ET PROPRIÉTÉS D'UN COMPOSITE PLA-ASCLÉPIADE

***Auteurs et affiliation :***

- *Ovlaque Pierre : Étudiant au doctorat, Université de Sherbrooke, Faculté de génie, Département de génie civil.*
- *Mohammadreza Foruzanmehr : Coordinateur scientifique, Université de Sherbrooke, Faculté de génie, Département de génie civil.*
- *Saïd Elkoun : Professeur, Université de Sherbrooke, Faculté de génie, Département de génie mécanique*
- *Mathieu Robert : Professeur, Université de Sherbrooke, Faculté de génie, Département de génie civil*

***Date de soumission :*** *16 mai 2019*

***Revue :*** *Polymer Engineering and Science*

***Titre :*** *On the effectiveness of the addition of milkweed floss fibers on processing and mechanical properties of PLA biocomposites*

## *4.1 Résumé*

Cette étude visait à étudier l'effet renforçant de l'asclépiade, une fibre naturelle lisse et homogène présentant un large lumen creux, sur les composites polymères biosourcés. Premièrement, l'asclépiade a fait l'objet d'une caractérisation approfondie sur le plan de sa morphologie, rugosité de surface, résistance à la traction et résistance thermique. Ensuite, les données ont été comparées à celles de la fibre de lin, l'une des fibres naturelles les plus utilisées dans l'industrie des composites. Des composites d'acide polylactique (PLA) et d'asclépiade (1 % en poids) ont été produits par injection et comparés aux composites renforcés des fibres de lin. Enfin, les propriétés mécaniques et la résistance aux chocs des composites ont été déterminées.

Les résultats ont montré que l'asclépiade présente un module de traction, une résistance à la traction et une rugosité de surface inférieure au lin. Néanmoins, la résistance en traction et la résistance aux chocs des composites asclépiade/PLA se sont respectivement avérées supérieures de 60 % et 15 % par rapport à celles des composites lin/PLA. Pour terminer,

les micrographies de l'interface entre le PLA et l'asclépiade ont révélé un manque d'adhérence critique entre les deux composants.

## *4.2 Abstract*

This study aimed at investigating the reinforcement effect of milkweed (MW) floss, a smooth and homogeneous natural fiber with a wide hollow lumen, on bio-based polymer composites. Firstly, MW floss was thoroughly characterized in terms of morphology, surface roughness, and tensile and thermal resistance. Then, MW floss was compared to flax fibers, one of the most widely used natural fibers in the composite industry. Subsequently, bio-based composites made of polylactic acid (PLA) and 1 wt.% MW floss were produced by injection molding and compared to composites reinforced with 1 wt.% of flax fibers. Finally, thermal behavior, mechanical properties and impact resistance of composites were determined. Results showed that MW floss, with respect to flax fibers, exhibits lower tensile modulus, ultimate tensile strength, surface roughness as well as a shorter critical length. Nonetheless, and despite the lower intrinsic properties of MW floss, UTS and impact resistance of MW/PLA composites were found to be 60% and 15% higher than those of Flax/PLA composites respectively. In addition, micrographs of MW/PLA interface revealed a lack of adhesion in MW/PLA, which should be overcome by surface treatment in upcoming work.

**Keywords:** Milkweed, Composite, Injection Molding, Polylactic Acid.

## *4.3 Introduction*

The depletion of oil stocks and environmental concerns force industries and researchers to develop more sustainable materials. Thus, over the last decade, efforts have been put into developing substitutes of conventional oil-based plastics from more sustainable resources. Among promising alternative bioplastics, polylactic acid (PLA) offers interesting properties and is available at a large scale for industrial applications. PLA is a bio-based polymer derived from agricultural crops such as corn, with a limited environmental impact [34]. In addition, PLA presents a melting point below 200 °C and can be therefore transformed using conventional molding processes [3], [121].

However, the use of PLA is still limited by several serious drawbacks such as a low strain at break at room temperature and a low thermal resistance due to its glass transition temperature at about 54 °C [36], [121]. Still, these drawbacks could be overcome by adding natural fibers (NF) as a reinforcement material. Indeed, NF such as flax fibers are successfully used to enhance thermal and mechanical properties and, even more, impact resistance of PLA [122]–[124]. For example, the addition of 40 wt.% of flax fibers in PLA leads to a 10 °C increase of the softening point and an enhancement of Young's modulus from 3.4 to 7.3 GPa as compared to neat PLA [122]. Also, Foruzanmehr *et al.* reported an improvement of more than 300% of the impact strength of PLA by reinforcing the matrix with 34 wt.% of flax fibers [123]. Several NF extracted from various species of plant could be suitable candidates for PLA reinforcement [124]. However, bast NF (i.e., fibers extracted from stems) such as hemp, flax, kenaf, nettle, ramie or jute are typically used as reinforcement of PLA. Indeed, compared to synthetic fibers, bast NF show lots of advantages like better specific properties, lower environmental footprints, lower density, lower price, safer handling and lower equipment abrasion [125] [126]. Nonetheless, the main drawbacks of NF are the dimensional inhomogeneity and inconsistent mechanical properties as compared to synthetic fibers [6], [70]. In addition, some NF such as flax fibers are strongly endemic, and a retting step is necessary to extract fibers from the bast.

Contrary to flax fiber and other bast fibers, milkweed (MW) floss does not exhibit these drawbacks. MW plants are not restrained by endemism and can be grown, harvested and used locally. Indeed, MW floss is not produced from a unique species of plants since milkweed designates a large variety of plants such as *Asclepias, Calotropis* or *Pergularia* that can grow in many regions of the world [72], [84]. For instance, *Calotropis Gigantea* plants appear to be a perennial shrub growing in Middle East regions whereas *Asclepias Syriaca* is produced by a wild weed that grows during the summer in the eastern part of North America [29][127]. Also, according to Karthik and Murugan, MW can be cultivated in poor soils and, unlike cotton or flax fibers, without need for fertilizers or regular watering [128]. Finally, MW floss is harvested at an ultimate fiber stage without the need of retting steps. Thus, the integrity and characteristics of the fibers are maintained and the risk of fiber damage is strongly limited.

Among the particularities of MW, the most interesting is undoubtedly the uncommon structure. Bast NF are generally depicted as solid cylinders composed of cellulose microfibrils bonded by hemicellulose and lignin molecules whereas these components are arranged in a tube-like structure with a thin wall and a wide hollow lumen in MW floss [20], [129]. Therefore, due to this wide, hollow lumen, MW floss is often associated with thermal and acoustic insulation applications [90], [115], [116]. Still, the wide hollow lumen also leads to a low density and, thus, great opportunities to produce lighter composites [20], [29], [84], [89]. Depending on the method of characterization, the density of MW floss densities ranging from 0.3 to 0.97 g/cc are reported in the literature, while bast fibers usually exhibit a density close to 1.5 g/cc [12], [84], [100]. The particular geometry of MW floss also leads to larger interphases with matrix thanks to the inner surface of the hollow floss. Consequently, the critical length (Lc) of MW floss is significantly reduced and MW leftovers or residues that are too short to be processed by carding operations (i.e., for thermal and acoustic insulation applications) can be valorized. Furthermore, with a shorter Lc, MW should be less impaired by automatic processes like extrusion that tend to reduce NF length to values below their Lc [54].

All studies dealing with the use of hollow fibers such as *Asclepias Syriaca*, *Calotropis Gigantea* or kapok floss reported quite impressive increases in mechanical properties and impact resistance that were ascribed to the empty tubelike structure of hollow floss [86], [105], [107]. Indeed, the higher aspect ratio of floss should lead to more interface breakage during fracture propagation. Venkata Reddy *et al*. reported a 130 and 182% increase of impact resistance and tensile strength of unsaturated polyester (UP) respectively after adding 9 wt.% of hollow kapok floss [108]. Similar improvements of UP mechanical properties were also reported by Srinivas and Babu [105]. Reddy and Yang also showed an improvement of impact strength, Young's modulus and tensile strength by 33, 65 and 57% respectively as compared to polypropylene reinforced with 50 wt.% of kenaf fibers using carding and thermoforming processing [86].

The present study aimed to investigate and compare the reinforcing effect of hollow MW floss fibers and solid flax fibers in PLA. Mechanical properties, density, roughness and theoretical critical length of MW floss were first characterized and compared to that of flax. Then, neat PLA and milkweed floss or flax fibers/PLA composites (1 wt.%) were

produced by injection molding. Mechanical properties, interfacial adhesion and water uptake of the different composites were finally characterized and discussed.

## *4.4 Material and method*

### *4.4.1 Materials*

MW floss fibers, extracted from *Asclepias Syriaca* plants grown in Quebec, and flax fibers were provided by Protec-Style (Quebec, Canada) and Biolin Research Inc. (Saskatchewan, Canada), respectively. PLA pellets, injection molding grade (PLA3100 HP), were purchased from Natureworks LLC.

### *4.4.2 Biocomposite Processing*

Neat PLA, MW reinforced PLA (MW/PLA) and flax reinforced PLA (Flax/PLA) samples were produced using the following method. First, 1 mm thick PLA sheets were obtained by compression molding of PLA pellets by using a Carver hydraulic press at 190 °C. Then, 1 wt.% of fibers were placed between two PLA sheets and pressed for 3 minutes at 190 °C to produce composite thin plates. The plates were then crushed to obtain 0.5 cm length homogeneous flakes of PLA/fibers composites. Finally, the flakes were extruded at 180 °C and pelletized by means of a Filabot single screw extruder coupled with a C.W. Brabender pelletizer. Eventually, composite and extruded neat PLA pellets were used to elaborate injected tensile test specimens using a MPM 55-2P vertical mini injector at 205 °C under 1 kPsi.

### *4.4.3 Methods*

#### *4.4.3.1 Mechanical Properties*

Tensile tests were carried out on a Zwick/Roell z050 tensile test machine. Mechanical properties of raw MW floss and flax fibers were determined, according to ASTM C1557-14 on 20 fibers, using a 5 N cell load with a crosshead speed set at 2 mm/min. It is noteworthy that displacement induced by the deformation of the cell under loading of MW floss was very low (i.e., 0.6% of the maximum load). Thus, crosshead displacement was directly used to determine the fiber elongation. To obtain accurate values of modulus and

ultimate tensile strength (UTS) according to ASTM C1557-14, fiber diameters at break were measured by optical microscopy.

Young's modulus and UTS of all the composites were measured according to ASTM D3039 at 2 mm/min crosshead speed with a 30 kN cell load using the built-in extensometer. Tests were carried out on five specimens for each condition.

Dynamic mechanical analysis (DMA) was performed by means of a Perkin Elmer DMA 8000. Storage modulus (E') and loss factor (tan δ) were obtained using the single cantilever mode at 1 Hz, a heating rate of 3 °C/min and a constant static force of 0.1 N. Tests were performed on five specimens for each condition.

Impact strength of composite and neat PLA was measured using an Instron/Ceast 9050 at ambient temperature following ASTM D256. For each condition, five notched samples were tested through Izod mode using a 1 J pendulum.

#### *4.4.3.2 Morphology*

Morphology of fibers and composites were examined by means of a Hitachi S3000-N scanning electron microscope (SEM) at 5 kV. Composite specimens tested under tensile were also analyzed to investigate the interfacial adhesion and effects of processing (i.e., extrusion and injection) on the MW floss geometry.

The transmission mode of a Nikon Optiphot optical microscope (OM) was used to determine the diameter of the fiber at break and the remaining lengths and dispersions of injected MW floss and flax fibers after processing. Average diameter and length of the investigated MW floss were also determined for more than 200 fibers. The images were acquired and analyzed by means of a Motic 580 digital camera and Motic Image Plus 3.0 software.

MW floss surface roughness was measured using a Veeco Nanoscope IIIA atomic force microscope (AFM). AFM observations were performed using the non-contact mode on five fibers. Prior to calculation of the arithmetical mean roughness (Ra), fiber surface curvature was flattened (third-order polynomial-Gwyddion software). Roughness was measured on 6 x 6 $\mu m^2$ square for each fiber and an average roughness was calculated.

#### *4.4.3.3 Thermal Behavior*

Differential scanning calorimetry (DSC) was carried out on different composites and neat PLA samples using a Perkin Elmer DSC 6000. The temperature range was from 20 to 200 °C and the heating rate 10 °C/min. Glass transition (Tg), cold crystallization (Tcc), melting temperature (Tm) and crystallinity (χ) were determined. Rates of crystallinity of neat PLA and composites were calculated according to equation 1 [123]:

$$\chi = \frac{\Delta H_m - \Delta H_c}{\Delta H_m°(1 - Wt_f)} \quad (1)$$

where $\Delta H_m$, $\Delta H_c$ and $\Delta H_m°$ are the enthalpy of melting, crystallization and melting of 100% crystalline PLA respectively. $Wt_f$ is the fiber weight fraction of the composite. A value of 93.7 J/g was used for the $\Delta H_m°$ of PLA [123].

Thermogravimetric analysis (TGA) was performed to investigate the thermal resistance and degradation of MW floss and flax fiber using a Mettler Toledo ATG/DSC 3+. All the analyses were conducted on three specimens under argon from 30 to 600 °C at 10 °C/min.

#### *4.4.3.4 Water Uptake*

Water uptake of composites was measured using the method described by Bayart et *al.* [29]. First, composites were dried for 48 hours at 50 °C under vacuum until constant dry mass ($m_d$) was obtained. Then, fibers were fully immersed in distilled water and held at 50 °C until a constant wet mass ($m_w$) was reached. Eventually, water uptakes ($\%_{water}$) of composites were calculated using equation 2:

$$\%_{water} = \frac{m_w - m_d}{m_d} \times 100 \quad (2)$$

Water uptake was measured for each condition on three samples and an average water uptake value was calculated.

## *4.5 Results and discussion*

### *4.5.1 Fibers Characterization*

#### *4.5.1.1 Fibers morphology*

Figure 4-1 presents SEM micrographs of MW floss (a and b) and flax fibers (c and d). As can be seen, MW floss and flax fibers exhibit different surface morphology and structure. On the one hand, MW floss can easily be isolated and presents a hollow structure and a remarkably smooth surface. Their average diameter and length determined by OM are 22.0 ± 7.4µm and 22.2 ± 6.1 mm respectively. These values are in accordance with those obtained by Dréan *et al.* on a two-year-old MW floss from *Asclepias Syriaca* [25]. On the other hand, flax fibers gather into a more cohesive bundle with a rougher surface, which is consistent with data reported by Nair *et al.* [131]. The cohesion of ultimate flax fibers (Figure 4-1c) leads to wider and longer fibers (i.e., technical fibers) as compared to MW floss. In addition, MW floss and flax fibers differ by the size of their lumens. Indeed, flax fibers present almost no visible lumen whereas MW floss exhibits a wall thickness of 1.27µm surrounding a lumen that occupies about 75% of the total volume of fibers [25]. Similar results were reported by Lim and Huang for kapok hollow fibers [83].

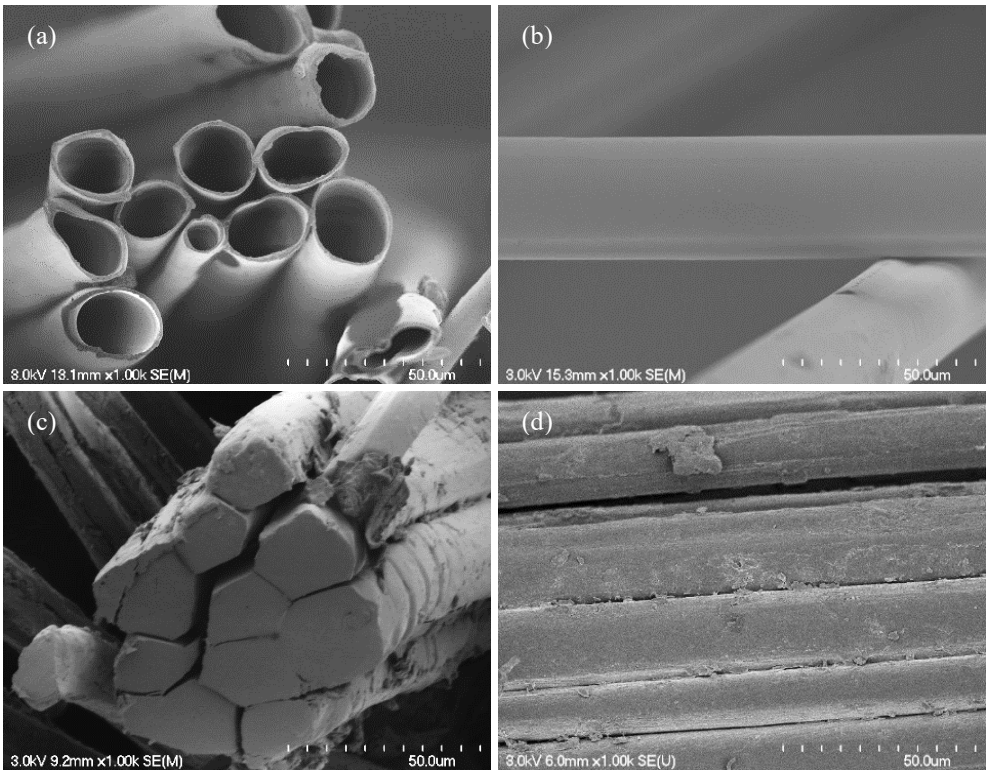


*Figure 4-1: Milkweed floss fibers (a and b) and flax fibers (c and d)*

### *4.5.1.2 Surface characterization*

As mentioned in the previous section, MW floss exhibits a very smooth surface. In order to compare the surface roughness of MW floss and flax fiber, AFM technique was used. MW floss shows an average surface roughness of 10.03 nm +/- 0.45 nm which is two times lower than the reported value for flax fiber (i.e., 21.7 nm +/- 2.5 nm) using the same method [132].

The smoother surface of MW floss (Figure 4-1 b) could be related to the higher amount of wax on the surface of the fiber. Indeed, MW floss exhibits an average wax content of 3 wt% as compared to 1.7 wt% for flax fibers [5], [133]. This high wax content is typical for hollow floss fibers (e.g., MW, kapok) which are known to exhibit a waxy coating on the surface due to the fact that floss is in direct contact with the environment as compared to bast fibers which are embedded [83], [112], [133]–[135]. This assumption is confirmed by the AFM surface topography view of MW floss presented in Figure 4-2, which shows nano-wrinkles aligned along the fiber axis. This particular structure was mentioned by Zhang *et al.* on the surface of kapok floss [136]. According to these authors, the association of nano-wrinkles and a thin external waxy layer induce a "lotus effect" on kapok surface and thus, explained the high contact angle found with water (116°-154°)[136], [137]. In the same way, MW floss presents a similar behavior with a contact angle of 129° with water [138].

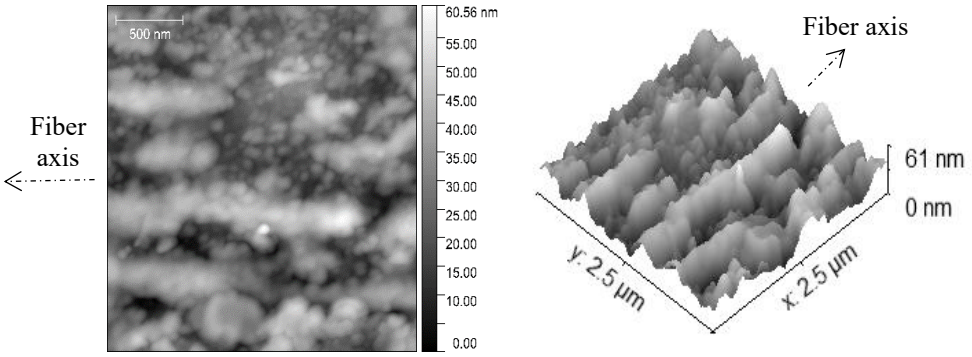


*Figure 4-2: Milkweed floss fiber surface topography*

### *4.5.1.3 Fibers mechanical properties*

Mechanical properties of MW floss were compared to those of flax fibers with a similar average diameter (i.e. 20 µm). Table 4-1 depicts Young Modulus (E), Ultimate Tensile Stress (UTS), and elongation at break (ε), of MW floss and flax fibers. These properties were obtained assuming MW floss as an empty cylinder (i.e., annular cross-section) with

a 1.27 µm wall thickness and flax fiber as a solid cylinder [25], [131]. MW floss exhibits a Young's modulus of 14 GPa and an UTS of 341 MPa which are significantly higher than values reported by Ashori and Bahreini (i.e., E = 8 GPa and UTS = 296 MPa) [29]. The difference might be ascribed to the milkweed species as Ashori and Bahreini characterized *Calotropis Gigantea* floss while this work deals with *Asclepias Syriaca* floss. Despite the fact that both species present a similar geometry and chemical composition, they may have different mechanical properties [21], [22], [25], [29]. In addition, it has been reported that growing conditions can influence, to some extent, the final mechanical properties of floss [103]. Moreover, the lower values reported by Ashori and Bahreini could also be explained by the cross-section geometry used for the calculation of the Young's modulus and UTS (i.e., plain vs annular cross-section).

The experimental results also show that MW floss presents lower mechanical properties than those of flax fibers. Indeed, E and UTS of flax fibers are 70 and 89% higher than those of MW floss respectively. These discrepancies in mechanical properties can be related to the cellulose content that reflected the respective roles of both fibers in the plant [139]. MW fibers exhibit a low cellulose content (i.e., between 40% and 55%) because their only purpose is to ensure the airborne dispersion of seeds. Conversely, flax fibers ensure the mechanical resistance of the stem and exhibit a significantly higher cellulose content (i.e., 71%) [36,43,44].

*Table 4-1: MW floss and flax fiber mechanical properties*

| | E (GPa) | SD* | UTS (MPa) | SD* | Strain (%) | SD* |
|---|---|---|---|---|---|---|
| Milkweed | 14 | 2 | 341 | 116 | 3 | 1 |
| Flax | 24 | 5 | 644 | 193 | 3 | 1 |

* Standard Deviation

#### *4.5.1.4 Fibers density*

The theoretical density of the fibers, $\rho_f$, was determined using equation (3) where R is the average outer radius, e the average wall thickness and $\rho_c$ the average wall density. An external diameter of MW floss of 22 µm measured by OM and an average wall thickness of 1.27 µm was considered [25]. The average wall density of MW floss was determined by gas pycnometry on 11 samples. A density of 1.48 +/- 0.01 g/cc was found for the cellulosic wall. According to Equation 3, MW floss presents an extremely low experimental density

close to 0.3 g/cc which is 4 times smaller than that of solid fibers such as flax fibers (1.2–1.5 g/cc) [40]. The theoretical value found for *Asclepias Syriaca* floss is in accordance with results obtained with kapok floss (0.3 g/cc) [16], [100], [101].

$$\rho_f = \frac{\rho_c \times (2Re - e^2)}{R^2} \quad (3)$$

#### *4.5.1.5 Fibers critical length*

It is well established that the fiber length of short fiber-based composites must be longer than a critical length (Lc) to achieve optimal strengthening [54], [140]. To calculate Lc, two MW floss geometries were considered: *i)* hollow fibers with an empty lumen and *ii)* hollow fibers with a polymer-filled lumen. Table 4-2 depicts the equation obtained for flax fibers and the two geometries of MW floss as well as their respective values of Lc in PLA matrices. Interfacial shear stress, $\tau_m$ , was also calculated from the equation (4) based on the Von Mises criterion where Rm is the matrix tensile strength [141].

$$\tau_m = \frac{Rm}{\sqrt{3}} \quad (4)$$

Tensile strength ($\sigma_{maxf}$) of MW floss, fiber average diameter (D) and wall thickness (e) were set at 341 MPa, 20 µm and 1.27 µm respectively [25]. For the sake of comparison, the Lc for flax fiber was calculated using an average diameter of 20 µm. Values of 644 MPa and 48.5 MPa for flax fiber and PLA tensile strength were respectively considered.

*Table 4-2: Assessment of Lc, critical fiber length, of hollow and solid fibers*

| Fiber geometry | Equation | Lc |
|---|---|---|
| *Flax (Solid) Fiber* | $L_C = \frac{\sigma_{maxf}}{\tau_m} \times \frac{\boldsymbol{D}}{\boldsymbol{2}}$ | 230 µm |
| *Hollow fiber with empty lumen* | $L_C = \frac{\sigma_{maxf}}{\tau_m} \times \boldsymbol{2}(\boldsymbol{e} - \frac{\boldsymbol{e^2}}{\boldsymbol{D}})$ | 29 µm |
| *Hollow fiber with filled lumen* | $L_C = \frac{\sigma_{maxf}}{\tau_m} \times \boldsymbol{e}$ | 15 µm |

As can be seen in Table 4-2, Lc of flax fibers, which is usually considered as a critical parameter for the reinforcement of polymer, increases with fiber diameter [54]. By contrast, MW floss outer diameter does not have a significant influence on the critical length. Thus,

and unlike flax fibers, the growing conditions and, to some extent, transformation steps seem to have no effect on the reinforcing capabilities of MW floss. Moreover, the values of Lc for MW floss are 87% and 93% smaller than that of flax fibers with empty and filled lumen respectively. Indeed, hollow fibers present a surface-to-volume ratio (S/V) much larger than solid fibers due to the inner and outer surfaces of the tube that facilitate stress transfers and thus decrease Lc. As an example, average S/V values of 0.2 $\mu m^{-1}$ and 1 $\mu m^{-1}$ were calculated considering the same diameter for a solid and a hollow fiber respectively. Furthermore, as the real average diameter of technical solid fibers tends to be much higher than that of a hollow fiber, S/V ratio differences tend to be even more pronounced.
Thus, thanks to its shorter Lc, MW floss should easily reinforce PLA compared to flax fibers. However, the reinforcement could be severely limited by the lower intrinsic mechanical properties of MW compared to that of flax fibers.

#### *4.5.1.6 Thermal resistance*

Thermal degradation of MW floss and flax fibers was assessed by TGA (Figure 4-3). TGA and DTG curves of MW floss and flax fibers exhibit the same global tendencies with three main mass losses resulting in three peaks on DTG curves. The first peak visible for both fibers at 100 °C was attributed to the loss of water with no significant difference between both fibers. Values of 4.5 ± 0.6 and 4.7 ± 0.3% were calculated for MW and flax respectively. However, the more pronounced peak for MW floss indicates that water evaporation occurs faster in MW floss than in flax fiber. This result can be related to the low thickness of the cellulosic wall of MW floss.

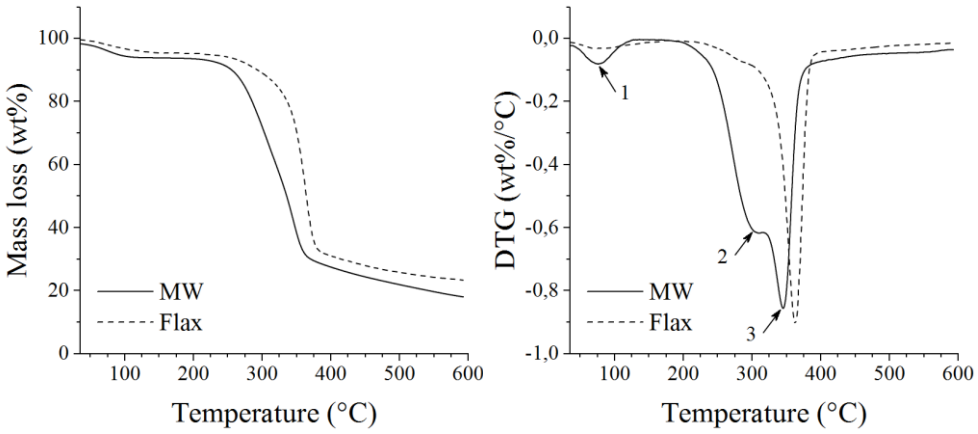


*Figure 4-3: TGA and first derivative (DTG) of MW floss and flax fibers*

The second peak between 290 and 300 °C was mainly attributed to lignin and hemicellulose degradation. Lignin presents a wide range of temperature of degradation from 244 to 309 °C [142], while hemicellulose presents a temperature of degradation ranging from 220 to 315 °C [95], [143]. However, the peak was more pronounced for MW floss due to its higher content of lignin and hemicellulose. It has been reported that hemicellulose and lignin contents of MW floss are about 27 and 15% respectively, and 20 and 2% for flax fibers [5], [22].

The major weight loss of both fibers, characterized by the third peak, was attributed to cellulose degradation. It is shown that the degradation of cellulose in MW floss occurs almost 20 °C earlier than for flax fiber (355 ± 0.7 °C as compared to 373 ± 1.1 °C). MW floss presents quite a low cellulose content (40–55%) and rate of crystallinity (30%) as compared to flax fibers (71% cellulose - 91% crystallinity) [5], [20]–[22], [144]. Therefore, the higher crystallinity of flax fibers leads to a higher temperature of degradation and a sharper peak [104].

With a temperature of degradation of 354 °C, MW floss is able to withstand heating steps during the molding process. However, fiber degradation was also studied through isothermal condition for 30 minutes at the processing temperature (i.e., 205 °C). Results showed that neither MW floss nor flax fibers demonstrate any degradation after 30 minutes at 205 °C which is in accordance with the results of Chen and Kuo [145]. The authors showed that hemicellulose, lignin and cellulose present no significant mass loss and consequently no degradation up to 225, 275 and 300 °C respectively [145].

## *4.5.2 Composite Characterization*

### *4.5.2.1 Effect of extrusion/injection process on fiber length*

Figure 4-4 shows a proper dispersion of both fibers with no evidence of agglomeration occurring during the extrusion and injection process. The difference in the number of fibers visible in the micrographs is related to the low intrinsic density of MW floss (0.3g/cc) compared to flax (1.2g/cc) and the constant volume rate of NF (1wt.%). The shortest length of MW after processing steps is mainly due to its natural brittle behavior, which is owed to its high lignin content [146].

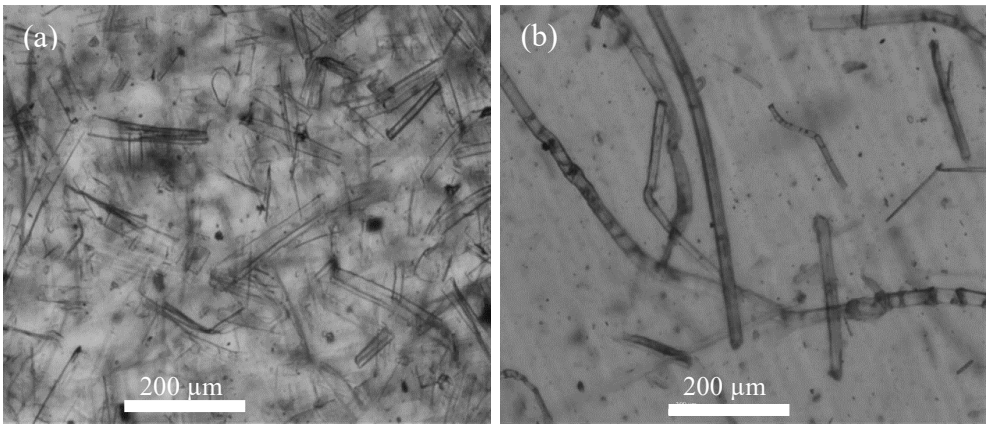


*Figure 4-4: Morphology of injected samples: a) MW/PLA, b) Flax/PLA.*

Figure 4-5 reports the cumulative distribution of post-processing length for MW floss and flax fibers which exhibit an average length ($\bar{L}$) of 106 ± 65µm and 251 ± 135 µm respectively. In regard to the standard deviations and maximum slopes of cumulative distributions (i.e., the population distribution width), flax fibers present a much broader distribution than MW floss. The longest length of flax fibers could be explained by less brittle behavior and better mechanical properties (Figure 4-5 and Table 4-1). In addition, Bos *et al.* showed that decreasing the content of fibers leads to fewer interactions during injection molding and thus, a longer final length [54]. As the volume of MW floss in the composite is almost four times larger than the volume of flax fibers for the same weight ratio, numerous interactions between MW floss fibers could happen resulting in a shorter final length.

The average lengths of the fibers after processing were compared to the theoretical Lc values determined above in Figure 4-5. Results showed that almost 87% of MW floss

presents an average length 3 to 5 times higher than the theoretical Lc ($Lc$ = 29-15 µm - $\bar{L}$ = 106 µm) depending on the filling of the lumen. On the opposite, 53% of the flax fibers are shorter than their theoretical Lc value with an average length almost equal to their theoretical Lc value in PLA ($Lc$ = 230 µm - $\bar{L}$ = 251 µm) and with a much broader distribution. The adhesion between flax fibers and PLA is therefore clearly more critical since half of the flax fibers do not reach their maximum reinforcement potential even in the case of a perfect interface stress transfer (i.e., the shortest Lc). As interfaces in composites are not perfect, the vertical lines representing the values of Lc will actually be shifted to longer lengths and the proportion of fibers below Lc will be even higher. Thus, the improvement of the mechanical properties of the Flax/PLA composites is limited as the population of flax fibers with a length below Lc will increase even more due to non-perfect bonding with the matrix (i.e., weak interfaces lead to longer Lc).

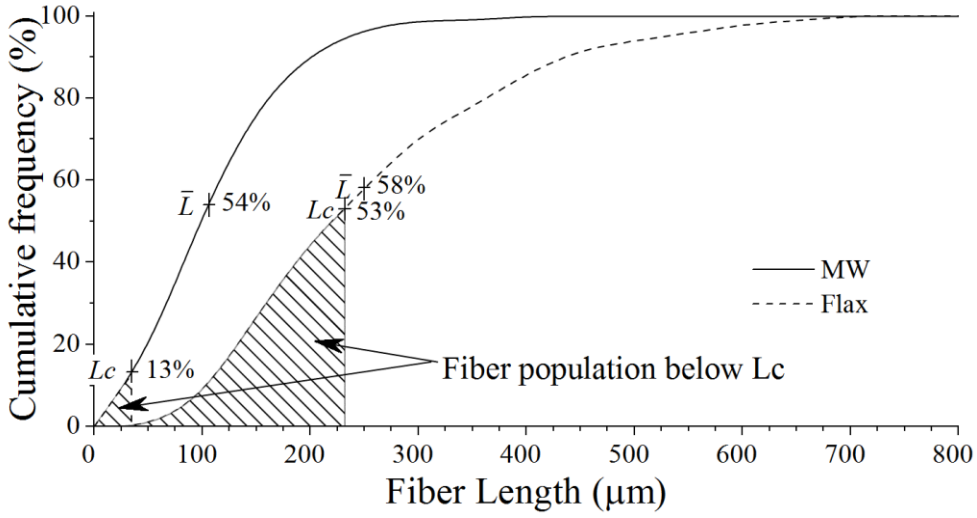


*Figure 4-5: MW floss fibers and flax fiber length cumulative distribution after injection molding*

### *4.5.2.2 Thermal behavior of composites*

The thermal behavior of the different composites was investigated using DSC. Flax/PLA and MW/PLA samples present a rate of crystallinity of about 15%, which indicates that neither flax fibers nor MW floss influence the crystallinity of PLA. No significant changes of the Tg, Tcc or Tm were observed.

### *4.5.2.3 Mechanical properties of the composites*

Tensile testing and DMA analysis were performed on PLA, MW/PLA, and Flax/PLA samples. Figure 4-6 shows their Young's modulus and UTS. The Young's modulus of MW/PLA and Flax/PLA composites increases by 11 and 9%, respectively, as compared to neat PLA. These results show that MW floss turned out to be more effective than flax fibers since MW floss exhibits an intrinsic tensile modulus 40% lower than that of flax fibers. Those results could be explained by the average length of MW floss that is higher than the critical one. Also, due to the higher volume ratio of MW compared to flax fibers, the probability of having a fiber that would fully participate to the composite tensile properties (i.e., oriented toward tensile solicitation axis) is much higher in MW/PLA.

The addition of MW floss and flax fibers to PLA leads to a decrease of 5 and 40% of the UTS, respectively. The same phenomenon was reported by David *et al.* and Oksman *et al.* for kenaf reinforced polypropylene and flax reinforced PLA respectively and was explained in both studies by a poor interfacial adhesion which leads to stress concentration and premature failure [122], [147]. Furthermore, the significant decrease of UTS found for Flax/PLA composite can also be related to the numerous surface defects found on the flax fibers as seen in Figure 4-4 and Figure 4-8. Indeed, flax fibers bending during extrusion led to the formation of numerous kink bands that induced stress concentrations and premature failure of flax fibers [148]. Finally, as previously discussed, it can be assumed that the remaining length of flax fibers compared to their respective Lc limits their reinforcing effect.

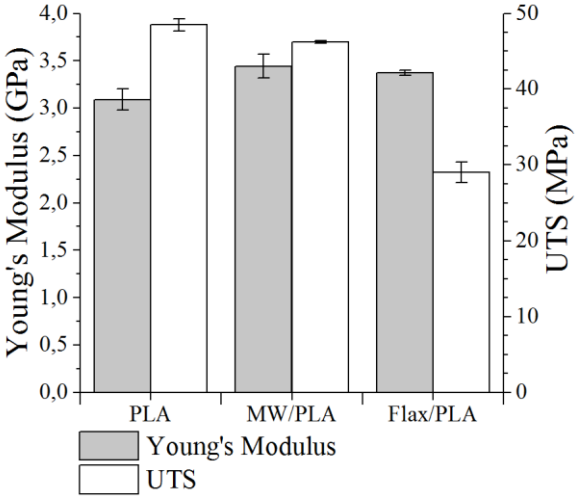


*Figure 4-6: Tensile test results of PLA, MW/PLA and Flax/PLA*

Figure 4-7 presents the storage modulus at 30 °C and the maximum tangent δ, measured using the single cantilever mode of composites. MW/PLA composite showed an increase of 11% of storage modulus as compared to pure PLA. However, and unlike tensile test results, Flax/PLA composite showed an increase of 29% of the storage modulus at 30 °C. This strong improvement can be explained by a longer length and better bending behavior of flax fibers compared to MW floss. Also, the moment of inertia of the cross-section of flax fiber (circular cross-section) is much higher than that of MW floss (annular cross-section).

Friction at the interface between fiber and matrix in composites is generally responsible for the increase of tangent δ as compared to neat matrices [149]. As presented in Figure 4-7, the consistency of the value of tangent δ between PLA, MW/PLA and Flax/PLA composite would tend to indicate that no further additional mechanisms of energy dissipation were induced by the addition of both NF in PLA. Therefore, regarding the constancy of the tangent δ, NF adhesion to PLA is extremely low for both composites.

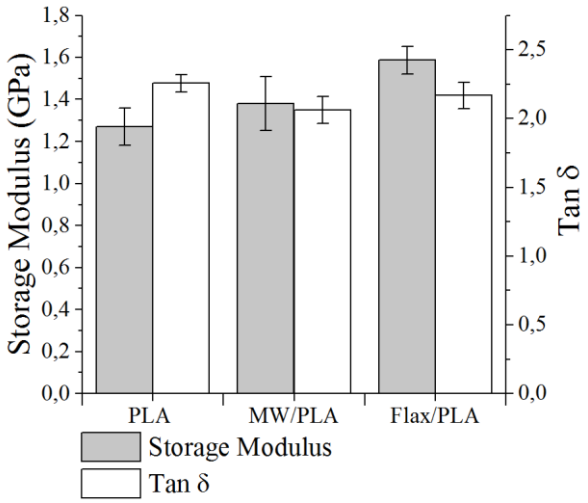


*Figure 4-7: Single cantilever results in DMA of PLA, MW/PLA and Flax/PLA*

### *4.5.2.4 Fractography and impact resistance*

Figure 4-8 presents typical micrographs of the rupture area of the composites after tensile testing. The fractography of the MW/PLA and Flax/PLA composites show numerous pulled out fibers and a lack of adhesion between PLA and both NF. It can also be noticed that the lumen of MW floss is filled with PLA despite its relatively high viscosity. Nonetheless, the adhesion of PLA with flax fibers seems to be better than with MW floss

since the surface of flax fibers appears strongly exfoliated by the debonding of the matrix. It is clear from Figure 4-7 andFigure 4-8 that the affinity between MW floss and PLA could be improved.

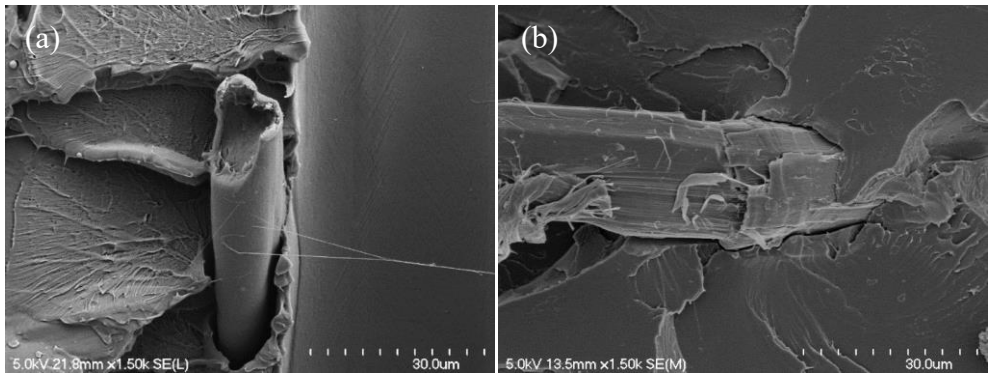


*Figure 4-8: Composite fractography, (a) MW/PLA, (b) Flax/PLA*

Results of Izod impact test are presented in Figure 4-9. It is clear from the results that the addition of MW floss in PLA has led to a significant improvement of the impact strength. An increase of 17% of the absorbed energy was measured for MW/PLA composite compared to pure PLA. On the opposite, the addition of flax fiber did not induce significant improvement of the toughness of PLA. The improvement of the fracture toughness induced by MW floss could mainly be attributed to the numerous interfaces induced by a better S/V ratio of MW.

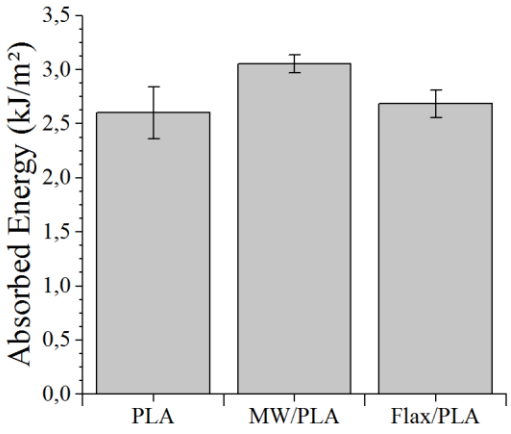


*Figure 4-9: Izod impact resistance of PLA, MW/PLA and Flax/PLA composites*

### *4.5.2.5 Water absorption*

The results of water uptake of composites and neat PLA are presented in Figure 4-10. For PLA, the water uptake was found to be equal to 1.18 ± 0.01% at equilibrium, whereas it was 1.32 ± 0.03 and 1.42 ± 0.04% for Flax/PLA and MW/PLA, respectively. The higher water uptake of both NF reinforced composites can be related to the hydrophilic behavior of cellulosic NF that absorb more water than PLA. Moreover, the gaps induced by the low compatibility between NF and PLA act as reservoirs and have certainly led to higher water absorption too [150]. Also, MW floss presents a much lower rate of crystallinity (56%) than flax fibers (71%) which may have contributed to higher water uptake in amorphous cellulosic phases [16,57].

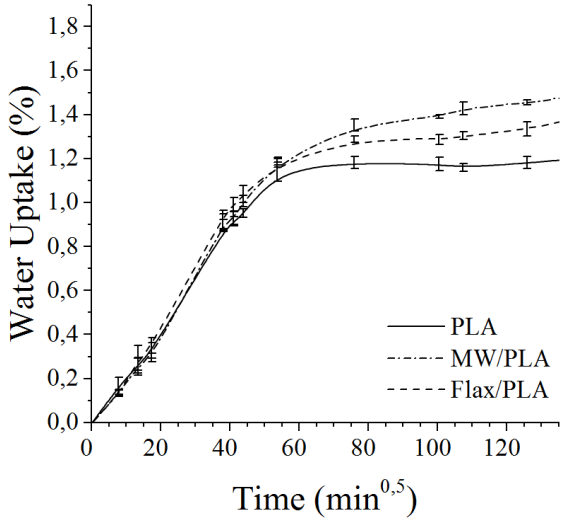


*Figure 4-10: Water uptake of PLA, Flax/PLA and MW/PLA*

## *4.6 Conclusions*

In this study, MW floss and flax fibers were used to reinforce PLA using conventional extrusion and injection processes. The interfacial adhesion between NF and PLA as well as the final mechanical properties of the composites were characterized. Based on the results presented in this study, the following conclusions can be drawn:

- Tensile tests have demonstrated that the mechanical properties of MW are not as high as those of flax fibers and other bast NF due to physiological differences between the two fibers. Still, an elastic modulus of 14 GPa and an UTS of 341 MPa were calculated for MW assuming an annular cross-section.

- MW demonstrates ground-breaking theoretical values of critical length (29-15 µm) and density (0.3 g/cc) compared to flax fibers (230 µm - 1.5 g/cc) but slightly lower thermal resistance that does not restrict its molding process.
- The processing of MW does not require special methods, as no fiber agglomeration was found after extrusion or injection molding. MW was found to be homogeneously dispersed and its structure did not collapse during processing because it was filled with PLA.
- Reinforcements of 11 and 9% were measured for the elastic modulus of MW/PLA and Flax/PLA respectively. A less severe decrease was measured on the UTS of MW/PLA than on Flax/PLA respectively compared to pure PLA. This result was related to a longer average length compared to the critical one (~5 for MW, ~1 for flax), fewer defects on MW surface and thinner fibers (i.e., better distribution of the reinforcements in the matrix for a steady percentage by weight).
- The better dispersion of MW associated with the pipe geometry were probably the main reasons for the 17% improvement in the fracture toughness compared to Flax/PLA and pure PLA.

The key results listed above demonstrate that MW leftovers, which are downgraded due to their length, could be used effectively as reinforcement for NF based composites. Moreover, the pipe geometry could induce unique opportunities on the lightness and insulation properties of composite materials. Nevertheless, the reinforcing effect of MW and, consequently, the mechanical properties of the composites, could be improved as a major lack of adhesion with PLA was demonstrated. However, this lack of adhesion, which should be the attention of future work, could be overcome by the use of surface treatments adapted to the thin structure of MW.

# *CHAPITRE 5 : EFFET D'UN TRAITEMENT ALCALIN OU D'UNE SILANISATION SUR LES PROPRIÉTÉS MÉCANIQUES DES BIOCOMPOSITES PLA-ASCLÉPIADE*

***Auteurs et affiliation :***

- *Ovlaque Pierre : Étudiant au doctorat, Université de Sherbrooke, Faculté de génie, Département de génie civil.*
- *Mohammadreza Foruzanmehr : Coordinateur scientifique, Université de Sherbrooke, Faculté de génie, Département de génie civil.*
- *Saïd Elkoun : Professeur, Université de Sherbrooke, Faculté de génie, Département de génie mécanique*
- *Mathieu Robert : Professeur, Université de Sherbrooke, Faculté de génie, Département de génie civil*

***Date de soumission :*** *16 mai 2019*

***Revue :*** *Composite Interfaces*

***Titre :*** *Milkweed floss fiber/PLA composites: effect of alkaline and epoxy-silanol surface modifications on their mechanical properties*

## *5.1 Résumé*

L'objectif de cette étude était d'améliorer les propriétés mécaniques des composites à base d'asclépiade et d'acide polylactique (PLA) en améliorant la compatibilité au niveau de l'interface. L'asclépiade est une fibre naturelle présentant une forme tubulaire unique, un large lumen et une section transversale mince. Ces fibres qui possèdent une surface spécifique élevée et peuvent conduire à une amélioration significative des performances mécaniques des composites. Cependant, l'asclépiade présente une mauvaise adhérence interfaciale avec le PLA. Cette étude évalue l'amélioration de l'adhérence et, par conséquent, des propriétés mécaniques des composites après traitement alcalin ou greffage d'agents de couplage époxy-silane sur la surface de l'asclépiade. La première partie de cette étude se concentre sur l'influence des différents traitements sur la géométrie, les propriétés mécaniques et la rugosité des fibres. La deuxième partie se penche sur l'étude et la caractérisation des composites constitués de 1 % en poids d'asclépiade traitée, produits par injection.

Les résultats ont montré que les propriétés mécaniques des fibres étaient significativement diminuées par les traitements de surface. Des diminutions respectives de 68 et 60 % du module de Young et de la résistance maximale en traction ont été mesurées pour l'asclépiade mercerisée. Les fibres traitées avec les epoxy-silanes suivent la même tendance avec des diminutions de 30 et 60 % du module et de la résistance des fibres. Néanmoins, des améliorations des propriétés mécaniques des composites ont été mesurées grâce aux traitements de surface. Des augmentations de la résistance maximum de 9 et 17% ont été calculées pour les composites avec fibres mercerisées ou traitées avec les epoxy-silanes, respectivement. Les micrographies de l'interface ont confirmé que l'adhérence entre les fibres et le PLA était améliorée, à plus forte raison dans le cas de l'utilisation d'epoxy-silanes.

## *5.2 Abstract*

The aim of this study was to enhance the mechanical properties of milkweed floss (MW)/polylactic acid (PLA) bio-based composites by compatibilizing the interface between the MW fibers and the matrix. MW floss is a natural fiber presenting a unique tube-like shape exhibiting a wide lumen and a thin cross-section. The addition of high specific surface area MW fibers to polymer matrix can lead to a significant improvement of mechanical performance of injection-molded composites. However, MW floss presents a poor bonding with PLA due to its smooth surface. This study evaluates the improvement of the adhesion and, consequently, of the composites' mechanical properties after alkaline treatment and grafting of epoxy-silane coupling agents onto the surface of MW floss. The first part of this study investigates the influence of the different treatments on the geometry, mechanical properties and roughness of MW fibers. Composites made of 1wt.% treated MW were then produced by injection molding and mechanical properties of composites were characterized. Results showed that the mechanical properties of MW fibers were significantly decreased by surface treatments. In fact, decreases of 68 and 60% of Young's modulus (E) and ultimate tensile stress (UTS) were respectively measured for alkali treated MW (NaOH-MW). Reductions of 30 and 60% were respectively calculated for E and UTS of epoxy-silane treated MW (Si-MW). Still, improvements in the composites' mechanical properties were measured, such as increases of the UTS of 9 and 17% for PLA reinforced

with NaOH-MW and Si-MW, respectively. SEM observations confirmed that the adhesion between the fibers and the PLA was greatly improved.

**Key-words:** Milkweed floss, Polylactic acid, Bio-based composite, Alkaline treatment, Epoxysilane.

## *5.3 Introduction*

Composite materials are widely used in many industrial fields, from automotive to aviation [152]. However, rising ecological concerns, as well as the strengthening of environmental laws, have become obstacles and forthcoming limitations for composite utilization [50], [153]. Indeed, the recycling of petroleum-based composites is still economically and technically hard to manage and consequently, 90% of the composites end their life in landfills [7].

Fortunately, several solutions arise to lay the foundations for a more sustainable composite industry. Among the solutions, the use of more sustainable materials such as bio-based matrices permits to produce greener composites. However, among all bio-based matrices available, only polylactic acid (PLA) reaches the requirements of availability and processability for large-scale applications. PLA is a thermoplastic matrix produced from renewable agricultural crops that competes the mechanical properties of well-established polypropylene resins [36]. However, PLA suffers from its low glass transition and low ductility, which restrict its utilization. Therefore, composites made of PLA reinforced with natural fibers (NF) have been intensely investigated and demonstrate great opportunities regarding price, brittleness, weight, carbon footprint, mechanical and thermal properties [122], [123], [130], [154]. Oksman *et al.* reported a 147% improvement of PLA stiffness by addition of 30 wt.% of flax fibers [122]. Nishino *et al.* showed that the storage modulus of PLA/Kenaf composites (70 vol.%) was maintained until PLA melting point (160 °C), whereas neat PLA showed a strong reduction of its mechanical properties above glass transition (i.e., 60 °C) [37].

Like bio-based matrices, NF also pave the way for a more sustainable composite industry by offering advantages such as weight reduction, low cost, high mechanical properties and low carbon footprint compared to synthetic fibers [6]. Among NF, bast fibers (i.e., fibers

extracted from the stem such as flax, hemp or jute) are frequently associated with composite applications due to their availability and superior mechanical properties [13], [27], [54], [69], [125]. Nevertheless, other types of fibers, such as hollow natural fibers (HNF) extracted from pods, like milkweed floss (MW) or kapok, can be used to reinforce organic matrices. Unlike bast fibers, which can be assimilated to cylinders with a very narrow lumen, HNF have a wide empty lumen that occupies 70 to 80% of their volume [23], [86]. HNF could induce several advantages including a very low density and good thermal and acoustic insulation properties[16], [100], [115]–[118].

Nevertheless, NF and therefore HNF show poor interactions with organic matrices that are mainly assigned to their surface chemistry [50]. Indeed, NF are composed of cellulose, which is reported to strongly limit their adhesion to polymeric matrices [63]. According to literature, the polarity and hydrophilicity induced by the numerous hydroxyl groups of cellulose are major obstacles to a good interaction with organic matrices. Thus, stress transfer is not optimal and the maximum shear stress at the interface is limited [50], [141]. In the case of HNF, the presence of waxes at the surface limits even more their interactions with matrices [83], [96], [112].

In spite of this natural lack of adhesion, strong bonding at the interface can be created through fiber treatments [121]. Of these, alkaline treatment is certainly the most common when it comes to NF [155]. It mainly aims at increasing the number of reactions with matrices by exposing cellulose microfibrils and converting hydroxide groups to alkoxide groups [5], [59]. Furthermore, alkaline treatment generally induces mechanical interlocking in composites by increasing NF roughness [59]. Alkaline treatments were applied to HNF by several researchers but no study focused on thermoplastic reinforcement purposes [94], [106]–[110]. Indeed, alkaline treatments of HNF are often used to improve their surface roughness in order to facilitate the transformation by spinning process [94]. Venkata Reddy *et al.* reported a great improvement of 17 and 46% of the tensile strength and modulus, respectively, of kapok fiber-based composites (unsaturated polyester) thanks to alkaline treatment (2% NaOH solution for 30 min) [109]. Less significant improvements of 6 and 4% of the flexural modulus and strength were reported, respectively, by the same researchers [106]. Another well-established way to enhance the interface of NF in polymeric matrices is using coupling agents. Silane-based coupling agents promote

covalent bonding between NF and polymeric matrices [13], [58], [59], [156]–[159]. Alcohol functions of hydrolyzed silanes are supposed to react with hydroxyl functions at the surface of NF to form covalent bonds. Wang *et al.* have shown that the use of epoxy-silane (3-Glycidyloxypropyl trimethoxysilane) provides good interactions between PLA and cellulose extracted from wood flour. An increase of 35% of the tensile strength was achieved with epoxy silanol as a coupling agent in PLA/cellulose composites [58].

The scope of the present study aims at investigating the effect of two different surface treatments (i.e., alkaline treatment and epoxy-silane coupling grafting) on the improvement of the interfacial adhesion between hollow MW fibers and PLA. The first part of the study was dedicated to the consequences of both treatments on the intrinsic properties of MW (i.e., geometry, mechanical properties and roughness). Knowing the influence of both treatments on the fiber, PLA samples reinforced with 1 wt.% MW were produced by injection molding and the effect of processing on the fiber morphology was studied. Eventually, the second part of the study focused on characterizing the resulting biocomposites and on assessing interfacial adhesion between MW and PLA.

## *5.4 Material and methods*

### *5.4.1 Materials*

Milkweed floss from species *Asclepias Syriaca* gown in Province of Quebec, Canada, was provided by Protec-Style (Canada). PLA 3100 HP pellets, injection molding grade, were purchased from Natureworks LLC. Sodium hydroxide pellets and epoxy-silane ((3-Glycidyloxypropyl)trimethoxysilane) were supplied by Sigma Aldrich. *Asclepias Syriaca* floss contains cellulose, hemicellulose and lignin in amounts ranging from 40 to 55%, 8 to 37% and 15 to 20%, respectively [21], [22], [160].

### *5.4.2 Fiber treatments*

#### *5.4.2.1 Alkaline treatment*

A concentration of 5 wt.% sodium hydroxide was used at room temperature to limit MW fibers degradation. The effect of soaking time on MW fiber structure as well as lignin and

hemicellulose removal were studied prior to composite manufacturing. MW fibers were immersed in the alkaline solution for 1, 5, 10, 30 and 60 min and then rinsed with distilled water. Afterward, MW fibers were briefly soaked in a 1% acetic acid solution and rinsed again with distilled water to adjust pH to 7. Eventually, alkaline treated MW fibers were dried in a vacuum oven at 50 °C for 24 hours.

#### *5.4.2.2 Silanization*

Prior to silanization, 5 wt.% of epoxy-silane was added to a 95:5 solution of water-ethanol to promote the hydrolysis of silane groups into silanol groups. MW fibers were pretreated with a boiling acetone reflux for 30 min under vigorous agitation to remove waxy components [123]. MW fibers were then immersed in the silanol solution for 90 min at room temperature. Afterward, treated MW fibers were dried in a vacuum oven at 105 °C for 24 hours to complete the epoxy-silane grafting [58].

### *5.4.3 Composite processing*

Neat PLA samples (PLA), MW fibers reinforced PLA (MW/PLA), alkaline treated MW fibers reinforced PLA (MW(NaOH)/PLA) and silane treated MW fibers reinforced PLA (MW(Si)/PLA) were produced using the following process. First, 1 mm thick sheets of PLA were produced by pressing pellets using a Carver press at 190 °C. Next, 1 wt.% of fibers were placed between two PLA sheets and pressed for 3 minutes at 190 °C to produce composite sheets, which were then crushed into flakes with an approximate size of 5 mm. Extrusion of the flakes was carried out with a Filabot single screw extruder at 180 °C using a 3 mm die and followed by a pelletizing step (a C.W. Brabender) to produce ready-to-inject composite pellets. Finally, pellets were injected in the form of tensile test specimens using a MPM 55-2P vertical mini injector at 205 °C under 1 kPsi.

### *5.4.4 Characterizations*

#### *5.4.4.1 Morphology*

A Veeco nanoscope IIIA atomic force microscope (AFM) was used in a non-contact mode to measure the roughness of fibers. Gwyddion software was used to calculate the

arithmetical mean roughness of 6 x 6 µm areas previously flattened with a third-order polynomial function. Five different fibers of each condition were tested in order to calculate their mean roughness (Ra).

Optical microscopy (OM) was performed using a Motic 580 digital camera mounted on a Nikon Optiphot microscope. Motic Image Plus 3.0. software was used to measure and analyze data. OM was carried out after tensile tests to determine the diameter at the fracture origin of MW fibers as well as the average length of the fibers and their dispersion in the composites.

A scanning electron microscope (SEM) Hitachi S3000-N was used to evaluate the effect of the two treatments on the fiber morphology. In addition, SEM observations were performed on fractured composite samples after tensile tests to assess the adhesion between the fibers and PLA.

#### *5.4.4.2 Mechanical properties*

Tensile tests on fibers were performed according to ASTM C1557-14 with a Zwick/Roell z050 machine. An average of at least 20 fibers was tested using a 5 N load cell and a crosshead rate of 2 mm/min. In order to calculate accurate values of Young's modulus (E) and ultimate tensile strength (UTS), diameter in the vicinity of the fractured area was measured for each fiber by OM. The cross-section area occupied by the lumen was not taken into account when calculating the mechanical properties of fibers. An annular cross-section with a constant cellulosic wall thickness of 1.27 µm was considered for MW and MW-Si fibers [25]. Due to the collapse of MW-NaOH fibers, the cross-section was approached as a rectangle with a thickness of 2.54 µm (twice the thickness of the cellulosic wall) and a width determined by OM.

Tensile tests on composites were carried out following ASTM D3039 standard test method at a rate of 2 mm/min with a 30 kN load cell. The strain of composites was determined with extensometers. Tests were conducted on five specimens for each condition.

Impact strength was measured with an Instron/Ceast 9050 at room temperature following ASTM D256 standard. Five Izod-type specimens were tested under impact loading with a 1 joule pendulum for each condition.

Dynamic mechanical analysis (DMA) was performed on a Perkin Elmer DMA 8000. The storage modulus (E') and maximum damping factor (tan δ) were determined. Five samples for each condition were tested using the single cantilever mode with a 0.1 N static force and a frequency of 1 Hz. Temperature scans were performed from 30 to 160 °C at 3 °C/min.

#### *5.4.4.3 Thermal properties*

Differential scanning calorimetry (DSC) was carried out on a Perkin Elmer DSC 6000. Temperature scans from 20 to 200 °C at 10 °C/min were performed on neat PLA as well as composites. Variations of glass transition temperature ($T_g$), cold crystallization temperature ($T_{cc}$) and melting temperature ($T_m$) were determined. Crystallinity was calculated following equation (1):

$$\chi = \frac{\Delta H_m - \Delta H_{cc}}{\Delta H_m°(1 - Wt_f)} \quad (1)$$

where $\Delta H_m$ and $\Delta H_{cc}$ are the melting and cold crystallization enthalpies, respectively, $\Delta H_m°$ the melting enthalpy of the 100% crystalline PLA and $Wt_f$ the weight fiber fraction of the composite. A value of 93.7 J/g was taken into account for $\Delta H_m°$ of PLA [123].

#### *5.4.4.4 Fiber modification*

Fourier-transform infrared spectroscopy (FTIR) was used to evaluate the efficiency of alkaline treatment and silanization of MW fibers. Characterization was performed with a JASCO 4600 FT-IR Spectrometer in attenuated total reflectance mode. Spectra were obtained after 32 scans from 600 to 4000 $cm^{-1}$ with a resolution of 4 $cm^{-1}$ at room temperature.

### *5.4.5 Statistical analysis*

Due to the low mass fraction of fiber in the composites, statistical analyses were performed to confirm the effect of fiber surface modification. Minimum confidence level was set at 5% (1 chance out of 20 that the results are not due to surface modification) to reject the null hypothesis. P-values were determined by using a one-tailed hypothesis from T scores results as the population was below 30. T scores were calculated according to equation 2.

$$Tscore = \frac{\mu_A - \mu_B}{\sqrt{\frac{\sigma_A^2}{n_A} + \frac{\sigma_B^2}{n_B}}} \quad (2)$$

where $\mu_A$ and $\mu_B$ are the mean values of the characteristic measured for samples A and B. $\sigma_A$ and $\sigma_B$ are the standard deviations found for these same samples and $n_A$ and $n_B$ the number of specimens tested for each condition.

## *5.5 Results and discussion*

### *5.5.1 Surface treatments*

#### *5.5.1.1 Silane grafting*

FTIR analyses and energy dispersive spectroscopy (EDS) were performed to verify the grafting of silanes on MW fibers. EDS spectra presented in Figure 5-1 revealed the presence of silicon atoms on MW floss surface that can confirm the presence of epoxysilanol. The nature of the bonds created between epoxy-silanol and MW was studied by FTIR and presented in Figure 5-2. Two new absorption peaks at 836 and 850 $cm^{-1}$ can be noticed on the MW-Si spectra compared to MW. According to Gañán *et al.*, the peak at 836 $cm^{-1}$ is induced by Si-C links and validates the presence of epoxysilanol on the surface of MW fibers, but not necessarily grafted, as revealed by EDS [161]. However, the peak at 850 $cm^{-1}$ is characteristic of bonding creation between silanol and cellulose and was related to a successful grafting of the epoxysilanol on MW fibers[162]. It is noteworthy that the presence of the cellulose-silanol bonding peak (i.e., 850 $cm^{-1}$) was only achieved after the pre-treatment with boiling acetone.

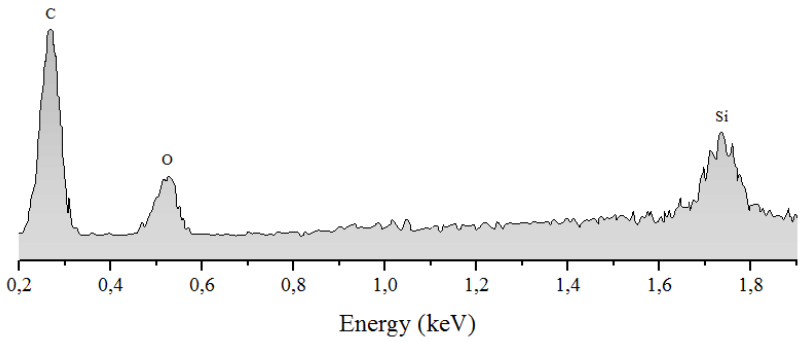


*Figure 5-1: EDS of the surface of a MW-Si fiber at 5 keV (normalized to carbon peak)*

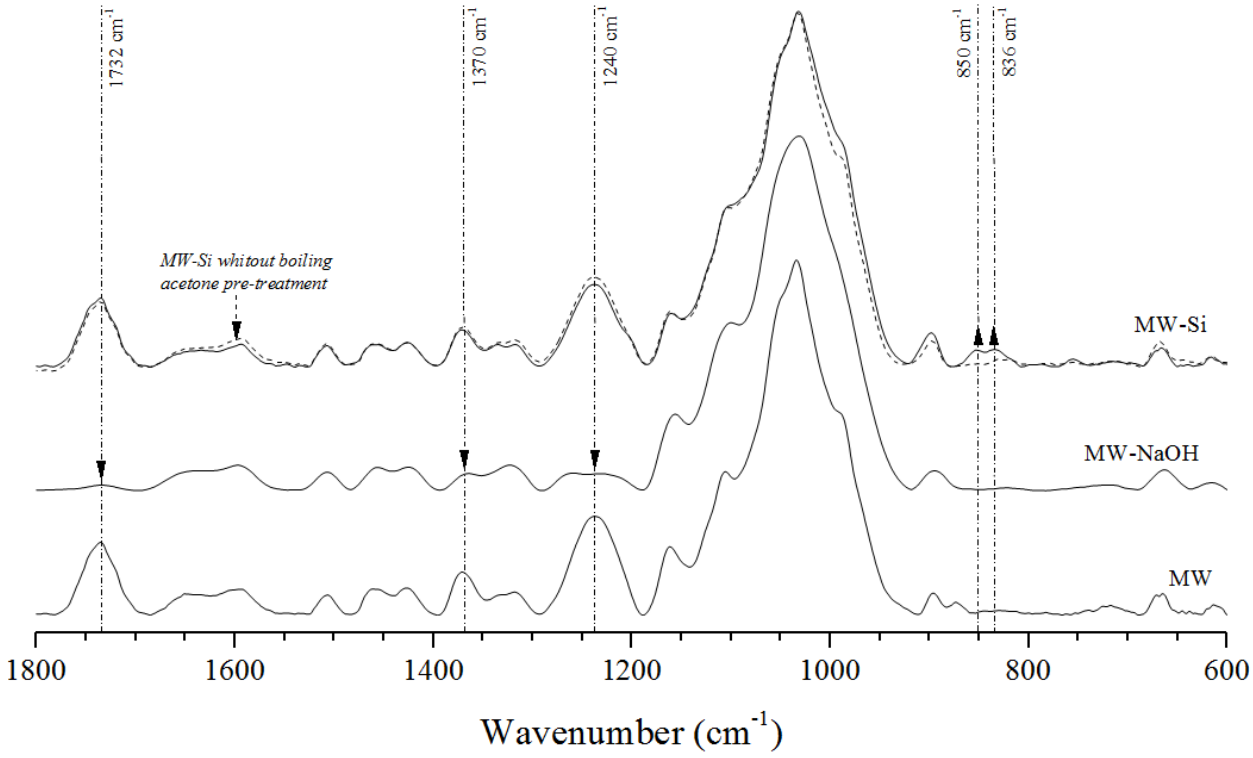


*Figure 5-2: FTIR spectra of MW, Mw-NaOH (5 min) and MW-Si (normalized to 1030 $cm^{-1}$)*

### *5.5.1.2 Alkaline treatment*

The effect of soaking time on the geometry of MW fibers is presented on the micrographs of Figure 5-3. According to SEM micrographs, a soaking time of 1 min did not induce any significant surface modification while soaking times longer than 5 min induced drastic alteration and collapsing of MW fibers. The attenuation of the absorption peaks at 1732 $cm^{-1}$, 1370 $cm^{-1}$ and 1240 $cm^{-1}$ on MW-NaOH spectra (Figure 5-2), corresponding to hemicellulose, polysaccharides and lignin, respectively, can be related to this alteration

[94]. The effect of soaking time on the absorbance of lignin (1240 $cm^{-1}$) and hemicellulose (1732 $cm^{-1}$) peaks after normalization to the 1030 $cm^{-1}$ peak was plotted and can be seen in Figure 5-4. It is noteworthy that the plateau starting after 5 min seems to correlate with the collapsing of the fiber noticed in Figure 5-3. Therefore, it may be concluded that the removal of lignin and hemicellulose, often considered as the cement that bonds cellulose microfibrils in NF, is responsible for the collapsing of MW fibers [5].Complete destruction of the hollow pipe geometry was also reported by Karthik and Murugan but for longer soaking times (10 min) [39].

As a result, a soaking time of 5 min was chosen to treat the fibers as most of lignin and hemicellulose were removed (Figure 5-4) and MW geometry seems less damaged than for longer times (Figure 5-3).

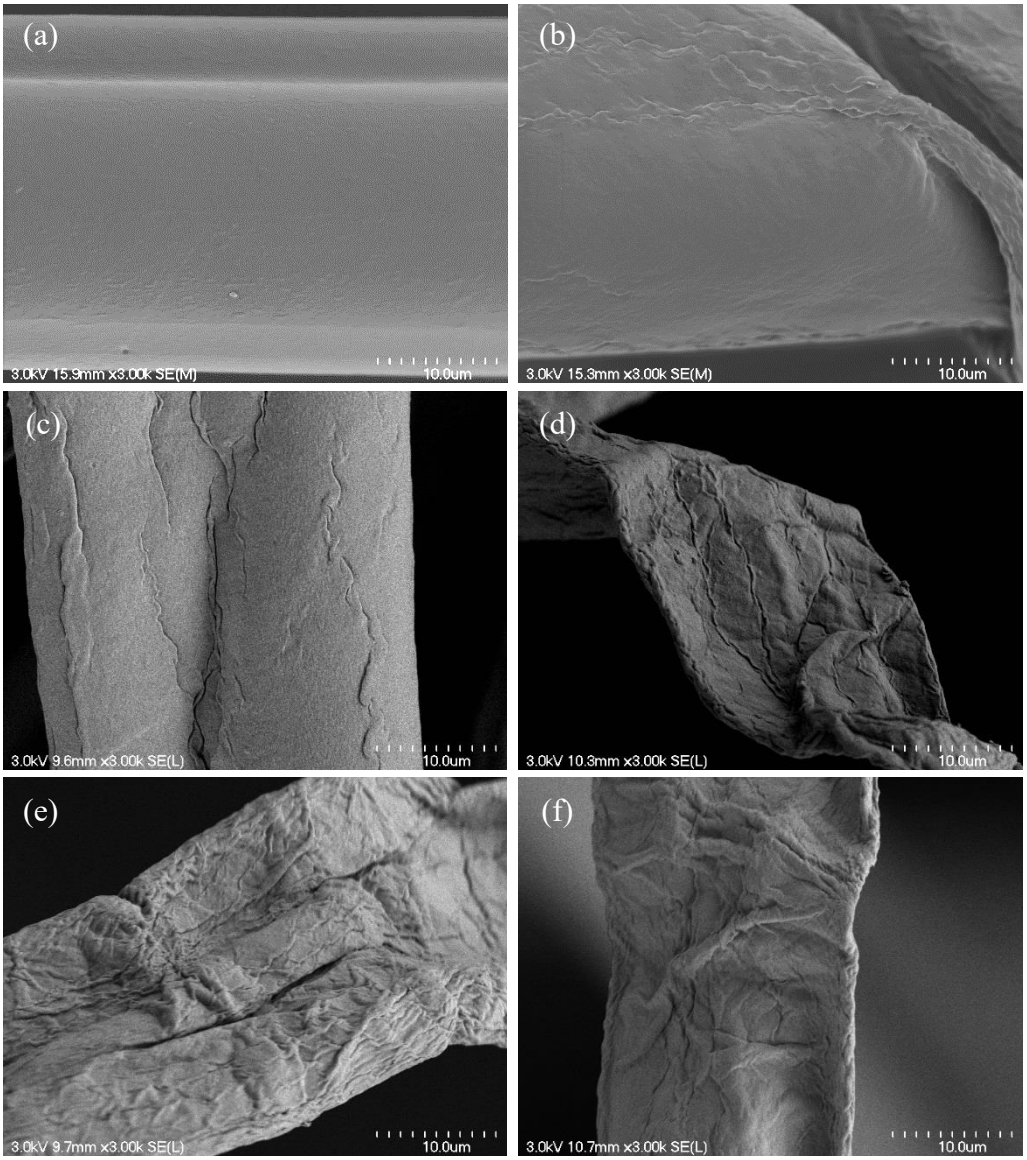


*Figure 5-3: Effect of soaking time in NaOH solution (5 wt.%) at room temperature on MW surface and geometry (a) raw MW, (b) 1 min, (c) 5 min, (d) 10 min, (e) 30 min, (f) 60 min*

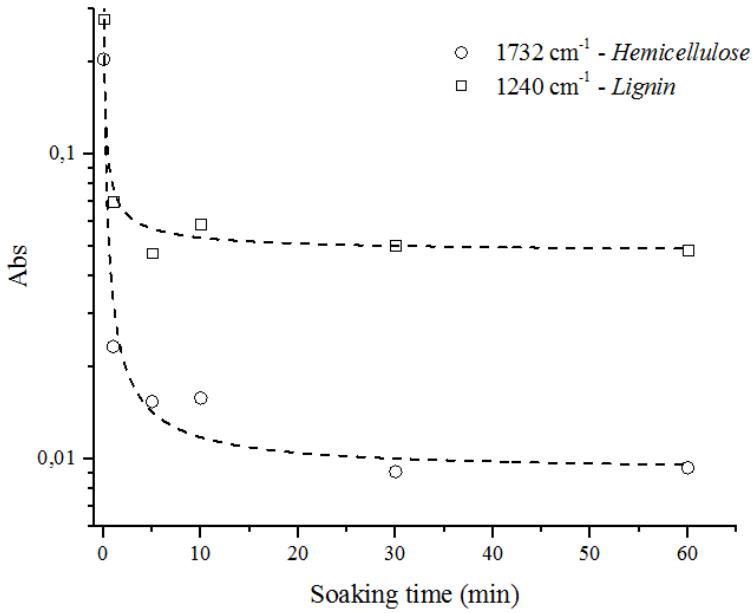


*Figure 5-4: Effect of MW soaking time in NaOH solution (5 wt. % - 25 °C) on the absorbance measured by FTIR on lignin (1240 $cm^{-1}$) and hemicellulose (1732 $cm^{-1}$) peaks. All FTIR spectra were normalized to the 1030 $cm^{-1}$ peak prior to a readout of values*

## *5.5.2 Fiber characterization*

### *5.5.2.1 Morphology and roughness of treated fibers*

Figure 5-5 presents the morphology of raw MW, MW-NaOH and MW-Si fibers. Alkaline treatment and silanization had a different effect on the resulting geometry and roughness of MW fibers. As mentioned before, the alkaline treatment affects MW-NaOH geometry and surface. Conversely, MW-Si did not suffer from any geometrical modification neither after the boiling acetone pretreatment nor the silanization soaking step.

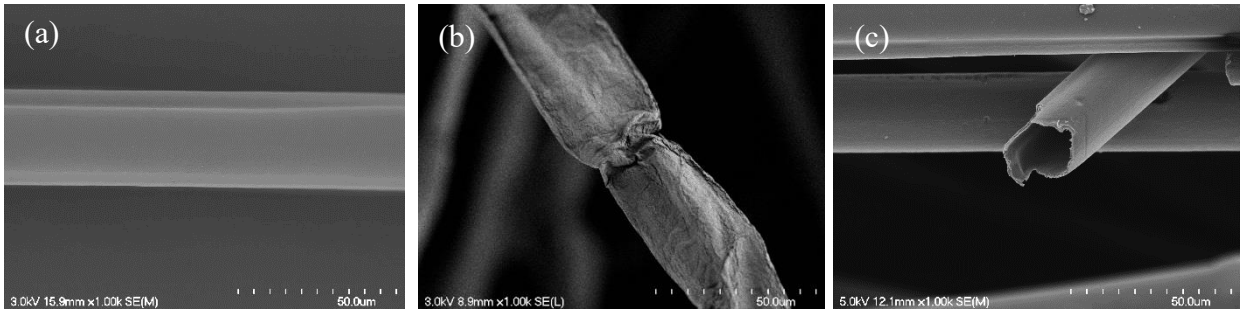


*Figure 5-5: SEM micrographs of MW (a), MW-NaOH (b) and MW-Si(c)*

The fiber roughness was characterized by AFM and topography of MW, MW-NaOH, and MW-Si fibers, using identical height and color scales, are presented in Figure 5-6. As

Figure 5-6 (b) suggests, MW-NaOH surface was highly impaired by the treatment, and rough spots and crevices can easily be noticed in comparison with the natural smooth surface of MW. Alkaline treatment had successfully increased the surface roughness and might help improve the MW/PLA interface by promoting mechanical interlocking. Average measured roughness demonstrated a remarkable increase of 108% from 10.03 ± 0.45 nm for MW to 20.9 ± 2.31 nm for MW-NaOH (p-value = 0.1%). On the contrary, and as Figure 5-5 (c) suggests, the roughness of MW-Si was not significantly modified (p-value = 16.6%). In fact, a roughness of 11.50 nm with a standard deviation of 2.26 nm was measured for MW-Si fibers.

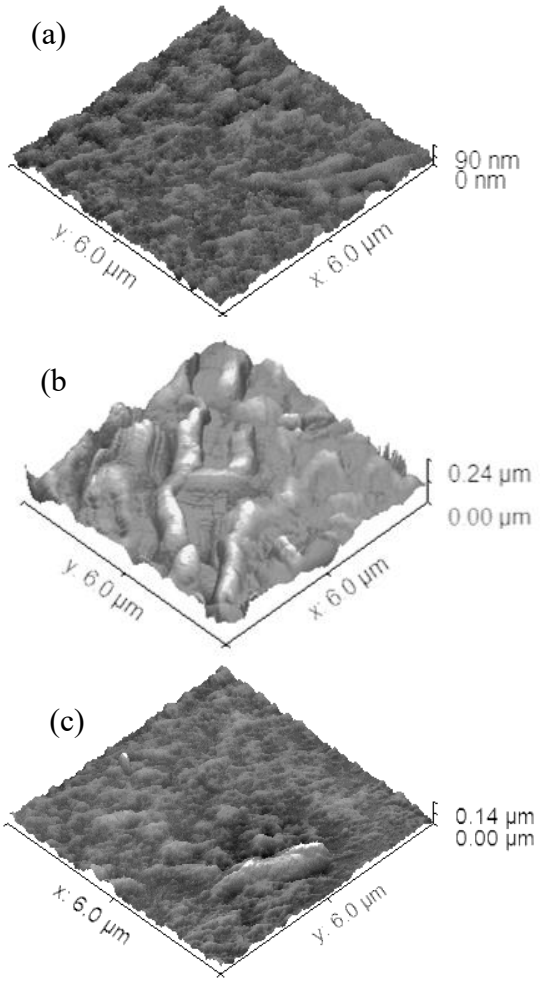


*Figure 5-6: Topography of (a) MW, (b) Mw-NaOH and (c) Mw-Si (homogenized scale and colors)*

### *5.5.2.2 Mechanical properties of fibers*

The effects of surface treatment on the elastic modulus, UTS and strain at break of different fibers are presented in Table 5-1. The results clearly showed that the use of alkaline treatment led to a large decrease in the mechanical properties of MW fibers as both modulus and UTS were decreased by 68 and 60% after treatment, respectively. This sharp decrease in MW-NaOH mechanical properties could be correlated to several phenomena. Firstly, the removal of lignin and hemicellulose that bind cellulose microfibrils inside NF can explain the decrease of mechanical properties[163]–[165]. Secondly, the increase of surface roughness after alkaline treatment leads to potential stress concentration in the thin wall of MW fibers that might induce premature failure. Thirdly, the significant increase of elongation (p-value = 3.1%) of MW-NaOH compared to MW could affect the measurements of the mechanical properties. Indeed, unlike MW, which is straight and directly aligned with the tensile axis, MW-NaOH appears curly. MW-NaOH may have adopted an additional low stiffness spring behavior because of its curliness that might have interfered with mechanical properties calculation, leading to higher elongation and, so, lower modulus. Finally, the alkaline treatment led, to some extent, to a conversion of cellulose I to cellulose II, which was reported to have lower mechanical properties [166].

Same tendencies were found regarding MW-Si fibers. However, the decrease of Young's modulus (30%) was less severe but UTS decreased by 60%, from 341 to 143 MPa. Finally, the maximum elongation of MW-Si appeared to be shortened by the silane treatment with a 30% decrease in the calculated strain (p-value = 0.8%). The modification of MW mechanical properties was somehow not expected for MW-Si, as no major components were removed from the fibers according to FTIR analysis. This may be due, to some extent, to drying at 105 °C of MW-Si, which may result in a decrease in E and UTS [53]. In addition, it was reported that silanol molecules are able to penetrate into the cellulosic wall (bulking treatment) [156]. Since MW fibers have a very thin cellulosic wall, silanol molecules may easily interfere with the structure of the cellulosic wall and act as a plasticizer in the fibers.

Reductions of fiber mechanical properties induced by alkaline or silane treatments were also reported in the literature dealing with bast fibers [121], [157]. Both chemical treatments induced a drastic fiber modification that could, at last, mitigate the improvement of the fiber matrix interface and thus, the global mechanical properties of composites.

| | Young's Modulus (GPa) | SD* | UTS (MPa) | SD* | Strain Max (%) | SD* |
|---|---|---|---|---|---|---|
| MW | 14.1 | 2.2 | 341 | 116 | 3.02 | 0.99 |
| MW-NaOH | 4.5 | 1.8 | 145 | 54 | 4.01 | 1.42 |
| MW-Si | 9.8 | 1.8 | 143 | 60 | 1.99 | 0.60 |

* Standard Deviation

*Table 5-1: Tensile properties of raw and treated fibers*

## *5.5.3 Composites improvement*

### *5.5.3.1 Length distribution*

The fiber length distributions and their related micrographs after injection molding are presented for each composite sample in Figure 5-7 and Figure 5-8, respectively. No major differences were measured between MW and MW-Si average length ($\bar{L}$) and distribution (108 ± 65 µm and 126 ± 63 µm for MW and MW-Si fibers, respectively). This result is surprising since the remaining mechanical properties of MW-Si were found to be much lower than those of raw MW. Moreover, MW-NaOH presented a higher $\bar{L}$ (213 ± 97 µm) with even lower fiber tensile properties. It is more than likely that $\bar{L}$ was related to the bending properties rather than the tensile properties. Unlike MW and MW-Si, MW-NaOH fibers were able to bend due to their collapsing (i.e., ribbon shape) as demonstrated in optical micrographs presented in Figure 5-8. Therefore, it was easier for MW-NaOH fibers to avoid a length reduction during extrusions. It should also be noticed in Figure 5-8 that neither alkaline treatment nor silanization induced fiber agglomeration during processing.

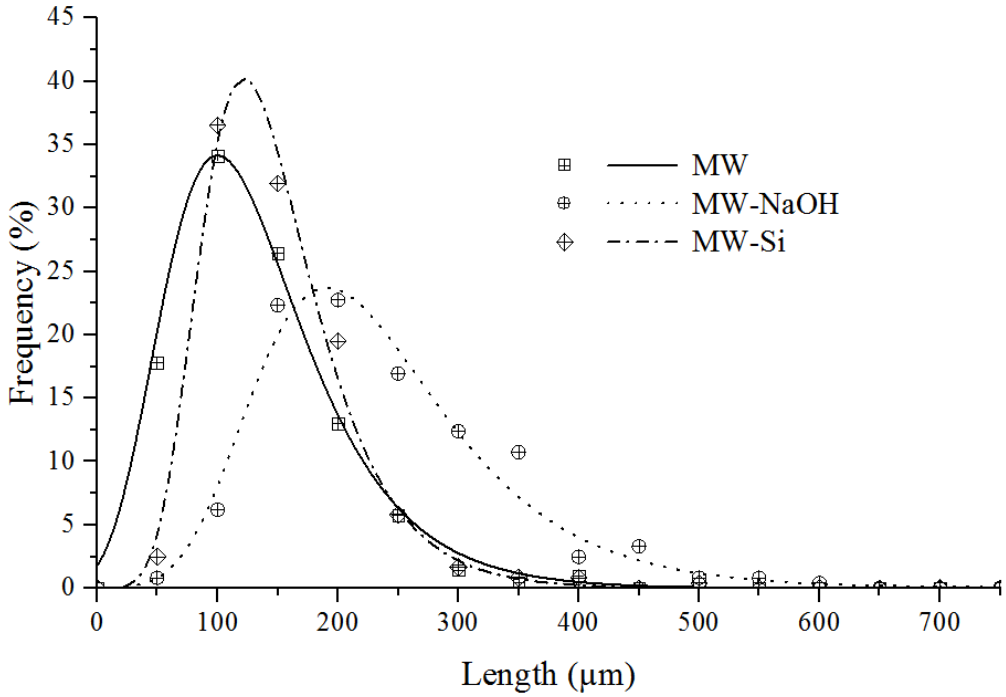


*Figure 5-7: Length distribution of MW, MW-NaOH and MW-Si after injection molding*

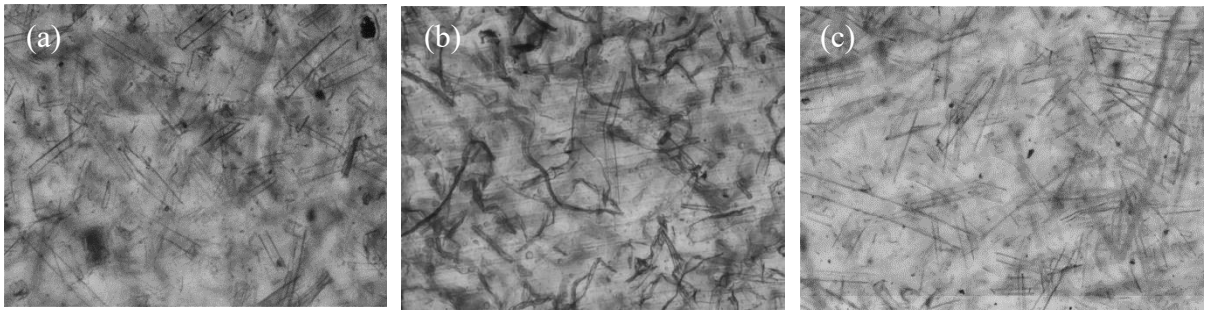


*Figure 5-8: Fiber dispersion in PLA after injection, (a) MW, (b) MW-NaOH and (c) MW-Si*

### *5.5.3.2 Thermal properties*

Crystallinity rates and characteristic temperatures ($T_g$, $T_{cc}$ and $T_m$) were measured in order to isolate mechanical properties results from a crystallinity difference or thermal degradation of PLA. Crystallinity rates were found to be constant (15%), regardless of the treatment, and could be explained by the high cooling rate of injected tensile specimens. Steady temperatures of 63, 96 and 183 °C were respectively determined for $T_g$, $T_{cc}$ and $T_m$ of PLA and composites. Therefore, only the interfacial adhesion and fiber intrinsic mechanical properties should be considered as the origin of the composites' mechanical properties changes.

### *5.5.3.3 Mechanical properties*

Composites tensile properties are presented in Figure 5-9. No significant differences were found between Young's modulus of MW/PLA, MW(NaOH)/PLA and MW(Si)/PLA composites. These results could show that the interface was successfully improved, as the two surface treatments induced a significant decrease of fiber modulus which was not reflected in that of composites. However, Young's modulus is determined for low deformations that only slightly stress the interface. Its variations are therefore not as relevant as those of the UTS to evaluate the quality of the fiber/matrix adhesion. Indeed, the UTS is measured at the very end of the tensile test when the interface is subjected to high stress.

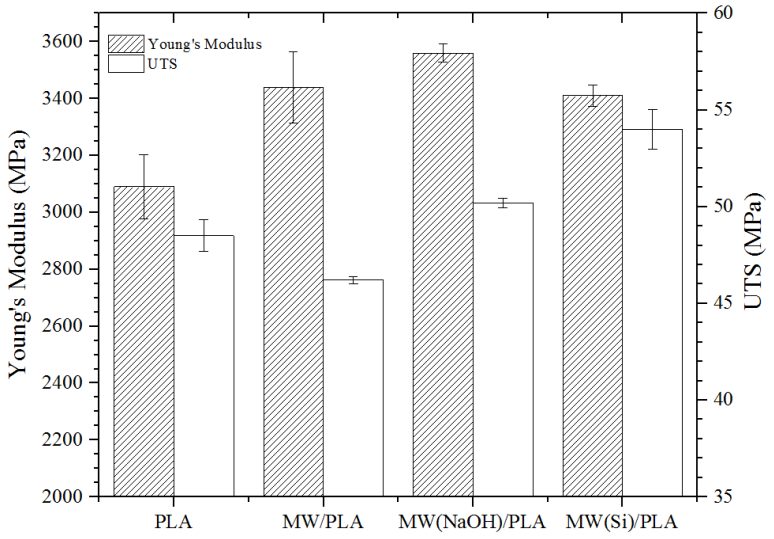


*Figure 5-9: Tensile properties (Young's modulus and UTS) of PLA and composites (SD as error bars)*

The addition of MW fibers in PLA led to a short diminution of the UTS (-5%) that was attributed to a lack of adhesion between MW and PLA, which generated stress concentration in the matrix. Significant differences (p-values lower than 0.01%) were found between MW/PLA and both treated composites. Increases of 9 and 17% of the UTS were measured for MW(NaOH)/PLA and MW(Si)/PLA, respectively, compared to MW/PLA. These increases would support an improvement of the interface related to both surface treatments. Nonetheless, UTS values were probably limited by the significant decrease of MW-NaOH and MW-Si intrinsic UTS.

The values of the storage modulus of composites obtained using the single cantilever mode are presented in Figure 5-10. The results show that MW(Si)/PLA composites present a higher storage modulus (1.62 GPa) as compared to other conditions (1.48 and 1.38 GPa for MW(NaOH)/PLA and MW/PLA respectively). This difference can be mainly attributed to the quality of the interface and possibly, to the higher length of MW(NaOH) fibers. Tan δ results supported an improvement of the interface. Indeed, the reduction of tan δ indicates a decrease of the viscoelastic behavior of the composites, and therefore a greater influence of MW fibers (elastic behavior) on the final properties. However, no significant difference was found between both treated MW composites.

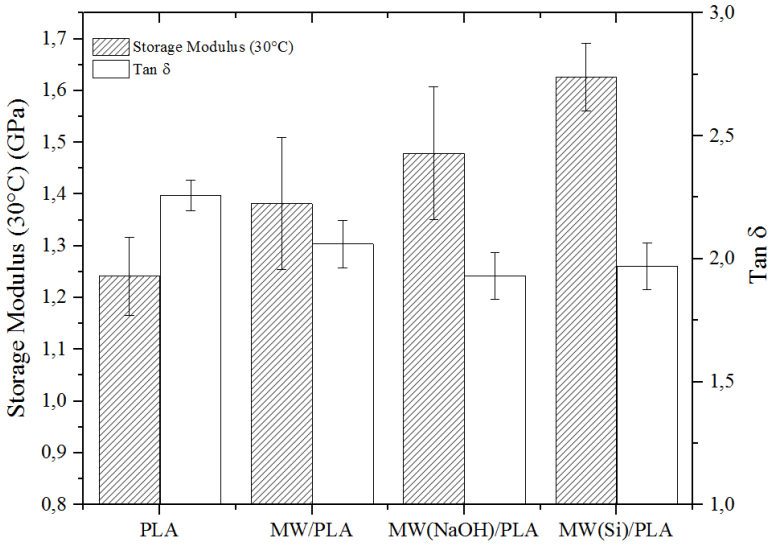


*Figure 5-10: Storage modulus and tan δ (single cantilever) of PLA and composites (SD as error bars)*

The improvement of mechanical properties reported in Figure 5-9 and Figure 5-10 can also be related to a decrease of the critical fiber lengths, which is the minimum length required for a fiber to reach its UTS when loading the composite. Its determination using conventional methods (single fiber fragmentation or pull out tests) was not successful with the MW/PLA system due to the low strain at break of PLA. Usually, the better the interfacial adhesion, the shorter the critical length and the greater the reinforcing effect in the composite. Thus, according to the decrease of damping factor in Figure 5-10, stress transfer at the interface was improved by the two surface treatments and logically led to shorter critical lengths for both treated MW. This reduction of critical lengths coupled with

longer average lengths of treated fibers resulted in a more efficient reinforcing effect and, to some extent, enhanced mechanical properties.

The mechanical properties presented in Figure 5-9 Figure 5-10 are clearly superior to those predicted by the rule of mixture (ROM). It should be remembered that the ROM is quite limited when used to describe and predict the mechanical properties of short natural fiber composites. Critical parameters such as voids, fiber orientation, curvature, lumen size, cross-section, packing, moisture content, densification, morphology and length are not considered in the ROM despite their influence on the mechanical properties of composites [53]. In addition, the mechanical properties presented in Table 5-1 were determined with a gage length much longer than the actual length of the MW fibers in the composites (about 100µm according to Figure 5-7). Thus the values reported in Table 5-1 cannot be used directly in the ROM because they underestimate the mechanical properties of MW fibers in composites. Indeed it was proven that the longer the gage length, the lower the mechanical properties appear due to the increased probability of failure [167], [168]. For instance, Anderson et al. found that the UTS of flax fibers decreased from 960 to 730 MPa with an increase of the gage length from 5 to 20 mm [167]. Moreover, it was shown that fibers with a small cross-section induced a better reinforcement effect [53]. In the present case, MW cross-section is extremely small compared to that of solid natural fibers. MW fibers exhibit an average cross-section of about 70 µm² while that of solid fiber with a diameter of 100 µm would be 8000 µm². Finally, according to the literature, it is not uncommon for the measured mechanical properties to exceed those predicted by the ROM for low fiber contents. 5 wt.% of hollow fibers (kapok fibers) used in unsaturated polyester led to an increase of 300 and 50% of the flexural modulus and strength, respectively [106]. Grande and Torres reported a 19% improvement in the tensile strength of high-density polyethylene with the addition of 1wt.% of jute fibers [63].

#### *5.5.3.4 Interfacial properties*

Figure 5-10 and Figure 5-11 present Izod impact results and SEM micrographs of fractured composite specimens, respectively. PLA exhibited an impact toughness of 2.6 kJ/m², whereas MW/PLA, MW(NaOH)/PLA and MW(Si)/PLA showed values of 3.05, 3.04, 2.71 kJ/m² respectively. The increase of impact toughness between neat PLA and composites

was attributed to the creation of numerous interfaces. Indeed, interfaces strongly interfere with fracture propagation and are responsible for the impact toughness increase in composites [169]. However, the differences between the composites can be mainly attributed to the quality of the interface because the fiber mass fraction was kept constant and the fiber lumens were filled by the PLA in each composite.

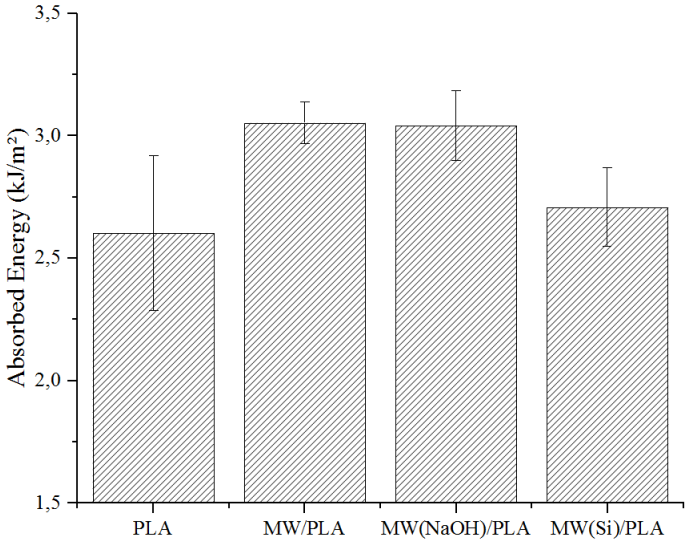


*Figure 5-11: Izod impact absorbed energy (SD as error bars)*

For MW/PLA composites, Figure 5-12 (a) shows fiber pull out that could be responsible for high energy dissipation during crack propagation. Pulled out fibers are characteristic of weak interfaces in which crack propagation takes place at the interface and results in a complete fiber debonding. This type of debonding would acknowledge a low stress transfer between PLA and MW and so, lower mechanical properties of MW/PLA as discussed previously in Figure 5-9 and Figure 5-10.

Concerning MW(NaOH)/PLA composites, it seems that the alkaline treatment did not strongly improve the interfacial adhesion. Indeed, the consistency between MW/PLA and MW(NaOH)/PLA in Figure 5-11 would indicate a similar mechanism of energy dissipation (i.e., through the interface).Figure 5-12 (b) tends to support this hypothesis since the failure of MW(NaOH)/PLA occurs at the interface between the fiber and the matrix. However, no fiber slippage was noticed by SEM. Slippage was possibly restrained by mechanical interlocking due to the improvement of the roughness as well as the tendency of MW-NaOH to bend. Therefore, the improvement of mechanical properties discussed before

could be mainly due to mechanical interlocking rather than a real improvement of the interfacial adhesion.

On the other hand, silanol grafting generated a significant decrease in the impact toughness (-11%, p-value = 1.5%). In addition, the SEM micrograph of MW(Si)/PLA (Figure 5-12(c)) displays a different mode of failure compared to that of MW/PLA and MW(NaOH)/PLA. It can be noticed that fracture mostly occurred through the fiber. The decrease of the impact toughness and the fracture behavior of MW(Si)/PLA composite confirmed a great improvement of the fiber/matrix adhesion. Indeed, a strong bonding at the interface leads to a more brittle behavior in fiber vicinity [13]. Therefore, the fracture propagation consumes less energy (less restrained) and is mainly driven through the fiber [123]. Still, this conclusion was only possible with PLA-filled fibers (Figure 5-12 (c)). Empty MW fibers, even with a strong interface, would have led to an increase in absorbed energy due to the high dissipation of energy generated by their lumens. Izod, DMA, SEM and tensile tests clearly showed that epoxy-silane grafting successfully improved the adhesion of MW fibers to PLA, which explains the improvement in the mechanical properties of composites.

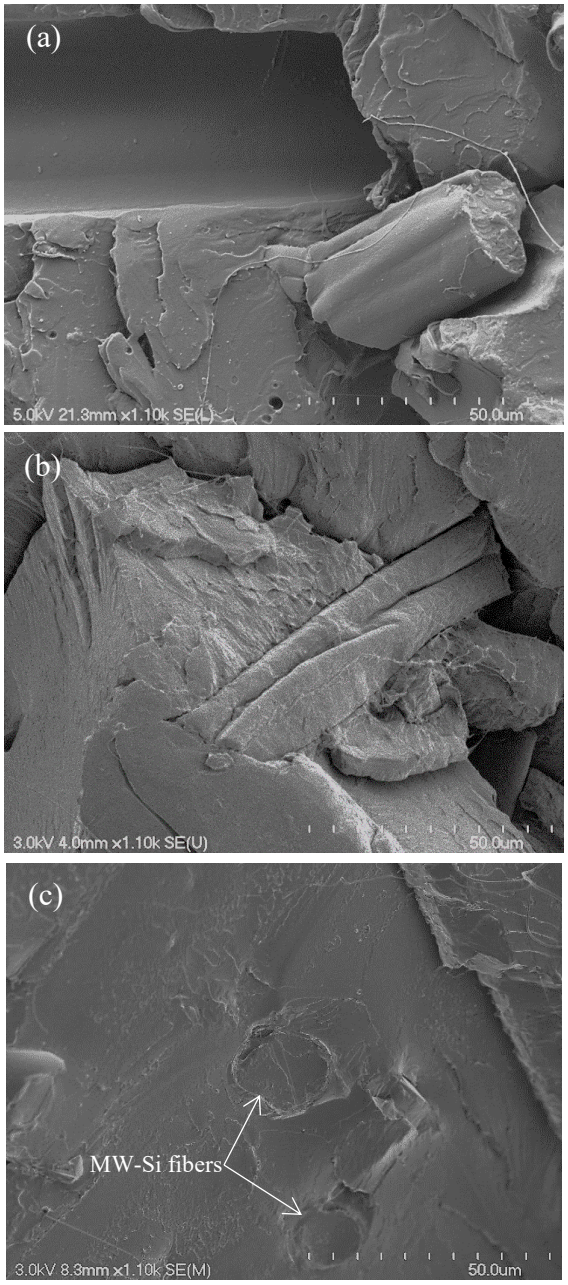


*Figure 5-12: Fractured samples interface (a) MW/PLA, (b) MW(NaOH)/PLA, (c) MW(Si)/PLA*

## *5.6 Conclusion*

In this study, MW fibers were treated with alkaline treatment and silanol coupling agents to improve the adhesion to PLA. MW/PLA bio-based composites were prepared by injection molding and characterized. Based on the results presented in this study, the following conclusions can be drawn:

- FTIR analysis shows that both treatments were successfully applied to MW hollow fibers. The alkaline treatment (5% -20 °C) was stopped after 5 minutes because most of the lignin and hemicellulose were extracted. Concerning the silanization, the dewaxing pretreatment was mandatory to form covalent bonds between fibers and silanols.
- Both treatments, mainly studied and developed on bast NF, have induced adverse effects. The alkaline treatment, which triggered a desired increase in roughness (+108%), led to a collapse of the fiber and a 68 and 60% decrease of E and UTS, respectively. Side effects were more limited with silanization, no change in morphology or roughness was induced. Only a smaller decrease in mechanical properties was measured (-30 and -60% on E and UTS, respectively).
- The alkaline treatment impacts the final average length of MW fibers in composites. While no difference was found between the average length of MW and MW-Si fibers, MW-NaOH fibers were 2 times longer. This was due to the collapse of the fiber, which limits the breakage during extrusion and injection.
- MW(NaOH)/PLA exhibited a higher UTS compared to MW/PLA biocomposites (+9%). This increase is mainly due to mechanical interlocking and fiber entanglement in PLA. Indeed, fractography and impact tests results did not show a significant improvement in the interface.
- MW(Si)/PLA biocomposites fractography acknowledged a significant improvement of the quality of the interface leading to a better stress transfer and increased UTS (+17%) compared to MW/PLA. This improved reinforcement may be related to the creation of a covalent bonding at the interface.

The epoxy-silanol surface treatment of MW fibers appears to be a good solution for improving interfacial affinity with PLA. However, the mechanical properties of the composites were probably limited by the degradation of MW fibers induced by the surface treatment. Therefore, in spite of the improvement of the properties, it makes little sense to degrade a natural product (MW) to make it compatible with a synthetic product (PLA). The poor interfacial adhesion that leads to poor bio-based composites should be managed by a modification of the matrix or by finding matrices that are naturally suited to MW. In this way, the original properties of MW fibers should be maintained in the final bio-based composites. Thus, the search for an appropriate matrix for MW-based biocomposites should be at the center of future work.

# *CHAPITRE 6 : DENSITÉ, ADHÉSION INTERFACIALE ET PROPRIÉTÉS MÉCANIQUES DE THERMOPLASTIQUES RENFORCÉS PAR FIBRE D'ASCLÉPIADE COURTE*

***Auteurs et affiliation :***

- *Ovlaque Pierre : Étudiant au doctorat, Université de Sherbrooke, Faculté de génie, Département de génie civil.*
- *Mohammadreza Foruzanmehr : Coordinateur scientifique, Université de Sherbrooke, Faculté de génie, Département de génie civil.*
- *Saïd Elkoun : Professeur, Université de Sherbrooke, Faculté de génie, Département de génie mécanique*
- *Mathieu Robert : Professeur, Université de Sherbrooke, Faculté de génie, Département de génie civil*

## *6.1 Résumé*

Cette recherche visait à évaluer l'amélioration des propriétés mécaniques et la diminution de la densité générée par l'utilisation de l'asclépiade, une fibre naturelle creuse. Comme l'asclépiade est fortement affectée par les traitements de surface, une bonne affinité naturelle avec la matrice est nécessaire pour obtenir un renforcement efficace. Ainsi, l'étude s'est concentrée sur le renforcement d'un polyamide d'origine biologique (PA11), qui aurait une bonne affinité interfaciale avec les fibres naturelles, ainsi que sur le polypropylène (PP) comme référence du fait de sa grande popularité. L'adhérence interfaciale entre l'asclépiade et les deux matrices a été déterminée à l'aide de tests de fragmentation de fibres simples (SFFT). Suite aux résultats de SFFT, des composites avec différentes fractions massiques d'asclépiade ont été produits par extrusion. En finalité, la distribution de la longueur des fibres, la diminution de la densité et les propriétés mécaniques ont été mesurées pour les composites PA11 et PP.

Selon les résultats de SFFT, le PA11 a montré une plus grande affinité naturelle avec l'asclépiade. Une longueur critique de 85 µm a été déterminée alors que celle-ci est de 306 µm dans le PP. Ces valeurs ont eu un impact direct sur le calcul du facteur d'efficacité de la longueur des fibres, qui s'est avérée beaucoup plus faible dans les composites de PP. Ainsi, l'ajout d'une fraction massique de 2,5 % de fibre dans le PA11 a entraîné une

augmentation de 29 % du module de Young, alors que l'augmentation a été limitée à 4 % dans le PP. La diminution de la densité a été très limitée dans les deux matrices, car les lumens des fibres se sont partiellement remplis lors du moulage par extrusion. Des taux de remplissage finaux allant de 80 à 100 % ont été mesurés en combinant les résultats de la microtomographie et de la densitométrie.

## *6.2 Abstract*

This research aimed to evaluate the improvement of mechanical properties and the decrease in density induced by the use of milkweed floss (MW), a hollow natural fiber. As MW is strongly affected by surface treatments, a good natural affinity with the matrix is required to obtain an effective reinforcement. Thus, the study focused on the reinforcement of a bio-based polyamide (PA11), which was reported to have a good interfacial affinity with natural fibers, and also on polypropylene (PP) as a reference. The interfacial adhesion between MW and the two matrices was determined using single fiber fragmentation tests (SFFT). Following the SFFT results, composites with different MW weight fractions were produced by extrusion molding. Finally, distribution of MW length, decrease in density and mechanical properties were measured for PA11- and PP-based composites.

According to SFFT results, PA11 matrix showed a greater natural affinity with MW. In addition, a critical length of MW fibers of 85 µm was determined with PA11 as compared to 335 µm with PP. This had a direct impact on the calculation of the fiber length efficiency factor, which was found to be much lower in PP than in PA11 for equivalent mass fractions. Thus, the addition of a mass fraction of 2.5% of MW fibers in PA11 led to an increase of 29% of the Young's modulus as compared to only 4% for PP-based composite. The decrease in the density was very limited for both matrices because the MW lumen tends to be filled during extrusion molding. Final filling proportion of the lumen of MW ranging from 80 to 100% were measured by combining the results of microtomography and densitometry.

## *6.3 Introduction*

The transportation industry is constantly looking for lighter materials, as the reduction of greenhouse gases is of growing importance [170], [171]. Nowadays, the use of natural

fiber-reinforced plastics (NFRP) is quite common in the automotive industry to reduce the weight of cars, which has a direct impact on their greenhouse gas emissions [172]. NFRP are very popular because they allow to improve the mechanical properties of conventional matrices without any major modification of techniques of molding typically used in the plastics industry [173]. In addition, NFRP present several advantages such as a lower carbon footprint, better sound absorption and lower cost compared to conventional materials [170], [174].

NFRP are generally produced with bast natural fibers (NF) due to their availability, price and mechanical strength [8], [33], [172], [175]. On the other hand, this study focuses on the use of hollow milkweed floss (MW) that could push the boundaries of NFRP even further. MW is by far, one of the lightest NF available thanks to its unusual tubular geometry, 70% of the volume of MW fiber can be considered as void leading to a density close to 0.3g/cc (20% of that of bast NF) [176]. Thanks to its cellulosic outer wall and its wide empty lumen, MW could be one of the only NF to be truly efficient on mechanical reinforcement and weight reduction of thermoplastics.

However, this promising new reinforced thermoplastic relies, on the one hand, on maintaining the hollow structure in the composite after the molding steps and, on the other hand, on sufficient stress transfer at the interface. Concerning the latter point, it is well established that NF are not naturally adapted to achieve good adhesion with organic matrices due to their surface chemistry [170]. Thus, surface modifications are generally performed to improve the stress transfer between fibers and matrices [50]. For instance, silanol or alkali treatments were reported to increase the mechanical properties of NF reinforced thermoplastics [9], [59]. Although the results of surface treatments are very impressive on solid fibers, their application to hollow fibers is more mitigated. For example, the alkaline treatment of MW (*Pergularia Daemia)* (5 % - 10 min – 25 °C) induced a 14 % decrease in the tenacity as well as the formation of a convolution like structure. According to the authors, this modification of MW morphology was also responsible for a decrease of the rigidity. [94].

Therefore, MW should be used with matrices that can interact with its surface and naturally lead to a good stress transfer at the interface. Of all the matrices available, polypropylene (PP) and nylon were considered for this study because they are both well established in the

automotive industry [175]. Although PP is well known for its lack of interaction with NF, it was chosen as a reference due to its predominance in automotive applications [177]. A biobased nylon (PA11) was considered since it is a more sustainable alternative to conventional nylon with a lower melting point (190 °C) that is compatible with NF extrusion [39]. Furthermore, the hydrophilicity of PA11 can lead to a good natural affinity with MW [178]–[181]. In addition, NF moisture content can be responsible, to some extent, for hydrolysis of PA11 that produces carboxylic acids that can react with the surface of NF [182].

Nevertheless, a good natural interfacial adhesion is not the only factor for achieving effective reinforcement. Proper management of the fiber length reduction during extrusion is also important [49]. It is commonly accepted that a fiber, to be effective, must be at least five times longer than its average critical length ($L_c$) to withstand an average stress close to its ultimate strength [183]. However, this situation is quite rare in short fiber reinforced composites [184]. Indeed, the general poor affinity between NF and the matrices leads to longer $L_c$ values while the average fiber length ($\bar{L}$) is greatly reduced by automatic mixing and molding techniques [62], [63], [184].

Therefore, to produce this promising new composite made of MW, it is important that (i) the matrix naturally leads to a short $L_c$, (ii) MW has a sufficient average length after extrusion, and (iii) the filling of the lumen is limited. This study aims at evaluating these three parameters as well as the final mechanical properties and weight reduction generated by the use of MW fibers in PP and PA11. Firstly, single fiber fragmentation tests (SFFT) were performed on MW/PP and MW/PA11 composites to determine the value of $L_c$ and assess the quality of the interface. Secondly, the configuration of the extruder was adjusted to induce the best dispersion of fibers and mechanical properties. Finally, the fiber efficiency factor and lumen filling rate were calculated and MW-reinforced composites were characterized with respect to the tensile properties for different MW weight fraction.

## *6.4 Materials and Methods*

### *6.4.1 Materials*

Raw MW and its leftovers were supplied by Protec-Style (Canada) and were extracted from the pods of *Asclepias Syriaca* species. These leftovers are composed of agglomerated fibers, too short to be carded. An average fiber length of 1.2 mm was calculated while raw MW has a typical average length of 22 mm. PA11 (LMFO) and PP (F006EC2 homopolymer) were supplied by Arkema and Braskem, respectively.

### *6.4.2 Processing*

As suggested in Figure 6-1, the volume occupied by MW leftovers (uncompressed) was difficult to manage in the hopper and it was chosen to limit the weight fraction to 10wt.% to ensure adequate and homogeneous extrusion conditions.

*Figure 6-1: Volume comparison of pellets and MW. From left to right: 25g PA11, 2.5g MW(leftovers), 2.5g MW(raw)*

A Thermo-Fisher twin screw extruder (process11- 40 L/D – D = 11 mm) was used to prepare the composites with MW weight fractions of 2.5, 5, 7.5 and 10wt.% in both matrices. The pellet feed rate and screws rotation speed were set at 4.5 g/min and 30 rpm respectively for PP and PA11 extrusion. The leftovers were introduced into a hopper located at 20 L/D from the die and added accordingly to the desired weight fraction. The screw configuration, temperatures and hopper position were kept constant between PA11 and PP extrusions and are shown in Figure 6-2. Although the mixing elements (90°) generate a reduction in fiber length [185], they were found to be mandatory because the pushing screw segments were not sufficient to separate the initial fiber agglomerates and

ensure homogeneous dispersion of the fibers in the composites. Nonetheless, it was reported that most of the fractures happened as soon as the fibers were introduced in the extruder, even with the use of mixing screw elements [62], [186], [187]. An atmospheric venting port was added downstream of the introduction of MW fibers to reduce the proportion of bubbles in the composites. The die pressures were measured respectively at 6 and 35 bars in the compression zone for pure PA11 and PP and their resulting composites. Die diameters of 3 and 2 mm were used for the extrusion of PA11 and PP, respectively.

The PA11 granules were vacuum dried at 80 °C for 24 hours according to the manufacturer's specifications. Composites were referred in the text as *x*MW/*y* where *x* is the weight fraction of MW fibers (i.e. 2.5, 5, 7.5 and 10) and *y* is the matrix (i.e. PP or PA11).

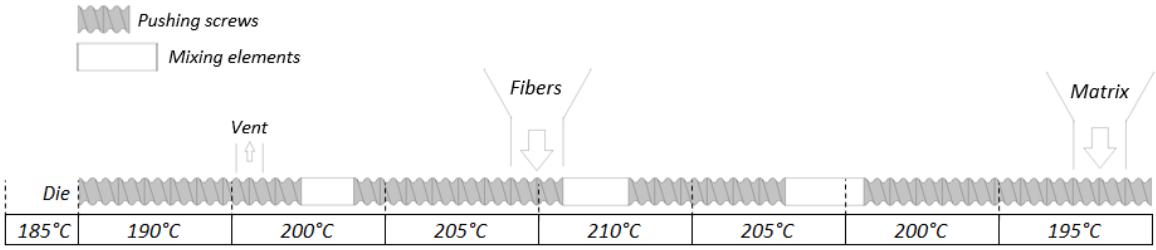


*Figure 6-2: Extrusion configuration for composite processing*

### *6.4.3 Characterisations*

#### *6.4.3.1 Interfacial adhesion*

The SFFT samples were prepared using the following procedure inspired by Graupner *et al.* method [124]. Firstly, PA11 and PP pellets were hot-pressed (Carver hydraulic press) to produce a 150 µm thick polymer film at 200 °C and cut into homogeneous 2 x 5 cm rectangles. Secondly, a single MW raw fiber was aligned between two films and held in position using high-temperature tape. This assembly was then placed between 2 glass lamellae and pressed at 200 °C for 2 min using a constant spacer. The assembly was then quenched to avoid crystallization. Glass slides (microscope slides) were used because they provide a low surface roughness on SFFT samples that would not induce optical interference during crack counting and fragments length measurements. Finally, samples were cut into 6 x 20 mm rectangles for tensile loading.

Tensile stress was applied to SFFT samples at 0.2 mm/min with a starting gage length of 15 mm using a Zwick/Roell with a 30kN load cell. In order to confirm that the fragmentation phenomenon reached its maximum, S-curves were performed by plotting the strain as a function of the crack density for PP and PA11 matrices. SFFT were performed on 6 samples for PP and PA11 and were stopped at 15% strain in both cases. The length of the fiber fragments was measured using an optical microscope (Nikon Optiphot), a digital camera (MoticCam580) and its acquisition software (MoticPlus 3.0). The critical length of MW fibers in PP and PA11 was calculated according to equation 1 [188], [189]:

$$L_c = \frac{4}{3}\bar{l} \quad (1)$$

Where $L_c$is the critical length and $\bar{l}$ is the average length of MW fragments after SFFT.
In order to validate the SFFT results, cross-sections of SFFT samples were prepared in liquid nitrogen using a microtome. The interface was observed on metalized samples (Pd-Au) by means of a Hitachi S3000-N scanning electron microscope (SEM).

#### *6.4.3.2 Fiber length dispersion*

Extrusion rods were hot-pressed at 200 °C and the resulting films were used to measure the length of the fibers in composites. The fiber length frequency was calculated in each composite on the length of 1000 fibers with an optical microscope (OM). The determination of the fiber length efficiency factor ($\eta_L$) was calculated from equation (2) [49] and using a log-normal distribution fitted to the experimental results for each composite [187], [190], [191]. The adjusted coefficient of determination ($R^2$) was found to be at least 98% for each log-normal adjustment.

$$\eta_L = \frac{1}{V_f}\left[\sum_i \frac{L_i V_i}{2L_c} + \sum_j V_j\left(1 - \frac{L_c}{2L_j}\right)\right] \quad (2)$$

Where L and V are referring to the length and volume fraction, respectively and, i and j indices to sub-critical and super-critical fibers, respectively.

#### *6.4.3.3 Matrix weight reduction and density*

Extrusion can induce a significant amount of voids (bubbles) in the extrusion rods that greatly decrease the composite density. In order to measure the real effect of MW on the decrease in density, a theoretical composite density ($\rho_c^*$) can be calculated according to the rule of mixture ((3). This theoretical density is not affected by voids but is directly related to the amount of MW and its empty lumens in composites.

$$\rho_c = \rho_c^* \times V_c + \rho_{air} \times V_{bubble} \quad (3)$$

$$\rho_c^* = \rho_w \times V_w + \rho_m \times V_m + \rho_{air} \times V_{lumen} \quad (4)$$

$$V_c = V_w + V_{lumen} + V_m \quad (5)$$

Where V and ρ respectively correspond to the volume fraction and density, and the indices *c, w* and *m* stand for composite, MW cellulosic wall, and matrix. The density of bubbles and lumens was considered equal to that of air at room temperature and 1 atm (0.001 g/cc). The true density of the composites ($\rho_c$) was averaged over 15 random measurements on the extrusion rod (30 mm long pieces) weighed in air and ethanol (23°C - 99.9%) according to ASTM D792-13. The density was determined using equation 6 where $\rho_c$ is the true composite density, $m_{air}$ and $m_{ethanol}$ are the mass of the rods in air and ethanol respectively, and $\rho_{ethanol}$ is the density of ethanol (0.787 g/cc)[192]

$$\rho_c = \frac{m_{air}}{m_{air} - m_{ethanol}} \times \rho_{ethanol} \quad (6)$$

The total volume fraction of bubbles ($V_{bubble}$) in the rods was determined using X-ray microtomography analyzes (skyscan 1172). 30 cross-sections were analyzed for each condition to assess the volume fraction of bubbles.

Finally, the determination of $\rho_c^*$ permitted to calculate $V_{lumen}$ using equation (4 and thus, the lumen filling rate in composites using equation (7.

$$\%F_{lumen} = \frac{(V_{lumen})^{MW} - V_{lumen}}{(V_{lumen})^{MW}} \quad (7)$$

Where $(V_{lumen})^{MW}$ is the volume fraction occupied by the fibers lumen in the weight fraction of MW introduced in the extruder, and $V_{lumen}$ , the remaining volume fraction of lumens that were not filled by the matrix during extrusion (equation (4). $V_{lumen}$ and $(V_{lumen})^{MW}$ were calculated assuming that the average diameter of MW is 22 µm and that the cellulosic wall has an average thickness and density of 1.27 µm and 1.5 g/cc, respectively [25].

#### *6.4.3.4 Thermos-mechanical properties*

Tensile tests were performed by means of a Zwick/Roell machine according to the recommendations of ASTM 3039. However, the production of samples with a rectangular cross-section was not feasible and extrusion rods were directly used to characterize the mechanical properties of pure matrices and composites. Nevertheless, the calculated mechanical properties for both pure matrices using cylindrical rods instead of rectangular ribbons were perfectly in line with the data provided by the manufacturers. Tests were conducted on 120 mm rods with a diameter calculated on an average of 6 measures in the gage length (50 mm). 15 rods were tested for each condition at a speed of 2 mm/min. The Young's modulus, ultimate tensile stress (UTS) and stress at yield were calculated when tensile test curves allowed it.

Dynamic mechanical analyses (DMA) were performed in tensile mode from 20 to 160 °C for PA11 and its composites since their Tg is known to be close to 50 °C. Scans from -35 to 160 °C were run for PP and its composites since their Tg is supposed to be close to 0 °C. The strain was set at 0.5% and the static force was automatically adjusted by the equipment to avoid excessive stretching or rupture of the sample. The storage modulus onset and tangent δ (tan δ) values were calculated at Tg.

The micrographs of composite cross-sections were prepared using the method described earlier to assess the interfacial adhesion of SFFT samples.

Fourier-transform infrared spectroscopy (FTIR) was used to evaluate the hydrolysis of PA11 after extrusion. Measurements were performed with a JASCO 4600 FT-IR spectrometer in attenuated total reflectance mode. 10 samples were tested for each composite. The spectra were obtained at room temperature after 32 scans from 600 to 4000 $cm^{-1}$ with a resolution of 4 $cm^{-1}$.

## *6.5 Results and Discussions*

### *6.5.1 MW fiber interfacial affinity*

#### *6.5.1.1 Single fiber fragmentation tests*

Since both matrices exhibit a significantly higher strain at break than that of MW fibers, the determination of the critical length ($L_c$) was possible in PP and PA11 using the SFFT method. The normalized crack density and fragment length frequency in SFFT samples are presented in Figure 6-3 for both matrices. According to Figure 6-3 a) and b), the crack density was stable after the application of a 15% strain on the samples, which confirmed that the maximum number of fragments was reached and allowed their measurement.

Based on the measurements of the length of 263 fragments (Figure 6-3 c), MW fragments showed an average length of 251 µm in PP while an average length of 64 µm was measured in PA11 (1422 fragments - Figure 6-3 d). Thus, using equation (*1*, the critical length of MW fibers in PP and PA11 was determined to be 335 and 85 µm, respectively. The lower $L_c$ value found in PA11 was related to a better stress transfer. Even though the $L_c$ in PP is significantly longer than that in PA11, they both remain very short compared to the values reported in the literature for NF, which are about a few millimeters. Awal *et al.* reported a $L_c$ close to 4.9 and 2.4 mm for flax fibers in PP and MAPP, respectively [193]. Herrera-Franco and Valadez-Gonzalez found a value of 12.96 mm for henequen fibers in HDPE [56]. Huber and Müssig calculated values of 3.2 mm for flax or hemp in MAPP [50]. As all these values were determined for bast NF, it is likely that the particular geometry of MW fibers was responsible for the shorter $L_c$ values found in this study.

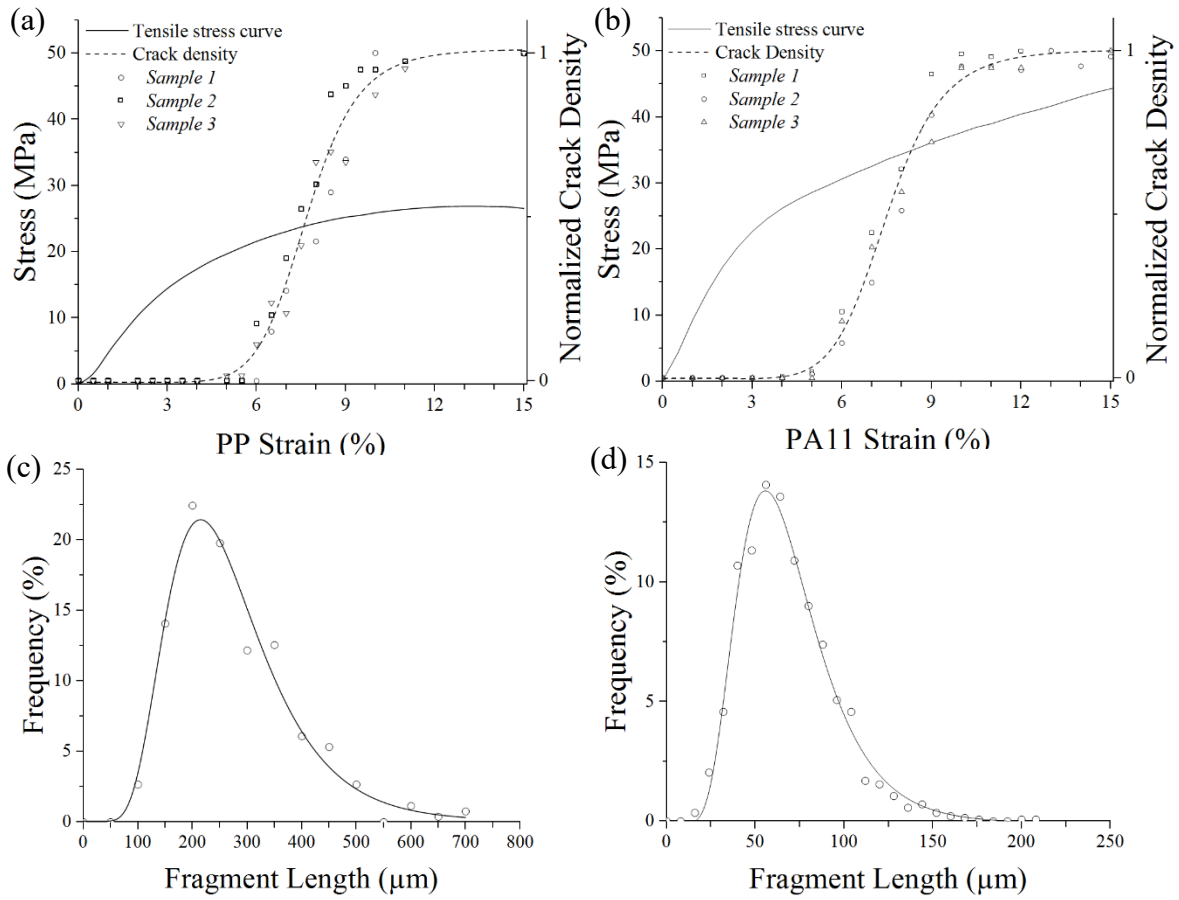


*Figure 6-3: Crack density and segment length frequency in PP (a and c) and PA11 (b and d)*

SEM micrographs of the cross-sections of SFFT samples (Figure 6-4) acknowledged the significantly lower value of the $L_c$ of MW fibers in PA11. Indeed, the adhesion between PA11 and MW fibers was better than with PP. As can be seen in the micrographs, no gap was visible at the interface with PA11 whereas a constant gap was revealed in the PP sample. The enhanced affinity was related to a more hydrophilic behavior of PA11 compared to PP, which favored good interactions with NF [178]–[181].

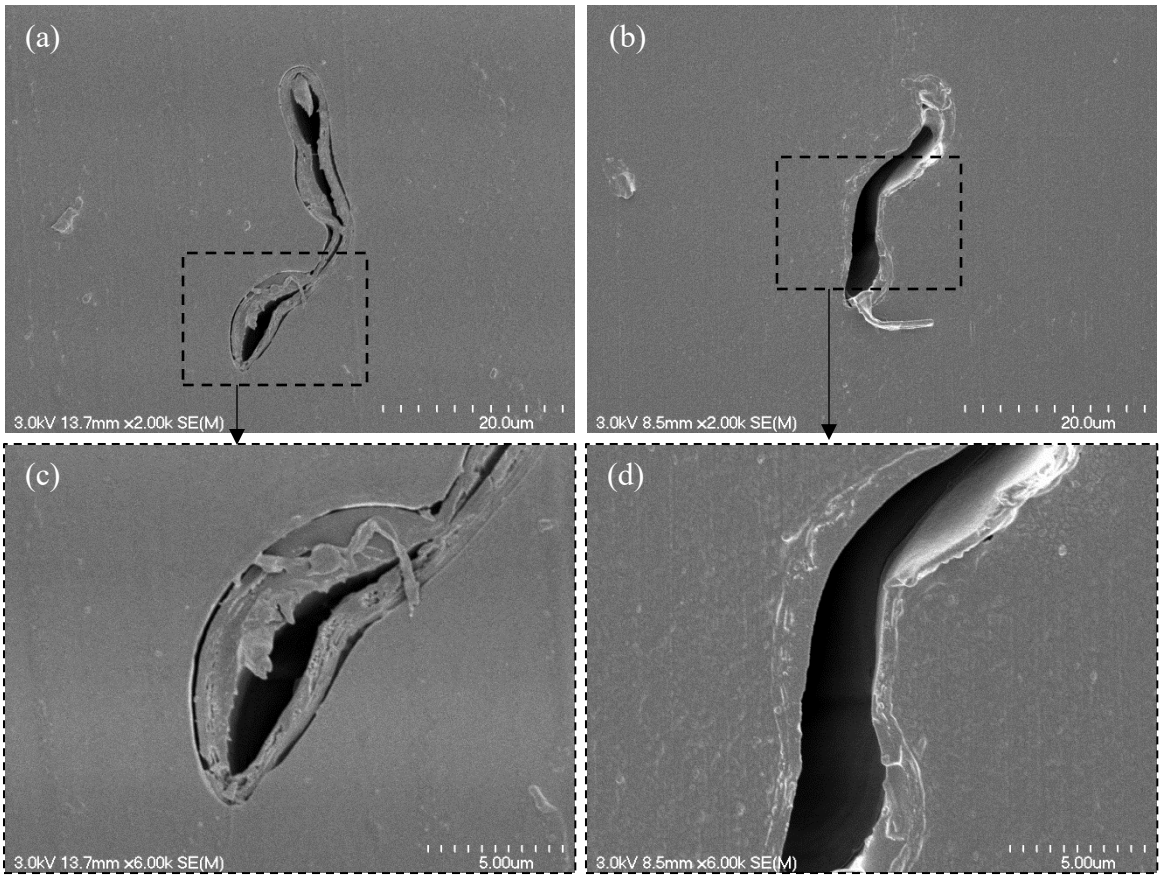


*Figure 6-4: Cross section of PP (a and c) and PA11 (b and d) of SFFT samples*

In addition, the higher affinity between PA11 and MW fibers was also validated by the fracture mode in SFFT samples. The OM micrographs of PP and PA11 SFFT samples are shown in Figure 6-5. In PP, the stress induced by the increase in strain was not efficiently transferred as suggested by SEM micrographs and the longer $L_c$ calculated. This resulted in a slippage of the fiber with the increase of strain as demonstrated by optical micrographs a) and c) in Figure 6-5. This behavior recognizes a poor natural bonding between PP and MW fibers [194]. Conversely, in PA11, the high natural affinity led to a propagation of cracks in the matrix. The small "V" surrounding the cracks in Figure 6-5 b) and d) are the 2D projection of a disk-shaped matrix crack, and confirm a strong interfacial adhesion [194], [195]. Therefore, it is possible to conclude, with regard to $L_c$ values, SEM micrographs and fracture modes, that PA11 and MW fibers have a much stronger interfacial affinity than PP and MW fibers.

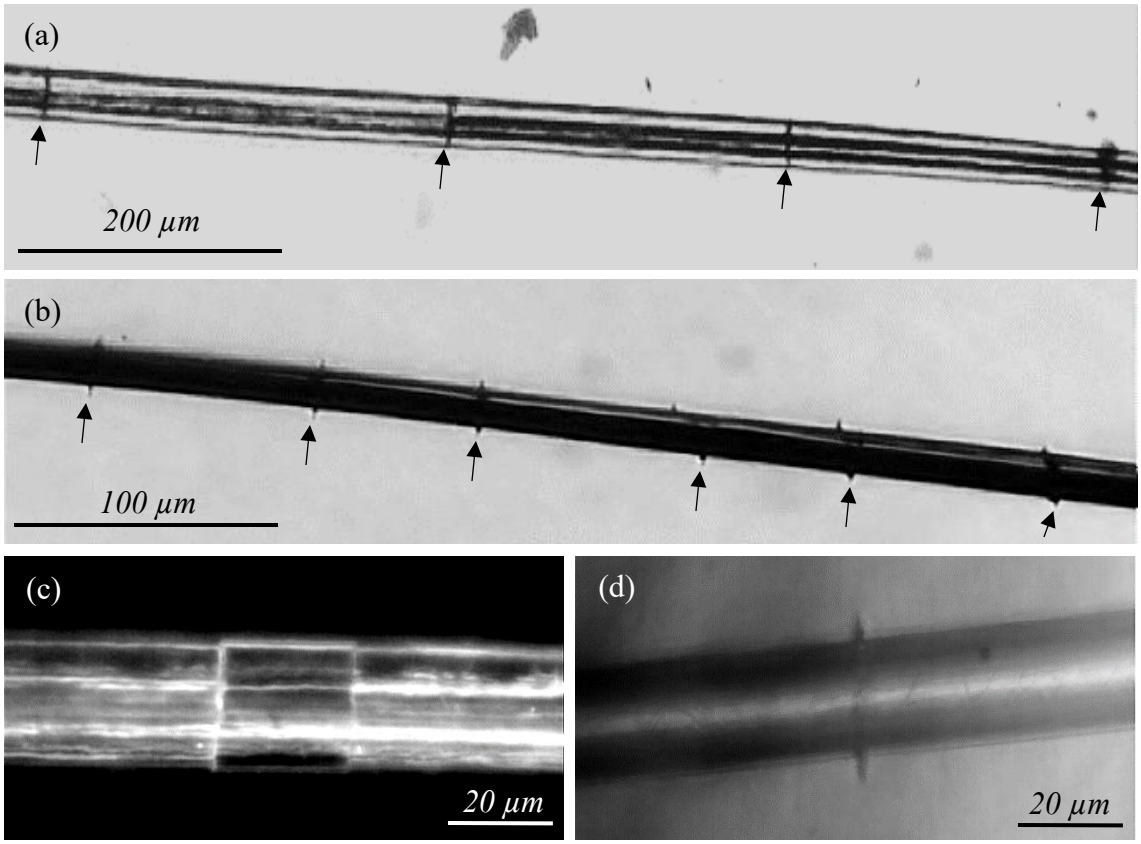


*Figure 6-5: Fracture mode in PP (a and c) and PA11 (b and d) in SFFT samples*

### *6.5.1.2 Quality of non-treated interfaces*

It is quite clear that natural affinity of PA11 and MW fibers is greater, but the results of SFFT do not indicate to what extent the interface was optimal and whether there was room for improvement. In order to quantify the quality of the interface, the $L_c$ values determined via SFFT were compared with their theoretical minimum values. From Kelly-Tyson equation [55] modified to adapt to an empty tubular structure (equation*(*8), it was possible to determine a theoretical minimum critical length ($L_{c_{min}}$) using equation (*9*. This calculation was not affected by the partial flattening of MW fibers, noticeable in Figure 6-4, because its outer perimeter (i.e. interface surface) was not modified.

$$L_c = \frac{\sigma_f}{\tau} \times 2\left(e - \frac{e^2}{D}\right) \quad (8)$$

$$L_{c_{min}} = \frac{\sigma_f}{\tau_{max}} \times 2\left(e - \frac{e^2}{D}\right) \quad (9)$$

Where e is the tube thickness, D is its diameter, $\tau$ is the interlaminar shear strength, $\sigma_f$ is the maximum fiber strength and $L_c$ is its critical length. $L_{c_{min}}$ in PA11 and PP was calculated assuming that the maximum interfacial shear strength achievable at the interface ($\tau_{max}$) was limited by that of the matrix, which was determined thanks to the Von Mises criterion:

$$\tau_{max} = \frac{Rm_m}{\sqrt{3}} \tag{10}$$

Where $Rm_m$ is the matrix maximum strength.

According to the study of Dréan et al., values of 1.27 µm and 22 µm were considered for e and D, respectively [25]. A $\sigma_f$ of 341 MPa was considered according to MW fibers tensile tests, values of 27 and 60 MPa were calculated for $Rm_m$ of PP and PA11 from their respective tensile tests. Theoretical values of 53 and 24 µm were calculated for $L_{c_{min}}$ in PP and PA11, respectively. The shorter $L_{c_{min}}$ in PA11 is linked to the better mechanical properties of PA11 (i.e. higher shear strength).

Therefore, knowing $L_{c_{min}}$ and its associated maximum interlaminar shear strength ($\tau_{max}$), it was possible to quantify the quality of the interface ($\varphi$) defined as the ratio of the interface shear strength to its maximum value (equation (*11*):

$$\varphi = \frac{\tau}{\tau_{max}} \tag{11}$$

In the end, φ can be plotted as a function of the value of the $L_c$ (equation (*12*).

$$\varphi = \frac{\sigma_f}{\tau_{max}} \times 2\left(e - \frac{e^2}{D}\right) \times \frac{1}{L_c} \tag{12}$$

Figure 6-6 presents the plotting of equation (*12* applied to PP and PA11. According to Figure 6-6, the natural interface quality in the PP/MW and PA11/MW systems were very low as they were close to 17 and 28% of their respective theoretical maximum value. Still, this 11% difference between both systems was in fact very significant. Indeed, the PA11/MW system seems to be at the beginning of the vertical asymptote while PP/MW is in the middle of the transition region of the curve. This would imply that any improvement in PA11/MW interfacial affinity would not induce a significant decrease in the $L_c$ while a slight improvement in PP/MW adhesion would result in a substantial reduction in the $L_c$.

For instance, assuming a hypothetical surface treatment that would induce a 15% increase of MW fibers interfacial affinity with the two matrices, a decrease of 31 and 143 µm in the $L_c$ of PA11/MW and PP/MW systems would be measured, respectively. Thus, it was possible to evaluate the relevance of a surface treatment for our composite. While surface treatment of MW fibers in PP seemed very relevant and would lead to a strong decrease of the $L_c$, it appeared to be partially meaningless in PA11, according to Figure 6-6.

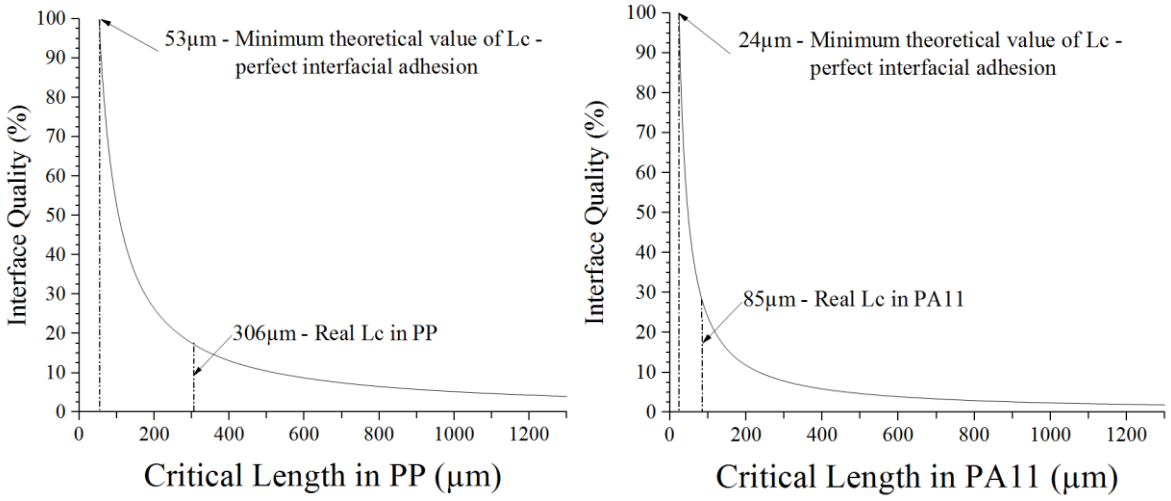


*Figure 6-6: Interface quality as a function of Lc for PP and PA11*

## *6.5.2 Composite Properties*

### *6.5.2.1 Extrusion configuration*

A proper extrusion configuration was important to ensure a correct fiber dispersion and composite homogeneity. Three different configurations (C1-C2-C3), presented in Figure 6-7, were studied to find the most efficient before processing the composites.

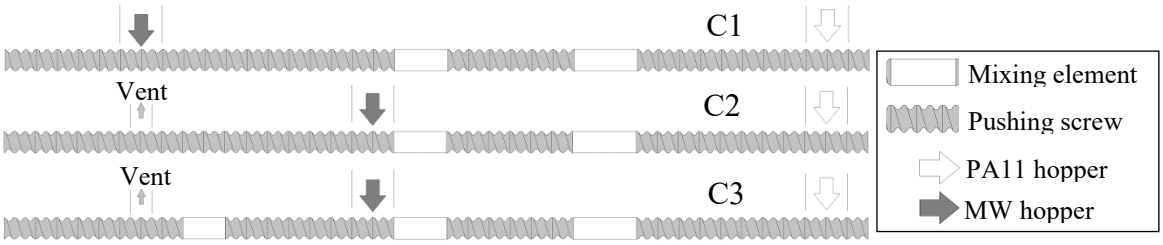


*Figure 6-7: Extrusion configuration*

The relationship between the different configurations and mechanical properties was studied on the 5MW/PA11 composite and is presented in Figure 6-8. Unfortunately, it was not possible to measure the length of the MW fibers due to the numerous agglomerates in

the rods produced with C1 and C2 that restricted OM observations. Nevertheless, it is clear from the results of mechanical characterization that the extrusion configuration had a significant impact on the mechanical properties of the composites and their standard deviation (SD) as well. Despite the fact that it was shown that the shorter the distance from the die, the longer the fibers in the final extrusion product, composites extruded using C1 had poor mechanical properties [196]. Indeed, these composites were mainly affected by low homogeneity and high fiber agglomerations. C1 was not able to disperse the fiber agglomerates over the short distance between the hopper and the die. The increase in the length between the MW hopper and the die from 5 to 15 L/D in C2 allowed a better homogeneity of the rods and therefore, better mechanical properties. Improvements of 17 and 40% were calculated for Young's modulus (E) and ultimate tensile stress (UTS), respectively, between C1 and C2. However, some important MW fiber agglomerates were detected in the rods from C2, which, in some cases, led to very poor mechanical properties and therefore, high final SD. Finally, C3 proved to be the most effective configuration to maximize the mechanical properties of composites. The addition of a short mixing element section (2 L/D) critically reduced fiber agglomerates and SD. It was found that E increased from 1361 to 1470 MPa and that its SD decreased from 196 to 103 MPa between C2 and C3. The same trend was calculated for the UTS value with an increase of 13% and a decrease of 51% in its SD.

The third configuration (C3) provided homogeneous composites with high mechanical properties and reduced SD. It was therefore used for the extrusion of all PA11 and PP composites described below.

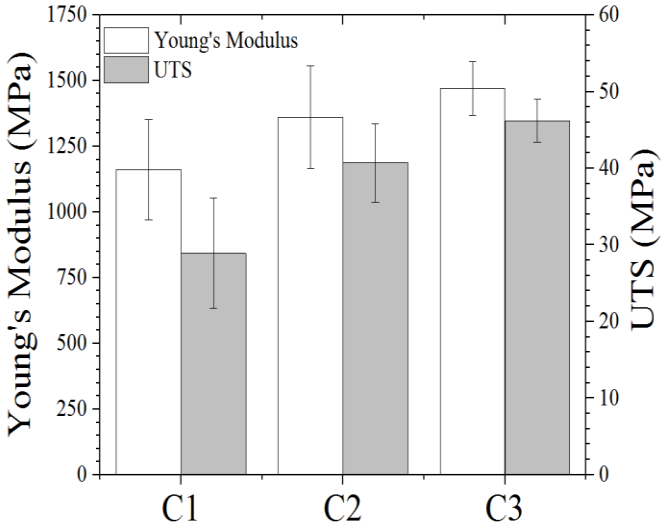


*Figure 6-8: Mechanical properties of 5MW/PA11 regarding the configuration of the extruder*

### *6.5.2.2 Fiber length efficiency factor*

The length distributions of MW fibers, shown in Figure 6-9, were typical of those of post-extrusion fibers because they were not symmetrical and extended to long fiber length [187], [197]. Parameters such as rpm of screws, mixing elements, and hopper position, which are reported to have a significant impact on fiber length, were kept constant between composites and cannot be responsible variations in distributions [62], [182], [185]. The slight shift in distributions to shorter lengths with the increase in the mass fraction of MW fibers was probably generated by an increase of fiber-fiber interactions as well as by the increase in MW fiber feed rates. Furthermore, the viscosity of the matrix was reported to have an impact on the average length of the fibers [197]. This can explain the difference between PP and PA11 composites as PP melt flow index was much lower (0.5 g/10min for PP and 18.5 g/10min for PA11 according to their respective datasheet).

According to the results of $L_c$, MW fibers must have lengths longer than 425 and 1675 µm (i.e. 5 times $L_c$) in PA11 and PP, respectively, to achieve an effective reinforcement. However, the distribution and the average length ($\bar{L}$) tended to show that MW fibers were shorter than these target lengths. For both matrices, average lengths were found to range around 100µm. Therefore, the fiber length efficiency factor ($\eta_L$) was calculated to evaluate the impact of a short $\bar{L}$ on the reinforcing effect of MW fibers. The average length of the fibers and their respective $\eta_L$ are presented in Figure 6-9.

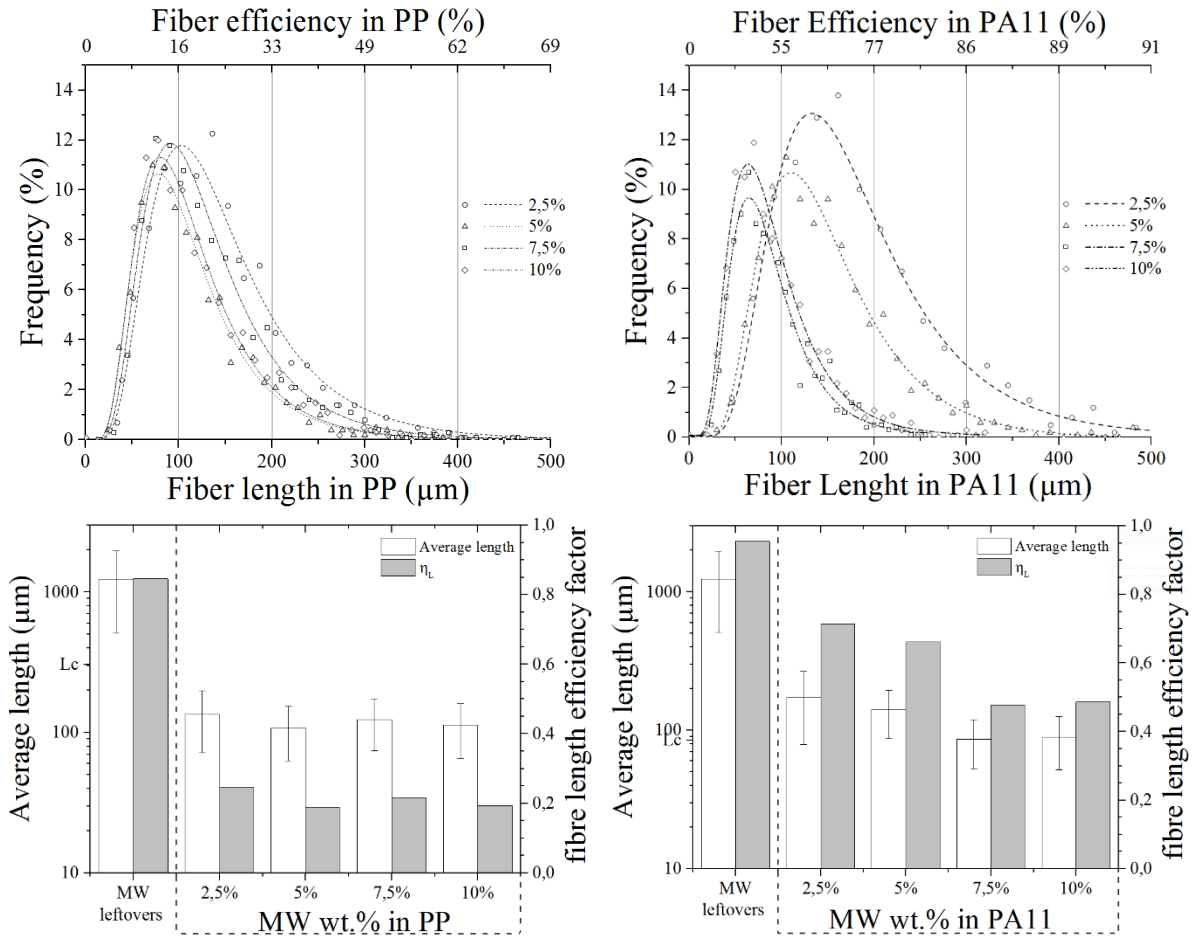


*Figure 6-9: Fiber average length, efficiency factor and dispersion in PP and PA11 matrices*

$\eta_L$ is usually directly used in the modified rule of mixtures to weigh the efficiency of the fiber reinforcement. Its calculation differentiates sub-critical and super-critical fibers. Sub-critical fibers (L< $L_c$ - index $i$ in equation (2)), which are not long enough to reach their strength, withstand an average stress proportional to their length. Conversely, the super-critical parameter (index $j$ in equation (2)) is not directly proportional to the length of the fiber. For these fibers, the average stress supported is slightly less than their UTS due to the linear increase in stress at both ends of the fibers.

The calculation of $\eta_L$ showed that reinforcement of PP composite was severely limited since $\eta_L$ decreased from 0.25 to 0.19 for 2.5 and 10 wt.% of MW fibers, respectively. It is noteworthy that even if the fibers were not reduced in length during extrusions, MW reinforcing effect would have been limited to 84% of its maximum. PA11 results seemed more promising with regard to the reinforcing effect of MW fibers. Thanks to a significantly shorter $L_c$, the super-critical parameter was more prominent in the $\eta_L$

determination and the values were logically higher. Still, since the average length was very close to the $L_c$, $\eta_L$ variations were of greater importance compared to that in PP. As for PP composites, calculations showed that $\eta_L$ values gradually decreased with the increase in MW fiber weight fraction from 0.71 for 2.5 wt.% of MW to 0.49 for 10 wt.% of MW. The reinforcing effect of MW fibers in PP was therefore quite limited due to the short length of MW fibers whereas a good reinforcement could be expected in PA11 composites.

#### *6.5.2.3 Composite density*

Figure 6-10 shows a representative microtomography of the composite 2.5MW/PA11. Microtomography made possible the visualization of the filling of the fibers but also the measurement of the volume of the bubbles and thus to evaluate the remaining empty lumens in the composites. It is clear from the enlarged area in Figure 6-10 that some MW fibers remained empty. The filled fibers appeared wider and more cylindrical, while empty fibers were more deformed and reminiscent of those incorporated in SFFT samples.

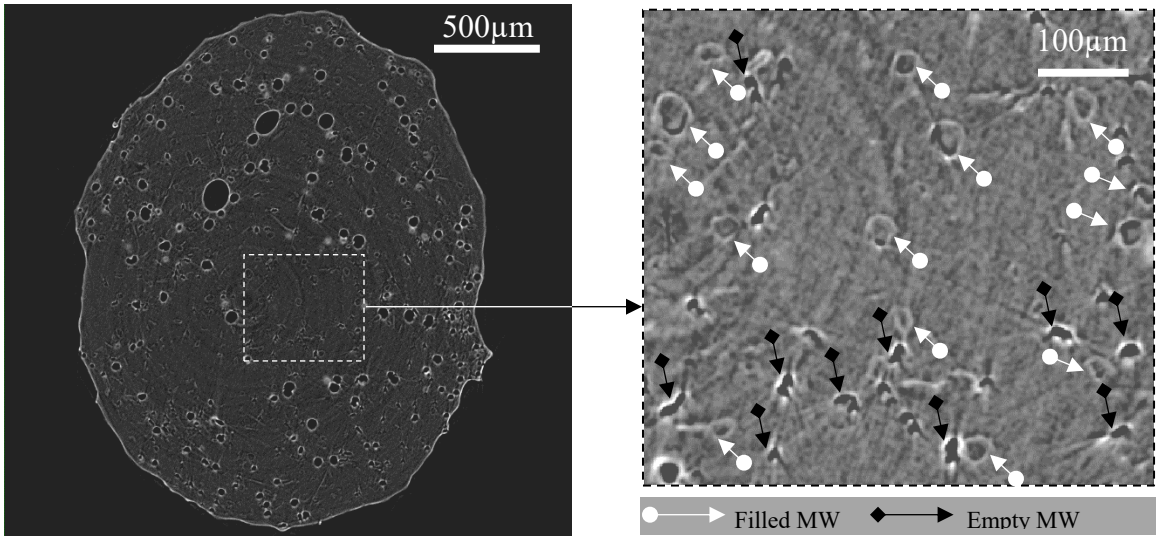


*Figure 6-10: Microtomography of 2.5MW/PA11*

The results of the density of composites ($\rho_c$) determined by densitometry as well as the theoretical density ($\rho_c^*$) calculated with equation (3) are presented in Figure 6-11. Decreases of density were found to be variable between conditions and not to follow the MW fibers weight fraction. The comparison between $\rho_c$ and $\rho_c^*$ values revealed that most of the weight reduction was actually related to the bubbles, which can be seen in the cross section presented in Figure 6-10. Thus, $\rho_c^*$ values demonstrated that MW lumens were

mostly filled and were not responsible for a lowering of the density. The lumen filling rate values were found to be between 80 and 100% in PP and PA11 composites. For example, values of 81, 82, 90, 86% were determined for MW weight fractions of 2.5, 5, 7.5 and 10% in PA11, respectively. The stability of the filling rate was consistent with the small variations in the average fiber length mentioned above. Several phenomena can be responsible for the formation of bubbles during the extrusion molding of NF-based composites. It was reported that the moisture content of NF as well as their agglomeration leads to the formation of bubbles in the extruded material [63]. In addition, the air escaping from MW lumens, which was almost totally replaced by the matrices during extrusion, may have also contributed to the formation of air bubbles in the material.

Therefore, it seemed that even with a relatively short distance from the hopper to the die, it was not possible to maintain an empty lumen in composites. Nevertheless, it appeared that MW fibers were responsible for the decrease of the density as they generated bubbles. However, these could induce stress concentrations and limit the mechanical properties of composites.

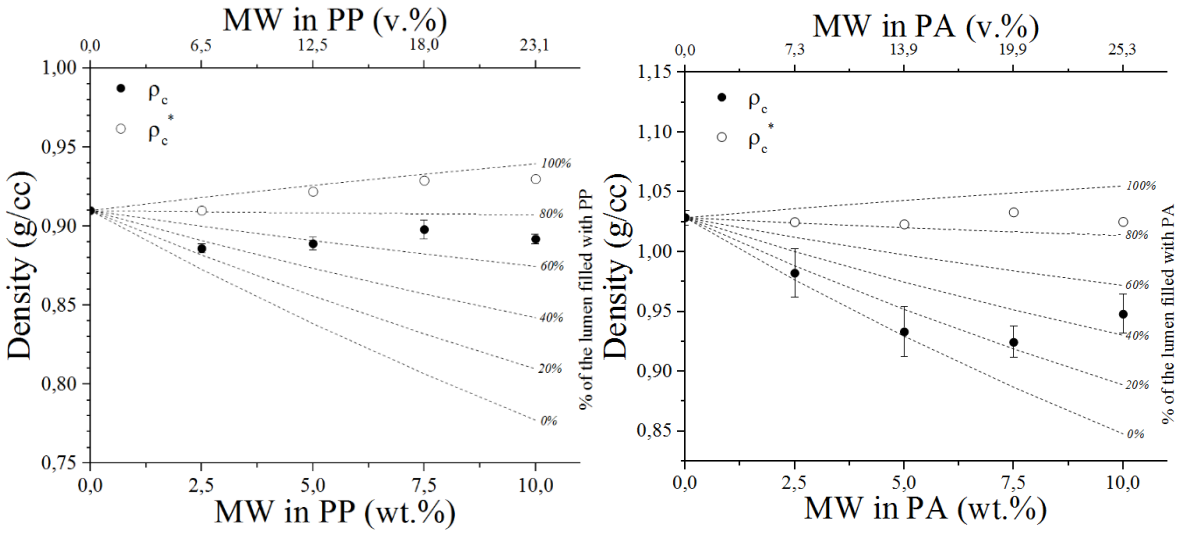


*Figure 6-11: Composites density and their respective theoretical density*

### *6.5.2.4 Mechanical properties*

Figure 6-12 shows the average tensile test curves for PP and PA11 composites. It is clear from the curves that the improvement in the tensile properties of PP composites was not significant compared to that of PA11. The tensile test curves of PP-based composites validated a limited influence of MW fibers on the tensile properties of the composites.

Indeed, plastic deformation occurred whereas effective fibrous reinforcements tend to give the composites a more fragile behavior. This insignificant influence of MW fibers was linked to the lack of adhesion demonstrated with SFFT. On the contrary, the addition of MW fibers to PA11 induced greater modifications in mechanical behavior for the same weight fraction. The tensile stress curves show less plastic deformation, and 10MW/PA11 seemed almost fragile.

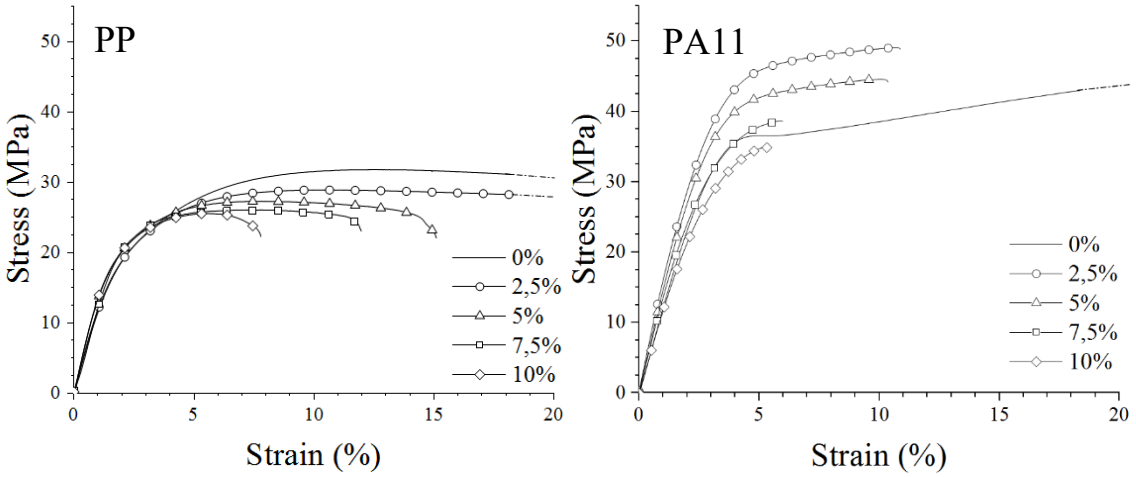


*Figure 6-12: Tensile stress curves of composites*

The evolution of Young's modulus is presented in Table 6-1: Young's Modulus of composites. PA11 and PP composites did not show the same evolution with regard to the tensile modulus. On the one hand, for PP-based composites, Young's modulus is proportionnal to the increase of the weight fraction of MW fibers. A logical maximum was reached for the 10MW/PP with an improvement of 14% of Young's modulus from 1210 for neat PP to 1380 MPa. On the other hand, for PA11-based composites, the evolution of tensile modulus was atypical and appeared to be inversely proportional to the MW content. The maximum improvement (30%) was achieved for 2.5MW/PA11 and a gradual decrease in the improvement was calculated for the other conditions. Improvements of 20, 10 and 2% of Young's modulus were calculated for 5MW/PA11, 7.5MW/PA11 and 10MW/PA11, respectively. The decrease in E could be related to the reduction of $\eta_L$ from 0.7 to 0.5 with the increase in the mass fraction of MW fibers [53]. In addition, PA11 may have undergone hydrolysis during extrusion because MW fibers were not dried before extrusion due to the high moisture absorption rate of hollow floss fibers [19], [25]. These reach a moisture equilibrium close to 10%, which represents 1wt.% of water in the composite for

10MW/PA11. As PA11 is produced by polycondensations, the presence of water during extrusion promotes hydrolysis, which reduces the length of molecular chains and leads to a significant drop in the mechanical properties of PA11. The estimation of the hydrolysis of PA11 between composites using DMA or differential scanning calorimetry was not succesful because it was not possible to subtract the influence of MW fibers on the thermal properties. Therefore, the hydrolysis of the matrix in PA11 composites was evaluated by calculating the ratio of 937/1161 $cm^{-1}$ peaks in the FTIR spectra of the composites [198]. According to Domingos *et al.*, an increase in the value of the ratio is likely to be related to a higher hydrolysis of PA11 [198]. Values of 0.565 and 0.693 with a standard deviation of 0.051 and 0.061 were measured for 2.5MW/PA11 and 10MWPA11, respectively. No significant differences were found between PA11 and 2.5MW/PA11 while intermediate values of 0.592 ± 0.049 and 0.670 ± 0.061 were calculated for 5MW/PA11 and 7.5MW/PA11, respectively. This increase in the peak ratio in relation to the mass fraction of MW fibers could indicate an increase in PA11 hydrolysis. In addition, PA11 hydrolysis generally induces a diminution of the strain at break [199]. As mentioned above, the reduction of the strain at break of PA11 composites could be related not only to the growing influence of MW fibers but also, to some extent, to an increase of PA11 hydrolysis. Therefore, a possible competition occurred between reinforcement and hydrolysis in PA11 composites.

*Table 6-1: Young's Modulus of composites*

| MW | Young's Modulus (MPa) | | | |
|---|---|---|---|---|
| wt.% | PP | *SD* | PA | *SD* |
| 0% | 1210 | *± 72* | 1230 | *± 87* |
| 2.5% | 1260 | *± 107* | 1590 | *± 54* |
| 5% | 1270 | *± 137* | 1470 | *± 103* |
| 7.5% | 1350 | *± 93* | 1350 | *± 94* |
| 10% | 1380 | *± 144* | 1250 | *± 89* |

Regarding the stress values presented in Table 6-2: Elastic limit, ultimate tensile stress and stress at yield of composites, no significant changes in the elastic limit were measured in PA11 or PP composites. Only the UTS values for both matrices and the stress at yield for PA11 were modified.

PP composites showed a linear decrease in their UTS with the increase of the weight fraction of MW fibers (-21% for 10MW/PP). This decrease is common with untreated NF

composites and confirms, once again, the poor natural adhesion between PP and MW fibers [63], [200]. The evolution of UTS in PA11 followed, to some extent, the same trend as that of PP composites. Nevertheless, the 2.5MW/PA11 composite showed a 9% improvement in its UTS compared to pure PA11, but 5MW/PA11 did not exhibit any significant improvement and the last two conditions (i.e. 7.5MW/PA11 and 10MW/PA11) showed respective decreases of 17 and 24%. The stress at yield followed the UTS variation, with a maximum achieved for 2.5MW/PA11 and a gradual decrease with the addition of MW fibers. The improvement of the UTS of 2.5MW/PA11 was related to the strong natural affinity existing between MW fibers and PA11. However, this good stress transfer was probably balanced by stress concentration (at fiber ends and in the perimeter of the bubbles), hydrolysis, fiber agglomeration, and decrease of $\eta_L$ with the increase of the weight fraction of MW fibers [197].

*Table 6-2: Elastic limit, ultimate tensile stress and stress at yield of composites*

| MW | Elastic limit (MPa) | | UTS (MPa) | | Stress at matrix Yield (MPa) | |
|---|---|---|---|---|---|---|
| wt.% | PP *SD* | PA *SD* | PP *SD* | PA *SD* | PP *SD* | PA *SD* |
| 0 % | 15.1 *± 0.8* | 26.1 *± 4.9* | 32.3 *± 1.3* | 45.7 *± 1.7* | - - | 36.6 *± 1.3* |
| 2.5 % | 14.9 *± 0.8* | 29.3 *± 6.0* | 28.4 *± 1.5* | 49.7 *± 3.4* | - - | 45.8 *± 1.5* |
| 5% | 15.3 *± 0.8* | 26.6 *± 4.9* | 26.8 *± 1.8* | 46.2 *± 2.8* | - - | 43.2 *± 2.2* |
| 7.5 % | 16.1 *± 2.1* | 21.4 *± 3.9* | 26.1 *± 2.2* | 37.8 *± 2.6* | - - | 37.0 *± 2.4* |
| 10 % | 15.9 *± 1.8* | 19.9 *± 2.9* | 25.4 *± 1.9* | 34.8 *± 3.0* | - - | 35.0 *± 2.2* |

#### *6.5.2.5 Thermo-mechanical properties*

The glass transition temperature (Tg) of composites, determined from the onset of storage modulus (E'), was not significantly modified. Tg temperatures of -9.9°C and 37.5 °C were measured for PP and PA11, respectively. The evolution of E' at the onset of the Tg was in line with Young's moduli of rods. Indeed, E' gradually increased in PP with the addition of MW fibers from 2446 MPa in PP to 3053 MPa in 10MW/PP. Like for tensile tests, the storage modulus of 2.5MW/PA11 was 30% higher than that of PA11 and the values decreased with the addition of MW fibers. This decrease led to a storage modulus similar to that of pure PA11 for 10MW/PA11.

The values of the tangent delta (tan δ) at Tg are reported in Figure 6-13 and reveal the importance of energy dissipation from viscous relaxation in the materials. The stability of tan δ in PP recognized that MW did not interact strongly with PP. Indeed, the addition of

MW elastic fibers should have led to a significant attenuation of viscous relaxations in the materials. This confirmed the poor quality of the interface and supported the conclusion of the SFFT. Conversely, the good interfacial affinity of PA11 and MW was confirmed by DMA, as the damping values are lowered by the addition of MW. This recognized a good interfacial affinity and therefore an increasing influence of MW fibers in the relaxation that occurred in the material.

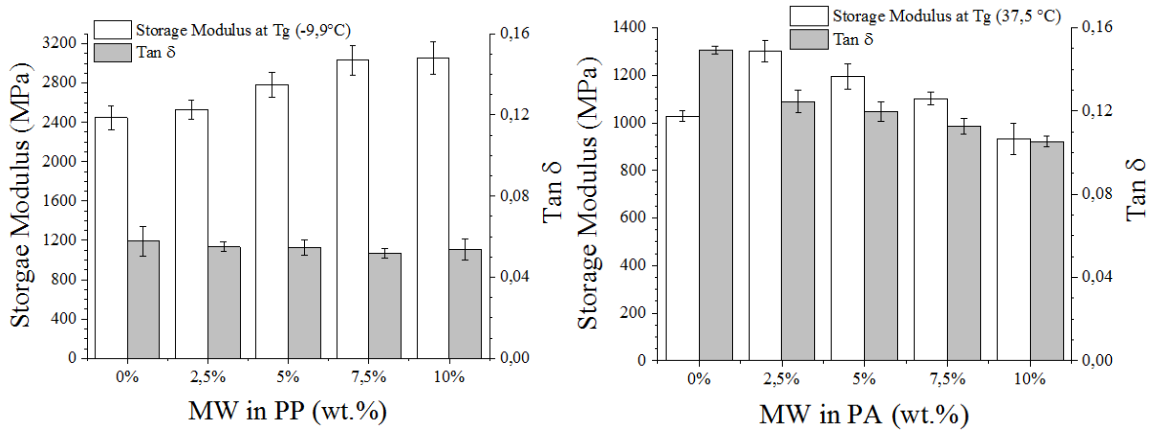


*Figure 6-13: Tangent delta peak values and storage modulus at Tg*

Finally, cross-sections of the best composites of each matrix were observed to assess the interfacial adhesion and remaining morphology of MW fibers after extrusion. SEM micrographs are presented in Figure 6-14. Most of MW fibers appeared to be flattened in PP composites while in PA11, the tubular structure remained constant. This could be related to the melt flow index of PP, which was close to 0.5g/10min (i.e. 37 times lower than that of PA11). Thus, PP was probably not able to fill the lumens and led to the flattening of MW fibers. This result was in line with the filling rates close to 100% found in PP composites, which means that lumens were no longer present in PP composites (i.e. flattened or filled). Concerning the interfacial affinity, the enlarged micrographs of composites were in agreement with those of the cross-sections of SFFT samples (Figure 6-4). As for SFFT samples, there were gaps at the interface between PP and most of MW fibers, while in PA11, these were less obvious.

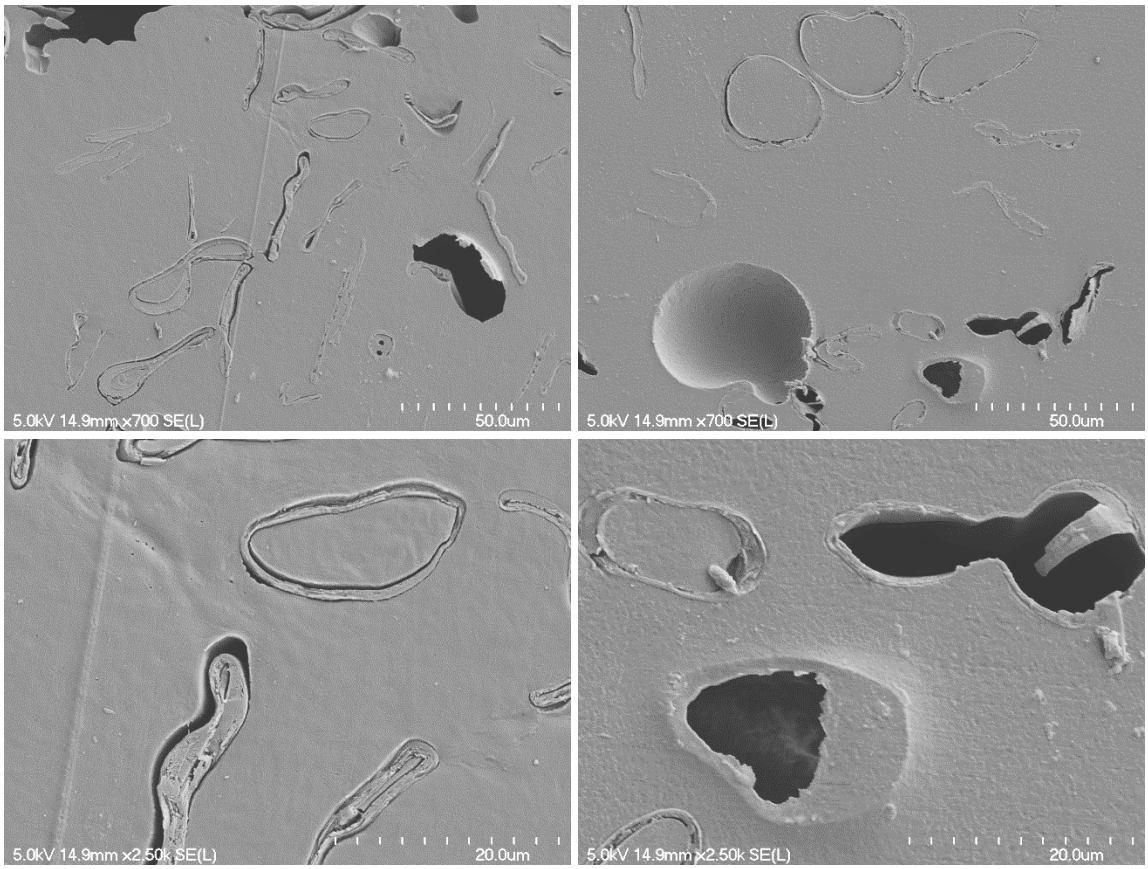


*Figure 6-14: Cross-sections of PP and PA11 composites (Left 10MW/PP; Right 2.5MW/PA11)*

## *6.6 Conclusion*

In this study, the natural affinity between MW and PP or PA11 was measured by SFFT before composite molding. The results of the critical fiber lengths, as well as the cracking modes and cross-sectional observations, suggested that the natural affinity of PA11 is higher than that of PP. Critical lengths of 85 and 235µm were calculated in PA11 and PP, respectively. It was also demonstrated that the surface treatment of MW fibers would not be relevant with PA11 because the interface is naturally strong. Following these results, composites consisting of 2.5, 5, 7.5 and 10% by weight of MW fibers residues were produced and characterized. The following conclusions can be drawn about the composites:

- Although MW fiber distributions in the two matrices were quite similar, the fiber efficiency factor was lower in PP due to the longer $L_c$. The values tend to be around 0.2 in the PP while they range from 0.7 to 0.5 in the PA11.

- A decrease in the density of the composite was measured. This was mainly related to bubbles generated during extrusion rather than empty MW lumens, which had a filling rate between 80 and 100%. The bubbles were probably generated by the air escaping from the lumens and also, to some extent, by the fiber agglomerates.
- The mechanical properties calculated with the tensile test and the DMA followed the same trends and validated a better affinity with PA11. Indeed, the improvement in mechanical properties was of greater importance in PA11 and the best composite was found to be 2.5MW/PA11 with a 30 and 9% improvements in its E and UTS, respectively. Nevertheless, it was found that the mechanical properties were probably in competition with hydrolysis of the matrix and stress concentration in PA11.

MW seems to be very effective in PA11, even at low weight fractions. According to the above conclusions, it is possible that adequate drying of MW fibers combined with thorough work on extrusion parameters improves mechanical properties because hydrolysis and bubble management could easily be reduced with adequate equipment.

# CHAPITRE 7 : CONCLUSION GÉNÉRALE

## 7.1 Conclusion

Ce projet de thèse s'est concentré sur la caractérisation et l'utilisation de la fibre creuse d'asclépiade pour le renforcement de matrices thermoplastiques. La fibre d'asclépiade est une fibre dont la mise en forme par cardage entraîne une séparation des fibres ayant une longueur trop courte. Le projet visait à valoriser ces fibres courtes en tant que renforts dans des matrices organiques thermoplastiques.

La première étude a démontré que la fibre d'asclépiade possède des propriétés mécaniques inférieures à celles des fibres libériennes en raison des différences physiologiques entre ces deux types de fibres. Un module d'élasticité de 14 GPa et une résistance à la traction de 341 MPa ont été calculés pour l'asclépiade en supposant une section annulaire. L'asclépiade présente cependant deux avantages pour le renforcement de thermoplastiques : sa longueur critique théorique (29-15 µm) et sa densité (0,3 g/cm3 - lumen vide) sont largement inférieures à celles des fibres libériennes.
La mise en forme de l'asclépiade par extrusion et injection n'entraîne pas d'agglomération de celles-ci. Dans le cas de sa mise en forme avec le PLA par extrusion/injection, le lumen de la fibre est rempli par la matrice ce qui maintient la structure tubulaire de la fibre.
Des améliorations de 11 et 9% ont été mesurées sur les modules d'élasticité des composites d'asclépiade et de lin respectivement. Une diminution moins sévère de la résistance en traction a été mesurée pour les composites d'asclépiade par rapport au lin. Le renforcement induit par l'asclépiade peut donc être jugé plus efficace au regard des propriétés mécaniques intrinsèques des fibres. Cette efficacité a été expliquée par un meilleur ratio de la longueur moyenne sur la longueur critique théorique des fibres (~5 pour l'asclépiade - ~1 pour le lin), moins de défauts sur la surface de l'asclépiade, et la section transversale plus faible qui amène à une meilleure distribution des renforts dans la matrice. Ce dernier point a permis d'expliquer l'amélioration de 17% de la ténacité des composites d'asclépiade par rapport aux composites renforcés de lin.

Les principaux résultats de cette étude laissent entrevoir que l'asclépiade peut renforcer les matrices organiques. Cependant, la fibre d'asclépiade, comme toutes autres fibres naturelles, montre une faible affinité naturelle avec le PLA qui limite probablement l'effet renforçant de celle-ci.

Ce manque d'affinité est au centre de la deuxième étude, car il n'existe que très peu de retours sur le traitement de surface des fibres d'asclépiade ou des fibres creuses en général. Les fibres d'asclépiade ont été traitées par mercerisation ou silanisation (époxy-silanol) pour améliorer son adhésion avec le PLA. Les résultats ont montré que les deux traitements ont été appliqués avec succès à l'asclépiade. Cependant, ils ont induit des effets indésirables sur les fibres. Le traitement alcalin, qui a amené une augmentation souhaitée de la rugosité (+108 %), a conduit à un effondrement de la structure tubulaire d'une diminution de 68 et 60 % du module et de la résistance en traction des fibres. Les effets secondaires étaient plus limités avec la silanisation. Aucun changement dans la morphologie ou la rugosité n'a été induit et seule une diminution des propriétés mécaniques a été mesurée (-30 et -60 % sur le module et la résistance, respectivement). L'écrasement des fibres mercerisées a amené à une longueur moyenne plus élevée après la mise en forme, car cette nouvelle géométrie laisse plus de liberté de flexion aux fibres pendant la mise en forme.

Les composites produits avec des fibres mercerisées présentaient une résistance à la traction supérieure à celle du PLA renforcé de fibres brutes (+9 %). Cette augmentation a été expliquée par l'enchevêtrement des fibres et les pincements mécaniques au niveau de l'interface induits par l'augmentation de la rugosité. En effet, les résultats de fractographie et des tests d'impact n'ont pas montré d'amélioration significative de l'affinité. La fractographie des composites mis en forme avec des fibres ayant reçu un greffage d'époxy-silanol en surface a reconnu une amélioration significative de la qualité de l'interface. Cette amélioration de l'affinité s'est marquée par une augmentation de la résistance à la traction (+17 %) par rapport aux fibres brutes. Le traitement de surface époxy-silanol des fibres d'asclépiade semble une bonne solution pour améliorer l'affinité interfaciale avec le PLA. Cependant, les propriétés mécaniques des composites sont probablement limitées par la dégradation des fibres induite par le traitement. La démarche apparait donc efficace, mais

reste peu logique, car elle consiste à dégrader une fibre naturelle pour la rendre compatible avec un produit synthétique (PLA). Une méthode plus sensée passerait par une modification de la matrice ou encore une utilisation de l'asclépiade dans une matrice thermoplastique naturellement compatible. De cette façon, les propriétés originales de l'asclépiade pourraient être conservées dans les composites finaux.

Le polyamide 11 est supposé avoir une bonne affinité avec les fibres naturelles et a donc été envisagé pour évaluer l'effet renforçant de la fibre d'asclépiade. Cette dernière étude cherchait principalement à mesurer concrètement cette affinité et la comparer à celle d'une référence (PP). L'adhésion a été mesurée par le biais de la détermination de la longueur critique par tests de fragmentation de fibres. Les résultats des longueurs critiques, des modes de fissuration et les observations des coupes transversales suggèrent que l'affinité naturelle du PA11 est très bonne et supérieure à celle du PP. Des longueurs critiques de 85 et 335 µm ont été calculées dans le PA11 et le PP, respectivement. Il a également été démontré que le traitement de surface de l'asclépiade ne devient plus pertinent dans le cas du PA11, car l'interface est naturellement forte. Suite à ces résultats, des composites constitués de 2,5, 5, 7,5 et 10% en poids d'asclépiade ont été produits et caractérisés.
Bien que les distributions des longueurs des fibres dans les deux matrices fussent assez similaires, le facteur d'efficacité de la fibre était logiquement plus faible dans le PP en raison de la longueur critique plus élevée. L'efficacité des fibres par rapport à leur longueur variait autour de 0,2 dans le PP alors qu'elle variait de 0,7 à 0,5 dans le PA11. Une diminution de la densité des composites a été mesurée grâce à l'ajout de fibres creuses. Cependant, les lumens des fibres se sont avérés remplis à 80 - 100% par la matrice. La baisse de densité a été principalement liée aux bulles qui ont probablement été générées par l'air s'échappant des lumens et aussi, dans une certaine mesure, par l'air amené dans les agglomérats de fibres. Les propriétés mécaniques calculées ont validé une meilleure affinité avec le PA11. En effet, l'amélioration des propriétés mécaniques a été d'une plus grande importance pour le PA11. La meilleure condition testée (2.5% d'asclépiade) montrait une amélioration de 30 et 9% du module et de la résistance du composite par rapport à la matrice pure. Néanmoins, les propriétés mécaniques des composites ont probablement été limitées par des phénomènes d'hydrolyse de la matrice et de

concentration des contraintes dans le PA11 due aux nombreuses bulles. Le couple asclépiade/PA11 apparait donc être très efficace même pour des fractions massiques de fibres faibles.

Ce projet de recherche a donc montré que l'asclépiade peut renforcer une matrice organique à condition qu'elle soit employée avec une matrice thermoplastique qui lui convienne. L'utilisation de rebuts de cardage ne limite pas l'effet renforçant grâce à la géométrie tubulaire qui induit une longueur critique faible. Ainsi la valorisation des rebuts en tant que renfort peut montrer de l'intérêt. Il n'y a que très peu de pertes au niveau de l'effet renforçant par rapport à des fibres brutes plus longues.

## *7.2 Perspectives*

*Améliorer les composites :*

La mise en forme des composites thermoplastiques à fibres courtes est une étape cruciale. Celle-ci a été améliorée dans la dernière étude grâce à l'utilisation d'une extrudeuse bi-vis plus modulable que celle employée dans les deux premières études (chapitre 4 et 5). Les résultats et les difficultés rencontrées sur cette dernière étude amènent plusieurs axes de réflexions pour améliorer les propriétés des composites :

(i) Désagglomérer les fibres. La séparation des fibres des rebuts de cardage devrait être traitée en amont de l'extrusion plutôt que par l'extrudeuse. Dans la dernière étude, l'emplacement de la trémie des fibres a dû être reculé pour assurer une dissipation correcte des amas de fibre. Ce changement de position s'est fait au détriment d'une augmentation du temps de résidence et un parcours plus long dans l'extrudeuse que l'on cherche généralement à minimiser. Si les agglomérats de fibres peuvent être séparés avant leur insertion dans la trémie, celle-ci pourrait être avancée au plus près de la filière pour limiter la diminution des longueurs et le remplissage.

(ii) Améliorer le séchage des fibres. Les fibres naturelles sont généralement séchées lorsqu'employées dans des matrices sujettes à hydrolyse. Ici pour les composites de PLA et de PA11, il n'était pas possible d'assurer une continuité entre l'étuve de séchage et l'extrudeuse. Des méthodes de séchage en continu

directement reliées à la trémie de l'extrudeuse devraient permettre d'améliorer l'efficience des composites et limiter l'hydrolyse des matrices.

(iii) Étudier le lien entre la viscosité de la matrice, le remplissage et l'écrasement des fibres. La dernière étude a montré que les fibres étaient globalement plus écrasées dans le PP que le PA11. L'influence de la viscosité de la matrice est donc un paramètre important qu'il faut maitriser pour réussir à former des composites efficients.

(iv) Mesurer les propriétés acoustiques. Les fibres creuses sont reportées comme étant efficaces pour l'amélioration des propriétés acoustiques des composites, notamment pour les applications automobiles [201]. Les composites d'asclépiade peuvent donc avoir des propriétés améliorées sur le plan acoustique. Les propriétés acoustiques n'ont pas été étudiées sur les composites d'asclépiade à cause de la présence de bulles qui fausserait l'effet des fibres. Également, les tubes à impédance nécessitent des plaques de composites et donc une filière adaptée pour éviter une étape supplémentaire de formage.

*Universalité des fibres creuses*

Comme évoqué au chapitre 3, il existe de nombreux types de fibres creuses. Le chapitre 3 a montré qu'il n'existe pas d'étude comparative de ces fibres faisant appel à des techniques et des méthodes de caractérisation identiques. Il pourrait donc être judicieux de caractériser ces fibres sur la base de méthodes communes. Les propriétés des fibres et des composites peuvent être ainsi évaluées pour statuer sur les similitudes et les possibles substitutions entre ces différentes fibres.

*Étudier le renforcement dans des thermodurcissables et l'auto réparation.*

Pour terminer sur ces perspectives, les fibres d'asclépiade pourraient être utilisées dans des matrices thermodurcissables. En effet, les fibres creuses de verre sont utilisées comme renfort et moyen d'auto réparation dans les composites thermodurcissables [202]–[204]. Comme la polymérisation des thermodurcissables peut se faire à température ambiante, l'imprégnation d'une partie des lumens par le monomère et une autre partie par un catalyseur permet de réparer les microfissures qui peuvent apparaitre. La fibre creuse

d'asclépiade pourrait donc être utilisée pour ces applications. Il faudrait cependant étudier la résistance de la fibre aux solutions contenant le monomère ou le catalyseur. Également, l'utilisation de fibre de verre creuse et plus généralement de fibres pour le renforcement de matrices thermodurcissables passe par l'utilisation de fibres assemblées en mats ou tissus. L'utilisation de fibres courtes est donc moins évidente. Enfin, la principale question reste à trouver un moyen d'imprégner des fibres courtes non assemblées et de maintenir l'imprégnation jusqu'à la mise en forme.

# RÉFÉRENCES


[1] R. Geyer, J. R. Jambeck, and K. L. Law, "Production, use, and fate of all plastics ever made," *Sci. Adv.*, vol. 3, no. 7, p. e1700782, Jul. 2017.

[2] "Biopolymeres facts and statistics," Institue for bioplastics and biocomposites, Hannover, 2018.

[3] K. Van de Velde and P. Kiekens, "Biopolymers: overview of several properties and consequences on their applications," *Polym. Test.*, vol. 21, no. 4, pp. 433–442, 2002.

[4] M. Jamshidian, E. A. Tehrany, M. Imran, M. Jacquot, and S. Desobry, "Poly-Lactic Acid: Production, Applications, Nanocomposites, and Release Studies," *Compr. Rev. Food Sci. Food Saf.*, vol. 9, no. 5, pp. 552–571, 2010.

[5] A. K. Mohanty, M. Misra, and L. T. Drzal, *Natural Fibers, Biopolymers, and Biocomposites*. CRC Press, 2005.

[6] A. Célino, S. Fréour, F. Jacquemin, and P. Casari, "The hygroscopic behavior of plant fibers: a review," *Front. Chem.*, vol. 1, no. 43, Jan. 2014.

[7] A. N. Netravali and C. M. Pastore, *Sustainable Composites: Fibers, Resins and Applications*. Pennsylvania: DEStech Publications, Inc, 2014.

[8] E. Zini and M. Scandola, "Green composites: An overview," *Polym. Compos.*, vol. 32, no. 12, pp. 1905–1915, 2011.

[9] J. George, M. S. Sreekala, and S. Thomas, "A review on interface modification and characterization of natural fiber reinforced plastic composites," *Polym. Eng. Sci.*, vol. 41, no. 9, pp. 1471–1485, Sep. 2001.

[10] A. K. Mohanty, M. Misra, and L. T. Drzal, "Surface modifications of natural fibers and performance of the resulting biocomposites: An overview," *Compos. Interfaces*, vol. 8, no. 5, pp. 313–343, Jan. 2001.

[11] Bourgeois Michel, *Fibre Agrosourcées*. Ed. Techniques Ingénieur, 2011.

[12] C. Baley, *Fibres naturelles de renfort pour matériaux composites*. Ed. Techniques Ingénieur, 2004.

[13] O. Faruk, A. K. Bledzki, H.-P. Fink, and M. Sain, "Biocomposites reinforced with natural fibers: 2000–2010," *Prog. Polym. Sci.*, vol. 37, no. 11, pp. 1552–1596, Nov. 2012.

[14] Faruk O. and Sain M., *Developments in Fiber-reinforced Polymer (FRP) Composites for Civil Engineering*, Woodhead Publishing. Uddin Nasim, 2013.

[15] Douglas D. Stokke, Qinglin Wu, and Guangping Han, *Introduction to Wood and Natural Fiber Composites*, John Wiley & Sons, Ltd. Christian V. Stevens, 2014.

[16] S. Meiwu, X. Hong, and Y. Weidong, "The Fine Structure of the Kapok Fiber," *Text. Res. J.*, vol. 80, no. 2, pp. 159–165, Jan. 2010.

[17] W. G. Hopkins, *Physiologie végétale*. De Boeck Supérieur, 2003.

[18] R. Zhong and Z.-H. Ye, "Secondary Cell Walls: Biosynthesis, Patterned Deposition and Transcriptional Regulation," *Plant Cell Physiol.*, vol. 56, no. 2, pp. 195–214, Feb. 2015.

[19] X. Yang, L. Huang, L. Cheng, and J. Yu, "Studies of Moisture Absorption and Release Behaviour of Akund Fiber," *Adv. Mech. Eng.*, vol. 4, no. 0, pp. 356548–356548, Jan. 2015.

[20] X. Yang, L. Q. Huang, and L. D. Cheng, "Study on the Structure and the Properties of Akund Fiber," *Appl. Mech. Mater.*, vol. 217–219, pp. 617–621, Nov. 2012.

[21] I. Spiridon, "Modifications of Asclepias syriaca fibers for paper production," *Ind. Crops Prod.*, vol. 26, no. 3, pp. 265–269, Oct. 2007.
[22] F. W. Barth and T. E. Timell, "The Constitution of a Hemicellulose from Milkweed (Asclepias syriaca) Floss," *J. Am. Chem. Soc.*, vol. 80, 1958.
[23] J. Müssig, Ed., *Industrial application of natural fibres: structure, properties, and technical applications*. Chichester, West Sussex, U.K. ; Hoboken, N.J: Wiley, 2010.
[24] M. Bouvier d'yvoire, "Etude de la voie de biosynthese des monolignols chez brachypodium distachyon," Paris 11, 2011.
[25] J.-Y. F. Dréan, J. J. Patry, G. F. Lombard, and M. Weltrowski, "Mechanical Characterization and Behavior in Spinning Processing of Milkweed Fibers," *Text. Res. J.*, vol. 63, no. 8, pp. 443–450, Aug. 1993.
[26] P. K. Mallick, *Fiber-reinforced composites: materials, manufacturing, and design*, 3rd ed., [expanded and rev. ed.]. Boca Raton, FL: CRC Press, 2008.
[27] M. Lewin, *Handbook of Fiber Chemistry, Third Edition*. CRC Press, 2006.
[28] A. D. Beshay, B. V. Kokta, and C. Daneault, "Use of wood fibers in thermoplastic composites II: Polyethylene," *Polym. Compos.*, vol. 6, no. 4, pp. 261–271, 1985.
[29] A. Ashori and Z. Bahreini, "Evaluation of Calotropis gigantea as a Promising Raw Material for Fiber-reinforced Composite," *J. Compos. Mater.*, vol. 43, no. 11, pp. 1297–1304, Jun. 2009.
[30] martine Guigere, "Asclépiade : une culture à part entiere," *Grandes cultures*, vol. 23, no. 3, 2013.
[31] "Asclépiade commune." Coopérative de solidarité Cultur'Innov.
[32] R. M. Rowell, *Handbook of Wood Chemistry And Wood Composites*. Taylor & Francis.
[33] D. N. Saheb and J. P. Jog, "Natural fiber polymer composites: A review," *Adv. Polym. Technol.*, vol. 18, no. 4, pp. 351–363, 1999.
[34] J. Ren, *Biodegradable Poly (Lactic Acid): Synthesis, Modification, Processing and Applications*. Springer Science & Business Media, 2011.
[35] H. Rosenheim, I. De, and S. Hyvedemm, "Bioplastics market data 2017," p. 4, 2017.
[36] V. L. Finkenstadt *et al.*, "Poly(lactic acid) green composites using oilseed coproducts as fillers," *Ind. Crops Prod.*, vol. 26, no. 1, pp. 36–43, Jun. 2007.
[37] T. Nishino, K. Hirao, M. Kotera, K. Nakamae, and H. Inagaki, "Kenaf reinforced biodegradable composite," *Compos. Sci. Technol.*, vol. 63, no. 9, pp. 1281–1286, Jul. 2003.
[38] Mr. Foruzanmehr, P. Y. Vuillaume, M. Robert, and S. Elkoun, "The effect of grafting a nano-TiO2 thin film on physical and mechanical properties of cellulosic natural fibers," *Mater. Des.*, vol. 85, pp. 671–678, Nov. 2015.
[39] P. Zierdt *et al.*, "Sustainable wood-plastic composites from bio-based polyamide 11 and chemically modified beech fibers," *Sustain. Mater. Technol.*, vol. 6, pp. 6–14, Dec. 2015.
[40] A. Le Duigou, A. Bourmaud, C. Gourier, and C. Baley, "Multi-scale shear properties of flax fibre reinforced polyamide 11 biocomposites," *Compos. Part Appl. Sci. Manuf.*, vol. 85, pp. 123–129, Jun. 2016.
[41] *CES EduPack*. UK: GrantaDesignLimited.
[42] E. M. Aizenshtein*, "Polypropylene fibres and yarns in the current state of development," *Fibre Chem.*, vol. 40, no. 5, pp. 399–405, Sep. 2008.

[43] D. Tripathi, *Practical Guide to Polypropylene*, Rapra Technology Limited. 2002.
[44] R. P. Babu, K. O'Connor, and R. Seeram, "Current progress on bio-based polymers and their future trends," *Prog. Biomater.*, vol. 2, Mar. 2013.
[45] R. Leblanc, "An Overview of Polypropylene Recycling," *The Balance*, 31-Jul-2017.
[46] M. A. AlMaadeed, R. Kahraman, P. Noorunnisa Khanam, and N. Madi, "Date palm wood flour/glass fibre reinforced hybrid composites of recycled polypropylene: Mechanical and thermal properties," *Mater. Des.*, vol. 42, no. Supplement C, pp. 289–294, Dec. 2012.
[47] L. Incarnato, P. Scarfato, and D. Acierno, "Rheological and mechanical properties of recycled polypropylene," *Polym. Eng. Sci.*, vol. 39, no. 4, pp. 749–755, Apr. 1999.
[48] M. A. S. Spinacé, K. K. G. Fermoseli, and M.-A. De Paoli, "Recycled polypropylene reinforced with curaua fibers by extrusion," *J. Appl. Polym. Sci.*, vol. 112, no. 6, pp. 3686–3694, Jun. 2009.
[49] M. J. Folkes, *Short Fibre Reinforced Thermoplastics*. Research Studies Press, 1982.
[50] T. Huber and J. Müssig, "Fibre matrix adhesion of natural fibres cotton, flax and hemp in polymeric matrices analyzed with the single fibre fragmentation test," *Compos. Interfaces*, vol. 15, no. 2–3, pp. 335–349, Jan. 2008.
[51] W. D. Callister, *Materials Science and Engineering: An Introduction*, 6 édition. New York, NY: Wiley, 2002.
[52] C.-P. Fung, J.-R. Hwang, and C.-C. Hsu, "The Effect of Injection Molding Process Parameters on the Tensile Properties of Short Glass Fiber-Reinforced PBT," *Polym.-Plast. Technol. Eng.*, vol. 42, no. 1, pp. 45–63, Jan. 2003.
[53] M. W. Tham *et al.*, "Tensile properties prediction of natural fibre composites using rule of mixtures: A review," *J. Reinf. Plast. Compos.*, vol. 38, no. 5, pp. 211–248, Mar. 2019.
[54] H. L. Bos, J. Müssig, and M. J. A. van den Oever, "Mechanical properties of short-flax-fibre reinforced compounds," *Compos. Part Appl. Sci. Manuf.*, vol. 37, no. 10, pp. 1591–1604, Oct. 2006.
[55] A. Kelly and W. R. Tyson, "Tensile properties of fibre-reinforced metals: Copper/tungsten and copper/molybdenum," *J. Mech. Phys. Solids*, vol. 13, no. 6, pp. 329–350, Dec. 1965.
[56] P. J. Herrera-Franco and A. Valadez-González, "A study of the mechanical properties of short natural-fiber reinforced composites," *Compos. Part B Eng.*, vol. 36, no. 8, pp. 597–608, Dec. 2005.
[57] A. K. Bledzki and J. Gassan, "Composites reinforced with cellulose based fibres," *Prog. Polym. Sci.*, vol. 24, no. 2, pp. 221–274, May 1999.
[58] Y. Wang, R. Qi, C. Xiong, and M. Huang, "Effects of coupling agent and interfacial modifiers on mechanical properties of poly (lactic acid) and wood flour biocomposites," *Iran Polym J*, vol. 20, no. 4, pp. 281–294, 2011.
[59] X. Li, L. G. Tabil, and S. Panigrahi, "Chemical Treatments of Natural Fiber for Use in Natural Fiber-Reinforced Composites: A Review," *J. Polym. Environ.*, vol. 15, no. 1, pp. 25–33, Feb. 2007.
[60] P. K. Kushwaha and R. Kumar, "Effect of Silanes on Mechanical Properties of Bamboo Fiber-epoxy Composites," *J. Reinf. Plast. Compos.*, vol. 29, no. 5, pp. 718–724, Mar. 2010.

[61] L. Petersson, K. Oksman, and A. P. Mathew, "Using maleic anhydride grafted poly(lactic acid) as a compatibilizer in poly(lactic acid)/layered-silicate nanocomposites," *J. Appl. Polym. Sci.*, vol. 102, no. 2, pp. 1852–1862, Oct. 2006.
[62] J. Ville *et al.*, "Influence of Extrusion Conditions on Fiber Breakage along the Screw Profile during Twin Screw Compounding of Glass Fiber-reinforced PA," *Int. Polym. Process.*, vol. 28, no. 1, pp. 49–57, Mar. 2013.
[63] C. Grande and F. G. Torres, "Investigation of fiber organization and damage during single screw extrusion of natural fiber reinforced thermoplastics," *Adv. Polym. Technol.*, vol. 24, no. 2, pp. 145–156, Jun. 2005.
[64] A. N. Oumer and O. Mamat, "A Review of Effects of Molding Methods, Mold Thickness and Other Processing Parameters on Fiber Orientation in Polymer Composites - SciAlert Responsive Version," *Asian J. Sci. Res.*, vol. 6, no. 3, pp. 401–410, 2013.
[65] M. J. T. Reaney, W. Hartley Furtan, and P. Loutas, "A critical cost benefit analysis of oilseed biodiesel in Canada : a BIOCAP research integration program synthesis paper," Mar. 2006.
[66] J. Pretty, "Agricultural sustainability: concepts, principles and evidence," *Philos. Trans. R. Soc. B Biol. Sci.*, vol. 363, no. 1491, pp. 447–465, Feb. 2008.
[67] S. K. Chattopadhyay *et al.*, "Biodegradability studies on natural fibers reinforced polypropylene composites," *J. Appl. Polym. Sci.*, vol. 121, no. 4, pp. 2226–2232, Aug. 2011.
[68] V. Sharma, H. K. Vinayak, and B. M. Marwaha, "Enhancing sustainability of rural adobe houses of hills by addition of vernacular fiber reinforcement," *Int. J. Sustain. Built Environ.*, vol. 4, no. 2, pp. 348–358, Dec. 2015.
[69] H. M. Akil, M. F. Omar, A. A. M. Mazuki, S. Safiee, Z. A. M. Ishak, and A. Abu Bakar, "Kenaf fiber reinforced composites: A review," *Mater. Des.*, vol. 32, no. 8–9, pp. 4107–4121, Sep. 2011.
[70] M. Smole, S. Hribernik, K. Stana-Kleinschek, and T. Kreze, "Plant Fibres for Textile and Technical Applications," in *Advances in Agrophysical Research*, IntechOpen., Stanislaw Grundas, 2013.
[71] N. Reddy and Y. Yang, "Extraction and characterization of natural cellulose fibers from common milkweed stems," *Polym. Eng. Sci.*, vol. 49, no. 11, pp. 2212–2217, 2009.
[72] M. A. Rahman and C. C. Wilcock, "A taxonomic revision of Calotropis (Asclepiadaceae)," *Nord. J. Bot.*, vol. 11, no. 3, pp. 301–308, 1991.
[73] G. Watt, "Madar. (Calotropis gigantea, R. Br.)," *Bull. Misc. Inf. R. Bot. Gard. Kew*, vol. 1900, no. 157/168, pp. 8–12, 1900.
[74] J. Cuoq, *Recueil des sources arabes concernant l'Afrique occidentale du 8 au 16 siècle. -Bilad Al-Sudan-.* Centre national de la recherche scientifique, 1975.
[75] J. M. Leprince, "Le Québec deviendra-t-il l'eldorado de la soie d'Amérique?," *Radio Canada*, 20-Oct-2014.
[76] C. S. Sonnini, *Traité des Asclépiades particuliérement de l'Asclépiade de Syrie: précédé de quelques observations sur la culture du coton en France*. 1810.
[77] C. Patterson, "Milkweed fruits: Pods of plenty," *The Washington Post*, 25-Sep-2012.
[78] J. M. Leprince, "La soie d'Amérique passe en production industrielle," *Radio Canada*, 26-Oct-2015.

[79] J. Bernstien, “How a Quebec company used milkweed to create a one-of-a-kind winter coat,” *CBC News*, 13-Oct-2016.
[80] A. A. Gharehaghaji and S. H. Davoodi, “Mechanical damage to estabragh fibers in the production of thermobonded layers,” *J. Appl. Polym. Sci.*, vol. 109, no. 5, pp. 3062–3069, Sep. 2008.
[81] M. Stevens, “USDA-NRCS Plant Guide - Common Milkweed (Asclepias Syriaca L.).” 25-Jul-2000.
[82] C. Holdrege, “The Story of an Organism: Common Milkweed,” *Nat. Inst.*, 2010.
[83] T.-T. Lim and X. Huang, “Evaluation of kapok (Ceiba pentandra (L.) Gaertn.) as a natural hollow hydrophobic–oleophilic fibrous sorbent for oil spill cleanup,” *Chemosphere*, vol. 66, no. 5, pp. 955–963, Jan. 2007.
[84] J. C. Sakthivel, S. Mukhopadhyay, and N. K. Palanisamy, “Some Studies on Mudar Fibers,” *J. Ind. Text.*, vol. 35, no. 1, pp. 63–76, Jul. 2005.
[85] A. Nourbakhsh, A. Ashori, and M. Kouhpayehzadeh, “Giant Milkweed (Calotropis persica) Fibers -- A Potential Reinforcement Agent for Thermoplastics Composites,” *J. Reinf. Plast. Compos.*, vol. 28, no. 17, pp. 2143–2149, Sep. 2009.
[86] N. Reddy and Y. Yang, “Non-traditional lightweight polypropylene composites reinforced with milkweed floss,” *Polym. Int.*, vol. 59, no. 7, pp. 884–890, Jul. 2010.
[87] M. H. Kish and S. S. Najar, “Strucutre and properties of a natural celulosic hollow fiber,” *Int. J. Eng.*, vol. 11, no. 2, pp. 101–108, 1998.
[88] S. Hassanzadeh, H. Hasani, and M. Zarrebini, “Analysis and prediction of the noise reduction coefficient of lightly-needled Estabragh/polypropylene nonwovens using simplex lattice design,” *J. Text. Inst.*, vol. 105, no. 3, pp. 256–263, Mar. 2014.
[89] N. Bahari, H. Hasani, M. Zarrebini, and S. Hassanzadeh, “Investigating the effects of material and process variables on the mechanical properties of low-density thermally bonded nonwovens produced from Estabragh (milkweed) natural fibers,” *J. Ind. Text.*, vol. 46, no. 3, pp. 719–736, Jun. 2015.
[90] H. Hasani, M. Zarrebini, M. Zare, and S. Hassanzadeh, “Evaluating the Acoustic Properties of Estabragh (Milkweed)/Hollow- Polyester Nonwovens for Automotive Applications,” *J. Text. Sci. Eng.*, vol. 4, no. 3, May 2014.
[91] A. A. Merati, “Reinforcing of Cement Composites by Estabragh Fibres,” *J. Inst. Eng. India Ser. E*, vol. 95, no. 1, pp. 27–32, Jun. 2014.
[92] O. K. Sunmonu and D. Abdullahi, “Characterization of Fibres from the Plant Ceiba Pentandra,” *J. Text. Inst.*, vol. 83, no. 2, pp. 273–274, Jan. 1992.
[93] G. L. Louis and B. A. K. Andrews, “Cotton/Milkweed Blends: A Novel Textile Product,” *Text. Res. J.*, vol. 57, no. 6, pp. 339–345, Jun. 1987.
[94] T. Karthik and R. Murugan, “Characterization and analysis of ligno-cellulosic seed fiber from Pergularia Daemia plant for textile applications,” *Fibers Polym.*, vol. 14, no. 3, pp. 465–472, Mar. 2013.
[95] P. Gu, R. K. Hessley, and W.-P. Pan, “Thermal characterization analysis of milkweed flos,” *J. Anal. Appl. Pyrolysis*, vol. 24, no. 2, pp. 147–161, 1992.
[96] K. Koch and H.-J. Ensikat, “The hydrophobic coatings of plant surfaces: Epicuticular wax crystals and their morphologies, crystallinity and molecular self-assembly,” *Micron*, vol. 39, no. 7, pp. 759–772, Oct. 2008.
[97] D. B. Anderson and T. Kerr, “Growth and structure of cotton fiber,” *Ind. Eng. Chem.*, vol. 30, no. 1, pp. 48–54, 1938.

[98] T. Kerr, "The structure of the growth rings in the secondary wall of the cotton hair," *Protoplasma*, vol. 27, no. 1, pp. 229–241, Dec. 1937.
[99] T. Karthik, "Studies on the spinnability of milkweed fibre blends and its influence on ring compact and rotor yarn characteristics," Anna University, Chennai, 2015.
[100] G. Cicala, G. Cristaldi, G. Recca, and A. Latteri, "Composites Based on Natural Fibre Fabrics," in *Woven fabric engineering*, Polona Dobnik Dubrovski., IntechOpen, 2010.
[101] Y. Zheng and A. Wang, "Kapok Fiber: Structure and Properties," in *Biomass and Bioenergy*, K. R. Hakeem, M. Jawaid, and U. Rashid, Eds. Springer International Publishing, 2014, pp. 101–110.
[102] K. K. Chawla, *Fibrous Materials*. Cambridge University Press, 2005.
[103] X. Yang, L. D. Cheng, L. Q. Huang, and W. H. Fan, "Study on the Correlation between the Property of Akund Fiber and its Growing Conditions," *Adv. Mater. Res.*, vol. 476–478, pp. 1934–1938, Feb. 2012.
[104] D. L. Morgado and E. Frollini, "Thermal decomposition of mercerized linter cellulose and its acetates obtained from a homogeneous reaction," *Polímeros*, vol. 21, no. 2, pp. 111–117, 2011.
[105] C. A. Srinivas and G. D. Babu, "Mechanical and Machining Characteristics of Calotropis Gigentea Fruit Fiber Reinforced Plastics," *Int. J. Eng. Res. Technol.*, vol. 2, no. 6, Jun. 2013.
[106] G. Venkata Reddy, S. Venkata Naidu, and T. Shobha Rani, "A Study on Hardness and Flexural Properties of Kapok/Sisal Composites," *J. Reinf. Plast. Compos.*, vol. 28, no. 16, pp. 2035–2044, Aug. 2009.
[107] G. Venkata Reddy, T. Shobha Rani, K. Chowdoji Rao, and S. Venkata Naidu, "Flexural, Compressive, and Interlaminar Shear Strength Properties of Kapok/Glass Composites," *J. Reinf. Plast. Compos.*, vol. 28, no. 14, pp. 1665–1677, Jul. 2009.
[108] G. Venkata Reddy, S. Venkata Naidu, and T. Shobha Rani, "Impact Properties of Kapok Based Unsaturated Polyester Hybrid Composites," *J. Reinf. Plast. Compos.*, vol. 27, no. 16–17, pp. 1789–1804, Nov. 2008.
[109] G. Venkata Reddy, S. Venkata Naidu, and T. Shobha Rani, "Kapok/Glass Polyester Hybrid Composites: Tensile and Hardness Properties," *J. Reinf. Plast. Compos.*, vol. 27, no. 16–17, pp. 1775–1787, Nov. 2008.
[110] L. Y. Mwaikambo, E. Martuscelli, and M. Avella, "Kapok/cotton fabric–polypropylene composites," *Polym. Test.*, vol. 19, no. 8, pp. 905–918, Sep. 2000.
[111] H.-M. Choi, "Needlepunched Cotton Nonwovens and Other Natural Fibers as Oil Cleanup Sorbents," *J. Environ. Sci. Health Part Environ. Sci. Eng. Toxicol.*, vol. 31, no. 6, pp. 1441–1457, Jul. 1996.
[112] H. M. Choi and R. M. Cloud, "Natural sorbents in oil spill cleanup," *Environ. Sci. Technol.*, vol. 26, no. 4, pp. 772–776, Apr. 1992.
[113] Y. Kobayashi, R. Matuo, and M. Nishiyama, "Method for adsorption of oils," US4061567A, 01-Mar-1976.
[114] K. Hori, M. E. Flavier, S. Kuga, T. B. T. Lam, and K. Iiyama, "Excellent oil absorbent kapok [Ceiba pentandra (L.) Gaertn.] fiber: fiber structure, chemical characteristics, and application," *J. Wood Sci.*, vol. 46, no. 5, pp. 401–404, 2000.

[115] P. C. Crews, S. A. Sievert, L. T. Woeppel, and E. A. Mccullough, “Evaluation of Milkweed Floss as an Insulative Fill Material,” *Text. Res. J.*, vol. 61, no. 4, pp. 203–210, Apr. 1991.
[116] M. S. Parmar, M. Bahl, and J. V. Rao, “Milkweed blended fabrics and their thermal insulation and UV protection properties,” *Indian J. Fibre Text. Res.*, vol. 40, no. 4, pp. 351–355, Jan. 2016.
[117] P. Cui, F.-M. Wang, A. Wei, and K. Zhao, “The Performance of Kapok/Down Blended Wadding,” *Text. Res. J.*, vol. 80, no. 6, pp. 516–523, Apr. 2010.
[118] P. Cui and F. Wang, “An investigation of heat flow through kapok insulating material,” vol. 19, pp. 88–92, Apr. 2009.
[119] B. Boris, “Insulated life preserver garment,” US2618257 A, 18-Nov-1952.
[120] M. E.-S. Ali, “Natural fiber insulation material and method for making the same,” US20130193365 A1, 01-Aug-2013.
[121] G. Bogoeva-Gaceva *et al.*, “Natural fiber eco-composites,” *Polym. Compos.*, vol. 28, no. 1, pp. 98–107, Feb. 2007.
[122] K. Oksman, M. Skrifvars, and J.-F. Selin, “Natural fibres as reinforcement in polylactic acid (PLA) composites,” *Compos. Sci. Technol.*, vol. 63, no. 9, pp. 1317–1324, Jul. 2003.
[123] Mr. Foruzanmehr, P. Y. Vuillaume, S. Elkoun, and M. Robert, “Physical and mechanical properties of PLA composites reinforced by TiO2 grafted flax fibers,” *Mater. Des.*, vol. 106, pp. 295–304, Sep. 2016.
[124] N. Graupner, A. S. Herrmann, and J. Müssig, “Natural and man-made cellulose fibre-reinforced poly(lactic acid) (PLA) composites: An overview about mechanical characteristics and application areas,” *Compos. Part Appl. Sci. Manuf.*, vol. 40, no. 6, pp. 810–821, Jul. 2009.
[125] G. Koronis, A. Silva, and M. Fontul, “Green composites: A review of adequate materials for automotive applications,” *Compos. Part B Eng.*, vol. 44, no. 1, pp. 120–127, Jan. 2013.
[126] M. John and S. Thomas, “Biofibres and biocomposites,” *Carbohydr. Polym.*, vol. 71, no. 3, pp. 343–364, Feb. 2008.
[127] E. E. Gaertner, “The history and use of milkweed (Asclepias syriaca L.),” *Econ. Bot.*, vol. 33, no. 2, pp. 119–123, 1979.
[128] T. Karthik and R. Murugan, “Milkweed—A Potential Sustainable Natural Fibre Crop,” in *Sustainable Fibres for Fashion Industry*, S. S. Muthu and M. Gardetti, Eds. Springer Science & Business Media, 2016, pp. 111–146.
[129] D. E. Akin, “Chemistry of Plant Fibres,” in *Industrial application of natural fibres: structure, properties, and technical applications*, J. Müssig, Ed. Wiley, 2010, pp. 13–22.
[130] M. Bayart, F. Gauvin, M. R. Foruzanmehr, S. Elkoun, and M. Robert, “Mechanical and moisture absorption characterization of PLA composites reinforced with nano-coated flax fibers,” *Fibers Polym.*, vol. 18, no. 7, pp. 1288–1295, Jul. 2017.
[131] G. R. Nair, A. Singh, M. Zimniewska, and V. Raghavan, “Comparative Evaluation of Physical and Structural Properties of Water Retted and Non-retted Flax Fibers,” *Fibers*, vol. 1, no. 3, pp. 59–69, Oct. 2013.

[132] L. Boulos, M. R. Foruzanmehr, A. Tagnit-Hamou, S. Elkoun, and M. Robert, "Wetting analysis and surface characterization of flax fibers modified with zirconia by sol-gel method," *Surf. Coat. Technol.*, vol. 313, pp. 407–416, Mar. 2017.
[133] H.-M. Choi and J. P. Moreau, "Oil sorption behavior of various sorbents studied by sorption capacity measurement and environmental scanning electron microscopy," *Microsc. Res. Tech.*, vol. 25, no. 5–6, pp. 447–455, Aug. 1993.
[134] M. Likon, M. Remškar, V. Ducman, and F. Švegl, "Populus seed fibers as a natural source for production of oil super absorbents," *J. Environ. Manage.*, vol. 114, pp. 158–167, Jan. 2013.
[135] B.-G. Lee, J. S. Han, and R. M. Rowell, "Oil sorption by lignocellulosic fibers," in *Kenaf properties, processing and products*, Mississippi State University, Ag. & Bio Engineering, 1999, pp. 423–433.
[136] X. Zhang *et al.*, "Superhydrophobicity determines the buoyancy performance of kapok fiber aggregates," *Appl. Surf. Sci.*, vol. 266, pp. 225–229, Feb. 2013.
[137] Y. Zheng, J. Wang, Y. Zhu, and A. Wang, "Research and application of kapok fiber as an absorbing material: A mini review," *J. Environ. Sci.*, vol. 27, pp. 21–32, Jan. 2015.
[138] Y. Zheng, Y. Zhu, A. Wang, and H. Hu, "Potential of Calotropis gigantea fiber as an absorbent for removal of oil from water," *Ind. Crops Prod.*, vol. 83, pp. 387–390, May 2016.
[139] K. Myrtha, O. Holio, and S. Anung, "Physical and Mechanical Properties of Natural Fibers Filled Polypropylene Composites and Its Recycle," *J. Biol. Sci.*, vol. 7, no. 2, pp. 393–396, 2007.
[140] S. K. De and J. R. White, *Short Fibre-Polymer Composites*. Elsevier, 1996.
[141] A. K. Bledzki, A. Jaszkiewicz, and D. Scherzer, "Mechanical properties of PLA composites with man-made cellulose and abaca fibres," *Compos. Part Appl. Sci. Manuf.*, vol. 40, no. 4, pp. 404–412, Apr. 2009.
[142] M. Brebu and C. Vasile, "Thermal Degradation of Lignin – a Review," *Cellul. Chem. Technol.*, vol. 44, no. 9, pp. 353–363, 2010.
[143] H. Yang, R. Yan, H. Chen, D. H. Lee, and C. Zheng, "Characteristics of hemicellulose, cellulose and lignin pyrolysis," *Fuel*, vol. 86, no. 12, pp. 1781–1788, Aug. 2007.
[144] J. Gassan and A. K. Bledzki, "Thermal degradation of flax and jute fibers," *J. Appl. Polym. Sci.*, vol. 82, no. 6, pp. 1417–1422, Nov. 2001.
[145] W.-H. Chen and P.-C. Kuo, "Isothermal torrefaction kinetics of hemicellulose, cellulose, lignin and xylan using thermogravimetric analysis," *Energy*, vol. 36, no. 11, pp. 6451–6460, Nov. 2011.
[146] M. S. Jasbi, H. Hasani, A. Zadhoush, and S. Safi, "Effect of alkali treatment on mechanical properties of the green composites reinforced with milkweed fibers," *J. Text. Inst.*, vol. 109, no. 1, pp. 24–31, Jan. 2018.
[147] N. V. David, S. Khairiyah, and P. P. A. Majeed, "Elastic and dynamic response characteristics of kenaf/polypropylene composites," in *Natural Filler and Fibre Composites*, Southempton: WIT Press, 2012, p. 183.
[148] C. Baley, "Influence of kink bands on the tensile strength of flax fibers," *J. Mater. Sci.*, vol. 39, no. 1, pp. 331–334, Jan. 2004.

[149] J. J. Yuan, J. M. Kennedy, and D. D. Edie, "Modeling the Dynamic Response of the Fiber/Matrix Interphase in Continuous Fiber Composite Materials," *ASTM Int.*, vol. STP38226S, no. STP1290, Dec. 1996.
[150] A. C. Karmaker, "Effect of water absorption on dimensional stability and impact energy of jute fibre reinforced polypropylene," *J. Mater. Sci. Lett.*, vol. 16, no. 6, pp. 462–464, Mar. 1997.
[151] R. S. Rengasamy, D. Das, and C. Praba Karan, "Study of oil sorption behavior of filled and structured fiber assemblies made from polypropylene, kapok and milkweed fibers," *J. Hazard. Mater.*, vol. 186, no. 1, pp. 526–532, Feb. 2011.
[152] S. Mazumdar, *Composites Manufacturing: Materials, Product, and Process Engineering*. CRC Press, 2001.
[153] C. Baillie, *Green Composites: Polymer Composites and the Environment*. CRC Press, 2005.
[154] R. Zah, R. Hischier, A. L. Leão, and I. Braun, "Curauá fibers in the automobile industry – a sustainability assessment," *J. Clean. Prod.*, vol. 15, no. 11, pp. 1032–1040, Jan. 2007.
[155] V. A. Alvarez, R. A. Ruscekaite, and A. Vazquez, "Mechanical Properties and Water Absorption Behavior of Composites Made from a Biodegradable Matrix and Alkaline-Treated Sisal Fibers," *J. Compos. Mater.*, vol. 37, no. 17, pp. 1575–1588, Sep. 2003.
[156] Y. Xie, C. A. S. Hill, Z. Xiao, H. Militz, and C. Mai, "Silane coupling agents used for natural fiber/polymer composites: A review," *Compos. Part Appl. Sci. Manuf.*, vol. 41, no. 7, pp. 806–819, Jul. 2010.
[157] A. Orue, A. Jauregi, U. Unsuain, J. Labidi, A. Eceiza, and A. Arbelaiz, "The effect of alkaline and silane treatments on mechanical properties and breakage of sisal fibers and poly(lactic acid)/sisal fiber composites," *Compos. Part Appl. Sci. Manuf.*, vol. 84, no. Supplement C, pp. 186–195, May 2016.
[158] T. P. T. Tran, J.-C. Bénézet, and A. Bergeret, "Rice and Einkorn wheat husks reinforced poly(lactic acid) (PLA) biocomposites: Effects of alkaline and silane surface treatments of husks," *Ind. Crops Prod.*, vol. 58, pp. 111–124, Jul. 2014.
[159] M. Abdelmouleh, S. Boufi, M. N. Belgacem, and A. Dufresne, "Short natural-fibre reinforced polyethylene and natural rubber composites: Effect of silane coupling agents and fibres loading," *Compos. Sci. Technol.*, vol. 67, no. 7–8, pp. 1627–1639, Jun. 2007.
[160] C. Richard, P. Cousin, Mr. Foruzanmehr, S. Elkoun, and M. Robert, "Characterization of components of milkweed floss fiber," *Sep. Sci. Technol.*, vol. 0, no. 0, pp. 1–9, Dec. 2018.
[161] P. Gañán, J. Cruz, S. Garbizu, A. Arbelaiz, and I. Mondragon, "Stem and bunch banana fibers from cultivation wastes: Effect of treatments on physico-chemical behavior," *J. Appl. Polym. Sci.*, vol. 94, no. 4, pp. 1489–1495, Nov. 2004.
[162] A. n. Frone, S. Berlioz, J.-F. Chailan, D. m. Panaitescu, and D. Donescu, "Cellulose fiber-reinforced polylactic acid," *Polym. Compos.*, vol. 32, no. 6, pp. 976–985, Jun. 2011.
[163] S. Mishra *et al.*, "Studies on mechanical performance of biofibre/glass reinforced polyester hybrid composites," *Compos. Sci. Technol.*, vol. 63, no. 10, pp. 1377–1385, Aug. 2003.

[164] N. Venkatachalam, P. Navaneethakrishnan, R. Rajsekar, and S. Shankar, "Effect of Pretreatment Methods on Properties of Natural Fiber Composites: A Review," *Polym. Polym. Compos.*, vol. 24, no. 7, pp. 555–566, Sep. 2016.
[165] S. Ouajai, A. Hodzic, and R. A. Shanks, "Morphological and grafting modification of natural cellulose fibers," *J. Appl. Polym. Sci.*, vol. 94, no. 6, pp. 2456–2465, 2004.
[166] R. J. Moon, A. Martini, J. Nairn, J. Simonsen, and J. Youngblood, "Cellulose nanomaterials review: structure, properties and nanocomposites," *Chem. Soc. Rev.*, vol. 40, no. 7, pp. 3941–3994, Jun. 2011.
[167] J. Andersons, E. Spārniņš, R. Joffe, and L. Wallström, "Strength distribution of elementary flax fibres," *Compos. Sci. Technol.*, vol. 65, no. 3, pp. 693–702, Mar. 2005.
[168] P. R. Hornsby, E. Hinrichsen, and K. Tarverdit, "Preparation and properties of polypropylene composites reinforced with wheat and flax straw fibres: Part I Fibre characterization," *J. Mater. Sci.*, vol. 32, no. 2, pp. 443–449, Jan. 1997.
[169] R. V. Silva, D. Spinelli, W. W. Bose Filho, S. Claro Neto, G. O. Chierice, and J. R. Tarpani, "Fracture toughness of natural fibers/castor oil polyurethane composites," *Compos. Sci. Technol.*, vol. 66, no. 10, pp. 1328–1335, Aug. 2006.
[170] O. Faruk, A. K. Bledzki, H.-P. Fink, and M. Sain, "Progress Report on Natural Fiber Reinforced Composites," *Macromol. Mater. Eng.*, vol. 299, no. 1, pp. 9–26, 2014.
[171] R. A. Witik, J. Payet, V. Michaud, C. Ludwig, and J.-A. E. Månson, "Assessing the life cycle costs and environmental performance of lightweight materials in automobile applications," *Compos. Part Appl. Sci. Manuf.*, vol. 42, no. 11, pp. 1694–1709, Nov. 2011.
[172] F. Ahmad, H. S. Choi, and M. K. Park, "A Review: Natural Fiber Composites Selection in View of Mechanical, Light Weight, and Economic Properties," *Macromol. Mater. Eng.*, vol. 300, no. 1, pp. 10–24, 2015.
[173] B. Ferrero, V. Fombuena, O. Fenollar, T. Boronat, and R. Balart, "Development of natural fiber-reinforced plastics (NFRP) based on biobased polyethylene and waste fibers from Posidonia oceanica seaweed," *Polym. Compos.*, vol. 36, no. 8, pp. 1378–1385, 2015.
[174] J. Chen and D. J. Gardner, "Dynamic mechanical properties of extruded nylon–wood composites," *Polym. Compos.*, vol. 29, no. 4, pp. 372–379, 2008.
[175] J. Holbery and D. Houston, "Natural-fiber-reinforced polymer composites in automotive applications," *JOM*, vol. 58, no. 11, pp. 80–86, 2006.
[176] M. Robert, P. Ovlaque, and M. R. Foruzanmehr, "Hollow Floss Fibers Characterization and Potential Industrial Applications," in *Chemistry of Lignocellulosics: Current Trends*, CRC Press, 2018, p. 516.
[177] R. Malkapuram, V. Kumar, and Y. S. Negi, "Recent Development in Natural Fiber Reinforced Polypropylene Composites," *J. Reinf. Plast. Compos.*, vol. 28, no. 10, pp. 1169–1189, May 2009.
[178] M. Tajvidi, M. Feizmand, R. H. Falk, and C. Felton, "Effect of Cellulose Fiber Reinforcement on the Temperature Dependent Mechanical Performance of Nylon 6," *J. Reinf. Plast. Compos.*, vol. 28, no. 22, pp. 2781–2790, Nov. 2009.
[179] K. Panyasart, N. Chaiyut, T. Amornsakchai, and O. Santawitee, "Effect of Surface Treatment on the Properties of Pineapple Leaf Fibers Reinforced Polyamide 6 Composites," *Energy Procedia*, vol. 56, pp. 406–413, Jan. 2014.

[180] E. Ozen, A. Kiziltas, E. E. Kiziltas, and D. J. Gardner, "Natural fiber blend—nylon 6 composites," *Polym. Compos.*, vol. 34, no. 4, pp. 544–553, 2013.
[181] D. Aydemir, A. Kiziltas, E. Erbas Kiziltas, D. J. Gardner, and G. Gunduz, "Heat treated wood–nylon 6 composites," *Compos. Part B Eng.*, vol. 68, pp. 414–423, Jan. 2015.
[182] P. A. Santos, M. A. S. Spinacé, K. K. G. Fermoselli, and M.-A. De Paoli, "Polyamide-6/vegetal fiber composite prepared by extrusion and injection molding," *Compos. Part Appl. Sci. Manuf.*, vol. 38, no. 12, pp. 2404–2411, Dec. 2007.
[183] S.-Y. Fu and B. Lauke, "Effects of fiber length and fiber orientation distributions on the tensile strength of short-fiber-reinforced polymers," *Compos. Sci. Technol.*, vol. 56, no. 10, pp. 1179–1190, Jan. 1996.
[184] M. Ho *et al.*, "Critical factors on manufacturing processes of natural fibre composites," *Compos. Part B Eng.*, vol. 43, no. 8, pp. 3549–3562, Dec. 2012.
[185] M. Feldmann, H.-P. Heim, and J.-C. Zarges, "Influence of the process parameters on the mechanical properties of engineering biocomposites using a twin-screw extruder," *Compos. Part Appl. Sci. Manuf.*, vol. 83, pp. 113–119, Apr. 2016.
[186] K. Ramani, D. Bank, and N. Kraemer, "Effect of screw design on fiber damage in extrusion compounding and composite properties," *Polym. Compos.*, vol. 16, no. 3, pp. 258–266, 1995.
[187] A. Vaxman, M. Narkis, A. Siegmann, and S. Kenig, "Short-Fiber Thermoplastics Composites: Fiber Fracture During Melt Processing," in *Wiley Encyclopedia of Composites*, American Cancer Society, 2012, pp. 1–19.
[188] D. Tripathi, T. Turton, F. Chen, and F. R. Jones, "A new method to normalize the effect of matrix properties on the value of interfacial shear strength obtained from the fragmentation test," *J. Mater. Sci.*, vol. 32, no. 18, pp. 4759–4765, Sep. 1997.
[189] S. Feih, K. Wonsyld, D. Minzari, P. Westermann, and H. Lilholt, "Testing Procedure for the Single Fiber Fragmentation Test," Forskningscenter Risø, Report, 2004.
[190] H. Chen and D. G. Baird, "Prediction of Young's Modulus for Injection Molded Long Fiber Reinforced Thermoplastics," *J. Compos. Sci.*, vol. 2, no. 3, p. 47, Sep. 2018.
[191] C. Wei-Kuo, L. Hsin-Tzu, and L. Yu-Der, "Effects of fiber length and orientation distribution on the elastic modulus of short fiber reinforced thermoplastics," *Polym. Compos.*, vol. 9, no. 1, pp. 27–35, Feb. 1988.
[192] J. A. Dean, *Lange's Handbook of Chemistry*. McGraw-Hill, 1967.
[193] A. Awal, G. Cescutti, S. B. Ghosh, and J. Müssig, "Interfacial studies of natural fibre/polypropylene composites using single fibre fragmentation test (SFFT)," *Compos. Part Appl. Sci. Manuf.*, vol. 42, no. 1, pp. 50–56, Jan. 2011.
[194] X.-F. Zhou, J. A. Nairn, and H. D. Wagner, "Fiber–matrix adhesion from the single-fiber composite test: nucleation of interfacial debonding," *Compos. Part Appl. Sci. Manuf.*, vol. 30, no. 12, pp. 1387–1400, Dec. 1999.
[195] A. Ho, A. N. Netravali, and S. L. Phoenix, "Interfacial shear strength studies of nicalon fibers in epoxy matrix using single fiber composite test," *Polym. Compos.*, vol. 16, no. 6, pp. 542–548, Dec. 1995.
[196] A. Keller, "Compounding and mechanical properties of biodegradable hemp fibre composites," *Compos. Sci. Technol.*, vol. 63, no. 9, pp. 1307–1316, Jul. 2003.

[197] S.-Y. Fu, B. Lauke, and Y.-W. Mai, “Major factors affecting the performance of short fibre reinforced polymers,” in *Science and engineering of short fibre reinforced polymer composites*, CRC Press., vol. 1, Fu S. Y., Lauke B., Mai Y-W., 2009.

[198] E. Domingos, T. M. C. Pereira, E. V. R. de Castro, W. Romão, G. L. de Sena, and R. C. L. Guimarães, “Monitorando a degradação da poliamida 11 (PA-11) via espectroscopia na região do infravermelho médio com transformada de fourier (FTIR),” *Polímeros*, vol. 23, no. 1, pp. 37–41, 2013.

[199] S. Maïza *et al.*, “Physicochemical and mechanical degradation of polyamide 11 induced by hydrolysis and thermal aging,” *J. Appl. Polym. Sci.*, vol. 136, no. 23, p. 47628, 2019.

[200] K. Oksman, A. P. Mathew, R. Långström, B. Nyström, and K. Joseph, “The influence of fibre microstructure on fibre breakage and mechanical properties of natural fibre reinforced polypropylene,” *Compos. Sci. Technol.*, vol. 69, no. 11, pp. 1847–1853, Sep. 2009.

[201] G. El-Shenawy, A. Mahmoud, and E. Ramadan, “Using Nonwoven Hollow Fibers to Improve Cars Interior Acoustic Properties,” *Res. J. Text. Appar.*, vol. 16, no. 3, pp. 49–56, Aug. 2012.

[202] J. L. Moll, S. R. White, and N. R. Sottos, “A Self-sealing Fiber-reinforced Composite,” *J. Compos. Mater.*, vol. 44, no. 22, pp. 2573–2585, Oct. 2010.

[203] S. Kling and T. Czigány, “Damage detection and self-repair in hollow glass fiber fabric-reinforced epoxy composites via fiber filling,” *Compos. Sci. Technol.*, vol. 99, pp. 82–88, Jul. 2014.

[204] R. S. Trask and I. P. Bond, “Biomimetic self-healing of advanced composite structures using hollow glass fibres,” *Smart Mater. Struct.*, vol. 15, no. 3, pp. 704–710, Apr. 2006.